Sede Amministrativa: Università degli Studi di Padova

Dipartimento di Science Biomediche Sperimentali

SCUOLA DI DOTTORATO DI RICERCA IN : Bioscienze e Biotecnologie
INDIRIZZO: Biologia cellulare
CICLO XXIV

"DMPK prevents ROS-induced cell death by assembling a HK II-Src complex on mitochondrial surface"

Direttore della Scuola : Ch.mo Prof. Giuseppe Zanotti
Coordinatore d'indirizzo: Ch.mo Prof. Cesare Montecucco
Supervisore :Ch.mo Dott. Andrea Rasola

Dottorando : Boris Pantic

Table of Contents

Summary **1**
Introduction **5**
DMPK and myotonic dystrophy type 1 5
Molecular features of DM1 6
DM1 and tumors 9
DMPK: structure and kinase activity 11
Proposed DMPK interactors 13
Other DMPK roles 15
Mitochondria in physiology and pathology 17
Mitochondria and cell death 18
The mitochondrial permeability transition pore (PTP) 20
Mitochondria and ROS 27
Mitochondria and signaling 32
Materials and Methods **37**
Cells 37
Cell transfection with calcium phosphate 37
Cell lysates 38
Isolation of mitochondria 38
Protein quantification 39
SDS-PAGE and Western immunoblotting 39
Co-immunoprecipitation assays 40
Fluorescence microscopy 40
ATP determination 41
Flow cytometry analysis of mitochondrial depolarization, mitochondrial superoxide, cell death and mitochondrial mass 42
Analysis of the oxygen consumption rate (OCR) of cell monolayers 43
Assay of thioredoxin reductase and glutathione reductase activities 43
Determination of glutathione concentration and redox state 44
Results **45**

Identification of cell models for the study of DMPK 45
DMPK expression does not affect mitochondrial membrane potential or mitochondrial mass 49
DMPK and stress 52
Mitochondrial metabolism and antioxidant defenses 56
Molecular mechanisms of DMPK-driven regulation of mitochondrial superoxide 60
How does DMPK increase HK II association with mitochondria? 67
Discussion **73**
References **81**

Summary

DMPK is a serine/threonine protein kinase that was initially proposed to be the cause of the most frequent adult muscular dystrophy, myotonic dystrophy 1 (DM1). Recently, it has been shown that DMPK is not the primary determinant of the DM1, but its deletion causes late onset myopathy and cardiac abnormalities in knock-out mice. Evidence present in the literature suggests a mitochondrial localization of high MW DMPK isoforms in muscle and cardiac tissue. However, to date, there is not a single association of mitochondria-anchored isoforms with the respective function of the organelle in the affected tissues. Therefore, we have examined the role of mitochondria-anchored isoform A, either by stably expressing it in cells lacking endogenous protein, or by stably silencing the endogenous one. DMPK significantly decreased levels of mitochondrial superoxide and consequently increased cell survival in prolonged serum and glucose depletion, both in SAOS-2 and rhabdomyosarcoma cells. At the molecular level we have found DMPK to interact with HK II and Src, increasing the HK II association to mitochondria. Detachment of HK II from mitochondria abolished differences in superoxide levels, while a HK II inhibitor 5-TG protected cells from death by stabilizing HK II on the OMM and by decreasing mitochondrial ROS in the absence of DMPK. Src activity was also important for HK II maintenance on OMM since its inhibition sensitized only DMPK-expressing cells to detachment of HK II. These data attribute an antiapoptotic role to DMPK due to an unprecedented link to HK II and its protective effect against mitochondrial ROS.

Abbreviations: 5-TG (5-thioglucose), DMPK (myotonic dystrophy protein kinase), HK II (hexokinase II), OMM (outer mitochondrial membrane).

DMPK è la serina/treonina protein kinasi, la quale è stata inizialmente proposta come la causa della più frequente distrofia muscolare negli adulti, la distrofia miotonica del tipo 1 (DM1). Recentemente si è visto che la DMPK non è la causa principale della DM1, ma la sua delezione causa miopatia ad insorgenza tardiva e anomalie cardiache nei topi *knock-out*. I dati presenti in letteratura attribuiscono la localizzazione mitocondriale alle isoforme ad alto peso molecolare nel muscolo e nel tessuto cardiaco. Comunque, finora non vi sono stati studi volti ad associare il ruolo delle isoforme mitocondriali della DMPK alla funzione dell'organulo nei tessuti in questione. Perciò, abbiamo deciso di esaminare il ruolo dall'isoforma A associata ai mitocondri, sia esprimendola stabilmente nelle cellule prive della DMPK endogena, sia silenziando stabilmente quella endogena. DMPK ha significativamente diminuito i livelli del superossido mitocondriale e, di conseguenza, ha aumentato la sopravvivenza delle cellule SAOS-2 e rabdomiosarcoma in deplezione di siero e glucosio. A livello molecolare, abbiamo trovato che la DMPK interagisce con HK II e Src aumentando l'associazione dell'HK II ai mitocondri. Il distacco dell'HK II dai mitocondri ha cancellato le differenze nei livelli di superossido, mentre l'inibitore dell'HK II 5-TG ha protetto le cellule dalla morte stabilizzando l'HK II sulla membrana mitocondriale esterna e diminuendo i livelli di ROS mitocondriali in assenza della DMPK. Src aveva la funzione di mantenere HK II sulla membrana mitocondriale esterna, in quanto la sua inibizione ha sensibilizzato le cellule al distacco dell'HK II solo se esprimevano la DMPK. Questo studio attribuisce un ruolo anti-apoptotico alla DMPK grazie all'interazione con HK II e la sua funzione protettiva contro i ROS di origine mitocondriale.

Abbreviazioni: 5-TG (5-tioglucosio), DMPK (distrofia miotonica protein kinasi), HK II (esokinasi II).

Introduction

DMPK and myotonic dystrophy type 1

Myotonic dystrophy protein kinase (DMPK) is a serine/threonine kinase whose discovery dates back to 1992, when a non-coding portion of the gene locus encoding for the DMPK protein was identified as causative for myotonic dystrophy type 1 (DM1) [1]. It was shown that DM1 is caused by the expansion of an unstable tri-nucleotide repeat in the 3'-UTR of the *dmpk* locus, thus including DM1 in the group of nucleotide repeat expansion disorders, right after fragile X syndrome and spinobulbar muscular atrophy discovered in the first 1990s. Since then, this family of diseases has been populated with more than 30 pathologies [1]. The common mechanism of pathogenesis is the expansion of tandem nucleotide repeats above a critical size, and this repeat extension can occur either in coding or non-coding regions of the gene. Depending on the context where the expansion occurs, the pathogenic mechanism will be either the accumulation of a mutated protein, or the suppression of gene expression caused by different molecular mechanisms, such as hypermethylation of the locus or production of aberrant mRNA that contains the repeats: this could compromise its own processing, or the maturation of other transcripts that share the same machinery for splicing or nuclear export [1, 2].

DM1 arises from a CTG repeat in the non-coding 3′UTR of *dmpk,* thus the repeat extension is transcribed into the mRNA but it is not translated into the protein. Myotonic dystrophy is the most frequent form of muscular dystrophy in the adult, with an incidence of 1 in 8000 individuals worldwide. It is inherited in an autosomal dominant way and disease severity generally correlates with repeat length. Affected individuals express heterogeneous and multisystemic symptoms with variable expressivity including myotonia (slow relaxation of the muscles after voluntary

contraction), progressive muscle weakness and wasting, defects in cardiac conduction, cataract development, cognitive impairment, hypogonadism and testicular atrophy [1, 2, 3]. In healthy individuals the repeat size ranges between 5 and 38 CTGs, whereas individuals with DM1 carry hundreds to thousands of repeats [2]. The progressive increase in the repeat number along the subsequent generations accounts for the anticipation phenomenon, *i.e.* the increased disease severity in the progeny of mildly affected individuals [3].

Molecular features of DM1

During the last two decades researchers have tried to reproduce DM1 features in mouse models, with the aim to investigate the molecular mechanisms that cause the multifaceted phenotype of DM1. Following these studies, three distinct molecular mechanisms have been proposed, which probably all contribute to different degrees in DM1 pathogenesis. It was observed that CTG repeats cause (*i*) a 50% reduction of DMPK protein levels, (*ii*) altered expression of the 5' flanking gene *Six5*, and (*iii*) nuclear accumulation of DMPK transcripts that sequester specific RNA binding proteins, thus altering the splicing of several DMPK unrelated genes [1, 2, 3]. The concurrent role played by these events in DMPK pathogenesis can be inferred by the following observations: (*i*) *dmpk* knock-out mice develop mild myopathy and cardiac abnormalities [4, 5, 6], (*ii*) knock-out mice for Six5 present cataracts [7] and (*iii*) mice expressing mRNA with CUG repeats manifest clinical myotonia and histological features of DM1 [8, 9, 10]. Molecular mechanisms other than DMPK haplo-insufficiency are not of primary interest for this thesis, and therefore will not be treated in further detail. However, it must be underlined here that, as molecular mechanisms different from a loss of DMPK activity recapitulate most of the DM1 features, research has not focused on the comprehension of the biological functions of DMPK, even if it is evident

that DMPK protein levels have an important role in muscle and heart physiology and pathology [3, 4, 5, 6].

Expression of the *dmpk* gene in skeletal muscle is driven by a low level promoter that operates in conjunction with an enhancer element containing conserved MyoD-responsive E-boxes [11]. DMPK expression is up-regulated in differentiating L6E9 and C2C12 muscle cells, through a canonical myogenic pathway (*i.e.* involving the PI3K, NF-κB, NOS, and p38 MAPK transduction pathways), supporting the idea that DMPK has a functional role in the generation and/or maintenance of skeletal muscle [12]. Mice lacking DMPK develop an adult-onset progressive myopathy, although the muscular phenotype of these mice is milder than that observed in DM1 patients [4]. However, the extrapolation of a skeletal muscle phenotype displayed by a mouse model to humans must be taken with caution, and the history of mouse models of human muscular dystrophies clearly shows that large discrepancy can be found between the two organisms. For instance, mutations that hamper collagen VI expression cause the Ullrich congenital muscular dystrophy (UCMD) in humans, a severe disease characterized by early onset symptoms and early adulthood lethality, whereas ablation of the entire gene in mice induces a mild dystrophic phenotype similar to the human Bethlem myopathy, in which collagen VI is mutated but partially expressed [13, 14].

Moreover, the cardiac phenotype of *dmpk*−/− mice reproduces different conduction defects observed in DM patients, including first-, second-, and third-degree atrioventricular block and abnormalities in intracellular Ca^{2+} cycling [5]. Heterozygous *dmpk*+/− mice develop first-degree heart block which is a conduction defect strikingly similar to that observed in DM1 patients [6]. This is remarkable, as cardiovascular disease, including progressive leftventricular dysfunction, ischemic heart disease, pulmonary embolism, or unexpected sudden death, is one of the most prevalent causes of death in DM1 patients [15].

Muscle is a key target tissue for insulin-dependent regulation of glucose metabolism, and *dmpk*−/− mice have higher levels of plasma insulin in confront to wild-type animals, in accord with

what is observed in DM1 patients [16]. Llagostera *et al.* [17] have shown that *dmpk−/−* mice exhibit decreased insulin sensitivity in cardiac and skeletal muscles, but normal insulin signaling in adipose tissue and liver, in which DMPK is not detected. Ablation of *dmpk* in muscle causes impairment of insulin-induced glucose uptake through inhibition of membrane translocation of the glucose transporter GLUT4, resulting in glucose intolerance and increased circulating insulin and lipid levels in fed *dmpk−/−* mice [17].

Phenotype	Pathomechanism	Model	Observations
Myopathy	DMPK dosage	$dmpk^{-/-}$ mice	Late-onset, progressive skeletal myopathy (fiber degeneration and fibrosis) Size changes in head and neck muscle fibres at older age.
		Transgenic murine line overexpressing hDMPK gene (Tg26-hDMPK)	Deficient exercise endurance, myotonic discharges, fiber degeneration
	RNA toxicity	Transgenic mice with expanded hDMPK 3'-UTR	Inhibition of myogenesis
		Inducible and skeletal muscle-specific expression of expanded CTGs	Severe muscle wasting.
		Disruption of the mouse Mbnl1 gene.	Myotonia at 6 weeks of age.
	Six5 deficiency	Mutant analysis of Six5 homologue in *Drosophila*.	Abnormal development of muscle.
Cardiac defects	DMPK dosage	$dmpk^{-/-}$ mice	Hypertrophic cardiomyopathy and enhanced neonatal mortality. First-, second-, and third-degree atrioventricular (A–V) block. Significantly prolonged PR and HV intervals. Enhanced basal contractility Impaired $Ca^{(2+)}$ uptake in SR, PLN is hypo-phosphorylated.
		Transgenic murine line overexpressing hDMPK gene (Tg26-hDMPK)	Cardiomyopathic remodeling
	RNA toxicity	Transgenic mice expressing the DMPK 3' UTR	Cardiac conduction abnormalities
	Six5 deficiency	$Six5^{+/-}$ mice	Cardiac conduction disease
Insulin Resistance	DMPK dosage	$dmpk^{-/-}$ mice	Muscle insulin resistance, abnormal glucose tolerance.
	RNA toxicity	siRNA for MBNL1 and MBNL2. Overexpression of CUG-BP	Abnormal insulin receptor (IR) splicing.
		Mice with human genomic DM1 region with expanded (>350 CTG) repeats.	Abnormal regulation of IR mRNA splicing in all the tissues investigated.
	Six5 deficiency	$Six5^{-/-}$ mice	Non-determined
Ocular alterations	DMPK dosage	Overexpression of DMPK in cultured lens epithelial cells.	Apoptotic-like blebbing of the plasma membrane and reorganization of the actin cytoskeleton.
	RNA toxicity	Disruption of the mouse Mbnl1 gene.	Ocular cataracts.
	Six5 deficiency	$Six5^{-/-}$ mice	Homozygous mutant mice developed lenticular opacities.
		$Six5^{+/-}$ mice	Cataracts. Rate and severity inversely related to Six5 dosage.
Ion channel gating	DMPK dosage	$dmpk^{-/-}$ mice	Altered intracellular calcium concentration Na^+ gating abnormality Non-inactivating Na^+ current
		Transgenic murine line overexpressing hDMPK gene (Tg26-hDMPK)	Myocardial intracellular calcium overload Reduced ClC-1 chloride channels in skeletal mucle sarcolemm
	RNA toxicity	Transgenic mice expressing the DMPK 3' UTR	Reduced ClC-1 protein expression
		HSA^{LR} transgenic mice (human skeletal actin mRNA with 250 CUG repeats inserted in the 3'UTR)	Loss of ClC-1 protein from the muscle surface membrane
	Six5 deficiency	$Six5^{+/-}$ mice	Normal Na^+ channel gating

Table 1. Synthesis of identified DM1 features in patients and observed phenotypes in mouse or cell models aimed to test the contribution of three proposed molecular mechanisms responsible for multisystemic DM1 clinical traits (adopted from [3]).

A comment must be done on data obtained from transgenic mice over-expressing the hDMPK gene. This transgenic murine model, named Tg26-hDMPK, carries approximately 25 extra copies of the intact hDMPK with non pathological repeat region $(CTG)_{11}$, and surprisingly it recapitulates various muscle traits of myotonic dystrophy [18]. It is therefore possible that the observed alterations were due to exaggerated DMPK expression, but they could also be caused by the introduction of supposedly non-toxic, but numerous, CUG binding sites in the expressed DMPK transcripts, thus mimicking the effect of expanded CUG triplet mRNA and its *trans* dysregulation of splicing [18].

DM1 and tumors

It is possible to envisage an association between DM1 and tumorigenesis. As discussed previously, instability of triplet repeats and altered levels of DMPK protein play a crucial role in tissue degeneration in DM1, and thus could potentially play a role in neoplastic transformation. Some of the hypothesized mechanisms include up-regulation of Wnt/β-catenin signaling pathway due to altered equilibrium of $CUG_{(n)}$ binding proteins and splicing factors [19], but could also be due to the DMPK function since the loss of one of the *Drosophila* homologous *lats/warts* leads to excessive growth and abnormalities of cell differentiation [20]. At present, few data are still available, but interesting correlations can be foreseen. A recent report [19] summarizes the association of DM1 and a high incidence of benign calcifying cutaneous tumors known as pilomatricomas, as well as other tumors. Pilomatricomas are rather rare, benign epithelial tumors that occur as solitary skin nodules measuring 0.5–6 cm. The prevalence of pilomatricomas in general population is unclear; however, one study showed that they represent one of every 500 specimens analyzed by dermatologists. In a study of 1,569 individuals with pilomatricomas, the

incidence of multiple pilomatricomas in the same individual was 3.5%. However, in the literature there are 35 published cases of DM1 patients with pilomatricomas, with multiple pilomatricomas present in 89% (31) of individuals. Beside pilomatricomas, a variety of benign and malignant neoplasms were described in 47 DM1 patients. Among these, thymoma was the most commonly reported tumor, followed by tumors of the parotid, parathyroid, and thyroid gland. Also multiple basal cell carcinomas, insulinomas, gastric cancer and pituitary tumors were reported. Since 2001 NIH keeps records of DM1 patients by asking them to complete a baseline medical history questionnaire at the time they enroll, and to provide annual health updates. A preliminary assessment of this National Registry revealed that 53 of the first 441 DM patients enrolled, reported having benign and/or malignant tumors. Unfortunately, these were all self-reported data lacking clinical or pathologic confirmation [19].

A very recent study of registered Swedish and Danish DM1 patients analyzed incidence of neoplastic malignancies compared to calculated incidence of overall population. The case study comprehended 1658 patients registered in the Swedish Hospital Discharge Register or Danish National Patient Registry between 1977 and 2008. One hundred four patients developed cancer during post-discharge follow-up which corresponds to an observed cancer rate of 73.4 per 10,000 person-years in the DM1 patient group *vs*. an expected rate of 36.9 per 10,000 person-years in the general Swedish and Danish populations combined. Significant excess risk of cancers of the endometrium, brain, ovary and colon was observed, and cancer risks were similar in both sexes after excluding genital organ tumors. This is the first report of such amplitude, both in the number of patients followed and also for the time span of the clinical follow-up, which clearly shows that genetic mechanisms underlying DM1 onset also double the risk of cancer development [21].

DMPK: structure and kinase activity

DMPK belongs to the AGC (protein kinase A, G and C) serine/threonine kinase family [22]. The most evolutionary conserved homologous are the p21-activated kinases MRCK, ROCK/rho-kinase/ROK, NDR1, warts/lats, and citron kinase [23]. At the mRNA level, it was shown that from a single gene locus at least six isoforms are transcribed by a combination of three different alternative splicing events (Figure 1). The six isoforms are present both in human and mouse, while in human an additional isoform was reported. All isoforms are composed by a N-terminal domain, a kinase domain and a coiled coil region, while the alternative splicing determines presence or absence of a penta-peptide VSGGG motif and the nature of the C terminal tail. Wansink *et al.* [23] showed that the internal VSGGG motif modulates DMPK auto-phosphorylation activity, while the C terminal tail of DMPK would define substrate specificity, as well as intracellular localization.

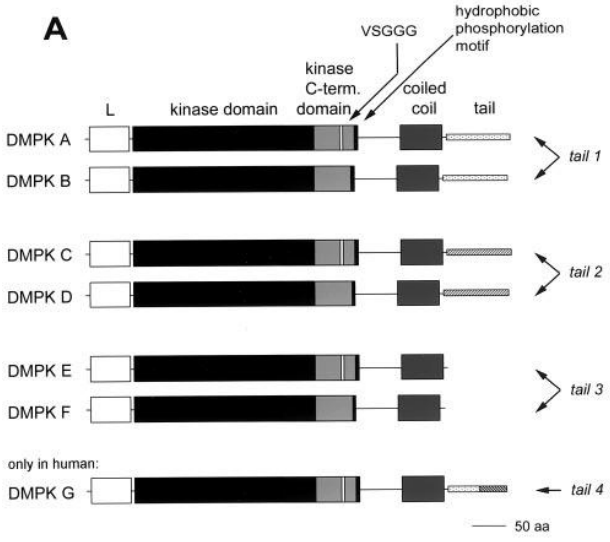

Figure 1. Structural organization of different DMPK isoforms. Combination of three alternative splicing events produces six major isoforms common to human and mouse. They differ for the presence of a VSGGG motif which regulates DMPK autophosphorylation activity, and for presence and length of a C-terminus tail. In humans, all isoforms bearing the hydrophobic C-terminal tail localize to the OMM, while short isoforms assume cytosolic localization (adapted from [23])

Comparison between the subcellular localization of individual DMPK isoforms of mouse and human indicated that orthologous splice isoforms behave differently. The four human DMPK

isoforms with the C terminus are all targeted to the outer mitochondrial membrane (OMM), while mouse orthologous isoforms A/B are targeted to the endoplasmic reticulum (ER), and C/D are targeted to the OMM [24]. The two remaining isoforms lacking a long C terminal tail adopt a cytosolic localization. DMPK displays a wide tissue distribution, but the various isoforms are differentially localized: short isoforms with the cytosolic localization were preferentially found in the smooth muscle, while long isoforms were found to be specific for skeletal muscle, heart and brain [25, 26].

In vitro phosphorylation study [23] of a library containing 35 peptides using an immunoprecipitated HA-tagged DMPK isoform E, has shown it to preferentially phosphorylate threonine residues surrounded by arginines and lysines. Derived consensus sequence for DMPK enzymatic activity was (R/K)XRRX(T/S)(L/V)X where X can be any aminoacid. Given the conservation of the kinase domain among all DMPK isoforms, this target sequence should be shared by all of them. However, in the same study it was shown with an *in vitro* phosphorylation assay that different DMPK isoforms have different trans-phosphorylation preference over a protein target (MYPT1), depending on the presence of VSVVG motif and the C terminal tail. The most active isoforms in phosphorylating the myosin phosphates target subunit 1 were the short cytosolic ones. This piece of data was interpreted as an auto-inhibitory propriety of the C-terminal tail, but it could also represent a specificity constraint which allows kinase activity only in the right sub-cellular compartment. Moreover, if we consider the distinct intracellular and tissue/cell type distribution of the different DMPK isoforms, it can be speculated that they could phosphorylate distinct panels of substrates *in vivo*.

Proposed DMPK interactors

Information on DMPK interacting partners is extremely scarce, and correlation of these data with the DMPK isoform specificity or sub-cellular localization is totally lacking. Interacting proteins were mostly searched in order to potentially explain some of the DM1 clinical features. What follows here is a brief summary of the proteins studied as possible DMPK partners and their possible role in determining pathological alterations found in DM1 patients.

Roberts *et al.* [27] reported a DMPK interaction with a RNA binding protein termed CUG-BP/hNab50, which is involved in various aspects of RNA processing and binds (CUG)n triplet repeats, the same triplet expanded in DM1. However, a detailed mechanistic explanation of the role played by the DMPK-CUG-BP/hNab50 interaction in DM1 pathogenesis is still missing [28].

Due to some observations on the function of Cl^- currents in healthy and myotonic muscle [29, 30], it was assumed that reduced Cl^- currents are responsible for myotonia. The over-expressing transgenic Tg26-hDMPK mice show reduced expression of the ClC-1 chloride channel in the sarcolemma of skeletal muscles [18], and the same Cl^- channel was shown to be mutated in *myotonia congenita* patients [30]. Phospholemman (PLM), a member of FXYD family of small ion transport regulators, inhibits the cardiac Na^+/Ca^{2+} exchanger (NCX1) when phosphorylated at Ser68 [31]. PLM is a membrane substrate for phosphorylation by protein kinases A and C, but it was also seen to be phosphorylated *in-vitro* by the short cytosolic isoform of DMPK [32]. Co-expression of DMPK with PLM in Xenopus oocytes reduced both Cl^- currents and expression of PLM in oocyte membranes. Lack of *in vivo* interaction and uncertainty about the mechanism by which DMPK would affect PLM expression or activity raises the doubt that PLM is a potential downstream effector of DMPK activity, rather than an interacting partner [32].

Myosin phosphatase target subunit 1 (MYPT1) is another possible DMPK interactor [33] that is involved in rearrangements of the actin cytoskeleton and of plasma membrane. The cytosolic

isoform of DMPK can phosphorylate MYPT1 in an *in vitro* phosphorylation assay [33]. It is however unclear what happens *in vivo*, since the DMPK and MYPT1 proteins are co-expressed only in brain and smooth muscle.

Pall *et al.* [34] observed an increase in basal contractility of single cardiomyocytes and an associated increase in cytosolic Ca^{2+} in *dmpk*-/- murine cardiomyocytes. This observation was correlated with an increased phosphorylation of the sarcoplasmic reticulum protein phospholamban (PLN), whose role is to modulate the activity of SR Ca^{2+} pump (SERCA2a). Active PLN is not phosphorylated and it inhibits SR Ca^{2+}-ATPase and Ca^{2+} uptake in SR, whereas phosphorylation of PLN abolishes this inhibition. However, the data presented in the manuscript do not show an increase in intensity of phospho-PLN band, but rather a mobility shift, not excluding the possibility of a different type of protein modification. Moreover, there is also a contrasting report on PLN phosphorylation status and SR Ca^{2+} uptake from *dmpk*−/− ventricular homogenates, where PLN phosphorylation was reduced and this correlated with decreased SR Ca^{2+} uptake [35]. This association was also confirmed by co-immunoprecipitation, and indirectly supported by a 2-fold decrease of Ser-16 PLN phosphorylation in *dmpk*-/- hearts [35].

As outlined above, the evidence of DMPK involvement in different signaling pathways is neither abundant nor sound, as some data is even contradicted in later reports. The search for putative mechanisms which would explain physiological features of myotonic dystrophy 1 often lacks a convincing mechanistic link between the observed molecular alteration and the downstream effect. Moreover, the role of DMPK in skeletal muscle or heart is extrapolated from data obtained on isoforms that are not typically found in the given tissue.

Other DMPK roles

As illustrated so far, the physiological role(s) of DMPK with regard on specific isoform and on the tissue or cell type where these are normally expressed is still somehow undefined. A small number of recent reports have added some information on roles of specific isoforms, and they will be critically described here.

Oude Ophuis *et al.* [36] reported on the effect of the mitochondria-anchored isoforms A and C. YFP-DMPK constructs were transiently expressed in different cultured cell lines, and their effect on mitochondrial distribution was followed by confocal immunofluorescence microscopy. An interesting observation from this manuscript was that the DMPK isoform A induced mitochondrial fragmentation and clustering in the perinuclear region. These morphological changes were also accompanied by mitochondrial membrane depolarization, increased autophagy activity, and release of cytochrome *c* from the mitochondrial intermembrane space. However, this effect on mitochondrial function and distribution was also obtained by the expression of YFP fused to the C terminus of hDMPK-A, strongly arguing for a consequence of membrane anchoring of the DMPK tail rather than for a function of the full-length protein. Moreover, in a previous work the same group had shown that the expression of the human isoform C also caused mitochondrial clustering, but to a lesser extent as compared to isoform A [24], and this observation was not reproduced in [36]. The particular nature of hDMPK-A C terminus and more importantly its dosage may account in an unpredictable degree for these phenomena.

The role of the short cytosolic DMPK isoform E was evaluated by Mulders *et al.* [37] in the context of proliferative and differentiating mouse myoblasts. This report emphasizes the dynamic regulation of the expression of different DMPK isoforms throughout myogenesis. YFP tagged DMPK isoform E was shown to induce alterations in actomyosin cytoskeleton by forming prominent stellar stress fibers after DMPK expression. Although the cytosolic isoform E is almost completely absent in differentiated myotubes, its expression is being progressively down-regulated

during differentiation of mouse myoblasts [25]. Introduction of mDMPK-E during this phase interferes with normal myotube formation by affecting cellular stress fibers organization, an observation which correlated with an increase in phosphorylation of regulatory myosin light chain 2 (MLC2). Thus, ectopic expression of cytosolic DMPK isoform E de-regulates actomyosin cytoskeleton organization and negatively influences myotube differentiation.

Intriguingly, a recent report from Harmon *et al.* [38] assigned to DMPK a critical role in maintaining the integrity of the nuclear envelope (NE). DMPK localization on the NE, rather than on endoplasmic/sarcoplasmic reticulum or mitochondria is unprecedented. Given references lack any evidence of DMPK localization on NE; in [35] a diffused perinuclear localization is observed when c-Myc tagged mDMPK-A is over-expressed (this could account for clustered mitochondria in perinuclear region as in [36]); while in [39] Harmon *et al.* comment on the distribution of DMPK, which can be seen throughout whole cell, exclusively as present on nuclear envelope/cell membrane.

From one side, the evidence present in the literature suggests a mitochondrial localization of high MW DMPK isoforms in cardiac and muscle tissue, without clarifying the functional role of the kinase for the organelle [23, 24, 25, 36]. On the other hand, the most affected tissues in mice lacking *dmpk* gene are muscle and heart, suggesting that absence of mitochondrial DMPK has indeed an important functional consequence on the maintenance and homeostasis of these tissues [4-6, 15-17]. Mitochondria participate actively in many crucial cell processes, and their correct function is critical from every aspect of cell existence. However, from this short overview of the literature, it results there is not a single association of mitochondria-anchored isoforms with the respective function of the organelle. Thus, in this study I evaluated (*i*) if mitochondria-anchored DMPK has any direct or indirect influence on mitochondrial function, (*ii*) and, if so, which are the underlying molecular mechanisms.

Mitochondria in physiology and pathology

In the last decades the mitochondrion has evolved in the scientist's view from a simple stand-alone power plant of the cell, to a complex organelle which interacts with the cellular environment in a multitude of ways. Apart from being the household of different metabolic and electrochemical processes such as oxidative phosphorylation, lipid metabolism, Ca^{2+} homeostasis, maintenance of mitochondrial membrane potential, mitochondria integrate their metabolic/electrochemical activities and connect them with the rest of the cell through dynamic cell signaling networks [40, 41]. For instance, mitochondria avidly take up Ca^{2+} from the cytosol due to their inside negative membrane potential, which in turn stimulates the activity of the electron transport chain and in the mean while this permits spatially and temporally delimited propagation of Ca^{2+} signaling waves in the surrounding cytoplasm [42]. If the matrix Ca^{2+} reaches a threshold concentration, opening of the inner membrane mega-channel called permeability transition pore (PTP) may occur, permitting the influx of ions and solutes along the gradient of osmotic pressure. This causes water entry and swelling of the IMM, with consequent rupture of the OMM, metabolic and bioenergetic failure and massive release of Ca^{2+} and of apoptogenic proteins. Signaling from the cytosol to mitochondria is influenced by multiple factors such as substrate availability, interactions with the cytoskeleton, post translational modifications, expression of nuclear genes targeted to mitochondria and modulation of their transcription level [43]. One of the factors that mediate the mitochondrion-to-cell cross-talk are reactive oxygen species (ROS). Low ROS levels can modify protein, lipid and nucleic acid function by direct oxidation, whereas higher ROS concentration elicits irreversible damage, leading to cell death [44]. For the purpose of this thesis I will cover mitochondria involvement in apoptosis and redox homeostasis, with a particular attention to the process of permeability transition and to organelle-restricted kinase signaling.

Mitochondria and cell death

Two intimately related and somehow redundant processes, termed apoptosis and necrosis, lead to cell death. Apoptotic or programmed cell death is characterized as an energy-dependent and highly regulated sequence of events which leads to an ordered disposal of the cell, avoiding the inflammatory perturbation of surrounding tissues by maintaining the plasma membrane integrity and prompting a removal of apoptotic cell bodies by phagocytosis [40]. Apoptosis is a highly conserved physiological process in metazoans and it maintains the organ and tissue homeostasis throughout cell proliferation and differentiation or by eliminating damaged, infected or neoplastic cells. On the other hand, necrotic cell death is typically referred to as a non-controlled pathological cell death which leads to an inflammatory response and is characterized by loss of plasma membrane integrity and random cleavage of DNA. However, apoptosis and necrosis are not two mutually excluding pathways: the type of cell engagement depends on the type, intensity and duration of the stimulus a cell is challenged with, and on the energy status of the cell, as ATP hydrolysis is required to carry out apoptosis [45]. Alterations in regulatory or executive components of the apoptotic machinery can lead to degenerative diseases like Parkinson, Alzheimer, AIDS and muscular dystrophies, which share an excess of apoptosis; alternatively, its suppression through mutations, altered expression levels or activity of regulators or executors of apoptosis is a step required for neoplastic transformation [40, 46].

Crucial component and obligatory participant in both apoptotic and necrotic cell death are mitochondria: both as a source of energy, whose availability determines the type of cell death, and as Pandora's boxes containing molecular promoters and executors of apoptosis. In order to trigger cell death, pro-apoptotic proteins such as cytochrome *c* (cyt*c*), which activates the executioner caspases by aggregating the apoptosome complex; AIF (Apoptosis Inducing Factor) and endonuclease G, which translocates into the nucleus and causes chromatin condensation and

fragmentation in a caspase-independent manner; HtrA2/Omi (high temperature requirement protein A2) and SMAC/Diablo (second mitochondria derived activator of caspase/direct IAP binding protein with low pI), which block the inhibitors of caspases (IAPs), must be liberated from the mitochondrial intermembrane or inter-cristae space following OMM permeabilization [40]. The OMM can be permeabilized by the action of pro-apoptotic members of the Bcl-2 family (like Bax and Bak) which would form oligomers with the function of a channel or by their interaction with pre-existing membrane channels such as VDAC, by altering its channel proprieties and allowing cyt*c* passage [47, 48]. Alternatively, OMM permeabilization could be a consequence of an increased permeability of the inner mitochondrial membrane (IMM), due to the opening of the PTP, a non-selective, high conductance channel, resulting in matrix swelling, cristae unfolding and subsequent rupture of OMM. Due to the undefined molecular nature of PTP, it is still debated whether the OMM permeabilization by Bcl-2 proteins and by PTP opening are two exclusive and separate mechanisms, or there is a certain degree of cooperativity [41].

Excess of cell death caused by mitochondrial dysfunction can be ameliorated by preventing PTP opening with cyclosporine A (CsA) in numerous human pathologies. The most important ones are ischemia-reperfusion (I/R) injury of the heart, ischemic and traumatic brain damage, muscular dystrophy caused by collagen VI deficiency (Bethlem myopathy and Ullrich congenital muscular dystrophy), amyotrophic lateral sclerosis, acetaminophen hepatotoxicity, hepato carcinogenesis by 2-acetylaminofluorene, and fulminant, death receptor-induced hepatitis [41].

Moreover, a list of human diseases caused by: (*i*) nuclear defects associated with mtDNA instability (either for mutations in mitochondrial DNA polymerase gamma or adenine nucleotide translocator 1), mtDNA maintenance (MPV17), synthesis of complex II assembly factors (SHDAF1 and SDHAF2), mutations affecting the mitochondrial fusion and fission system (mitofusin 2, optic atrophy 1, ganglioside-induced differentiation-associated protein 1) or (*ii*) due to mutations in mitochondria-encoded genes; represents a sum of very heterogeneous but not rare disorders, underlying the importance of proper mitochondrial function from every aspect of its being [49, 50].

The mitochondrial permeability transition pore (PTP)

The PTP is the mediator of the mitochondrial permeability transition (PT). PT consists in a sudden increase of IMM permeability to solutes smaller than 1500 Da induced by the opening of a high conductance, CsA sensitive, voltage and calcium-dependent channel termed PTP. Normally, the IMM is impermeable to solutes and ions, which are transported across the membrane in a strictly regulated manner in order to maintain the proton electrochemical potential difference (Δp) and its major component, the membrane potential difference ($\Delta\psi_m$, negative inside). The potential energy stored in the proton gradient across the IMM is responsible for the synthesis of 90% of the total cellular ATP by the F_0F_1 ATP synthase [42]. Prolonged PTP opening leads to mitochondrial depolarization, loss of pyridine nucleotides and inhibition of respiratory chain activity. These events are followed by a massive Ca^{2+} release and extensive swelling of mitochondria caused by osmotic equilibration of ions and solutes with molecular masses below the pore size: in its open state, the PTP has an apparent diameter of 3 nm and allows the flux of molecules up to 1.5 kDa. As a consequence, the unrestricted cristae unfolding causes breaks in the OMM and intermembrane pro-apoptotic proteins are released [41].

The molecular nature of the PTP is still missing, but its regulatory mechanisms are widely studied. PTP proneness to opening is modulated by a variety of physiological, pharmacological, ionic and protein regulators. Both components of Δp affect PTP opening: the optimum matrix pH for PTP opening is 7.4 while opening probability sharply decreases both by lowering matrix pH (through reversible protonation of histidyl residues) or by increasing it. A high inside negative membrane potential stabilizes PTP in closed conformation and a large number of pathophysiological effectors can move the threshold voltage at which opening occurs. PTP inducers move the threshold voltage closer to the resting potential, whereas PTP inhibitors move the threshold voltage for PTP opening away from the resting potential [51]. Sensing of the

transmembrane voltage is achieved through redox-sensitive sites: one is modulated by matrix PN, with oxidation promoting PTP opening; another by the GSH pool acting on proximal protein thiols [52], another redox-sensitive site is activated by the thiol oxidant copper-o-phenanthroline [53]. PTP regulation through the surface potential is indirectly supported by observations that amphipathic anions (i.e. arachidonic acid) facilitate the permeability transition, whereas polycations, amphipathic cations and positively charged peptides inhibit the pore [54]. These data imply that the effect of amphipathic compounds depends on their net charge which would affect the pore voltage sensor.

Free matrix Ca^{2+} is widely considered to be a key factor for regulation of the PTP open-closed transitions acting as an inducer of PTP opening in the case of Ca^{2+} overload or as a permissive factor for most pore inducers. Its activity can be competitively inhibited by other Me^{2+} ions, such as Mg^{2+}, Sr^{2+} and Mn^{2+} [51].

Different proteins are known to regulate the PTP. Some of these are components of signal transduction cascades, and will be discussed in the last paragraph. The OMM voltage-dependent anion channel (VDAC) had been regarded as a PTP component, given some striking similarities in its electrophysiological and regulatory proprieties [55].

Despite these similarities, Baines *et al.* showed that individual or double VDAC *knock-outs* are not components of PTP, since $VDAC1^{-/-}$, $VDAC3^{-/-}$ and VDAC1/VDAC3-null mitochondria exhibited oxidative stress and Ca^{2+}-induced PT indistinguishable from WT mitochondria [56]. The same was observed in fibroblasts isolated from the above-mentioned mice, and notably in $VDAC1/VDAC3^{-/-}$ fibroblasts where VDAC2 was silenced, thus formally ruling out a role of VDAC as a pore component [56].

Cyclophilin D (CyP-D), a mitochondrial matrix *cis-trans* peptidyl-prolyl isomerase, is so far the most relevant PTP modulator, both from the genetic and pharmacological point of view. CyP-D genetic ablation (the $Ppif^{-/-}$mice, [57]) or its inhibition with the drug CsA desensitizes PTP to opening by Ca^{2+} and oxidants, as seen in CyP-D-deficient MEFs and hepatocytes which are

significantly more resistant to necrosis induced by a Ca^{2+} ionophore (A23187) or by H_2O_2 [58, 59]. Also, cardiac ischemia/reperfusion injury causes less damage in *Ppif*$^{-/-}$ animals, similarly to what is observed following the treatment of wild-type animals with CsA. However, different cell types obtained from *Ppif*$^{-/-}$ mice normally undergo apoptosis in response to various stimuli, including etoposide, staurosporine, TNFα, and tBID or Bax caused cyt*c* release from isolated mitochondria [41]. These observations however cannot be used to rule out the involvement of PTP in apoptosis, but they can be used to rule out the regulatory function of CyP-D in apoptotic cell death (as discussed in [41]). The complexity of this molecular regulation is further highlighted by the work of Basso *et al.* [60], which recently showed that inorganic phosphate is essential for the inhibitory effect of CyP-D ablation or its inhibition with CsA. When P_i was replaced by vanadate, arsenate, or bicarbonate the inhibitory effects of CsA and of CyP-D ablation disappeared, whereas in the absence of phosphate, the pore sensitivity to Ca^{2+} and oxidative stress was identical in WT and *Ppif*−/− mitochondria. These data suggest that PTP is not inhibited directly by the ablation of CyP-D or by treatment with CsA, but rather the role of CyP-D is to mask an inhibitory site for Pi.

Another important observation is the recent finding that PT is an inner membrane event which occurs both in intact mitochondria as well as in digitonin-prepared mitoplasts [61]. Therefore, OMM proteins are not molecular constituents of the PTP, but its function can be regulated by a variety of OMM proteins like TSPO, hexokinase (HK) isoform II, VDAC1 and Bcl-2 family members (for a review see [41]).

Among these molecules, HK II seems to be particularly relevant for PTP modulation. The mammalian HK isoforms HK I and HK II catalyze the first reaction of glucose metabolism: they use ATP to convert glucose into glucose-6-phosphate (G-6-P), which is then processed either in glycolysis or in the pentose phosphate pathway (PPP). HK association with mitochondria and its dynamic movement between mitochondrial and cytosolic compartments is influenced by a variety of factors like levels of its end product glucose-6-phosphate, ATP, divalent cations, Pi and intracellular pH [62]. HKs can function as metabolic sensors: as HKs on the OMM selectively

utilize intramitochondrial ATP for glucose phosphorylation, they directly couple glycolysis to oxidative phosphorylation. HK II is particularly up-regulated in tumors that exhibit increased rates of aerobic glycolysis ("Warburg effect"), providing at the same time fast source of energy through glycolysis and both building blocks for biosynthetic pathways and anti-oxidant defenses through PPP [63]. Binding of HK II to mitochondria provides several kinetic benefits that facilitate the enzymatic reaction: (*i*) HK II binding affinity for ATP is enhanced approximately ~5-fold; (*ii*) it becomes insensitive to end-product (G-6-P) inhibition; (*iii*) and it gains preferential access to ATP generated in mitochondria [63]. HK II binding to mitochondria is prompted by activation of the protein kinase B/Akt signaling pathway which increases HK II binding to its proposed OMM binding target VDAC1. Both HK I and HK II anti-apoptotic activity was reported to be dependent

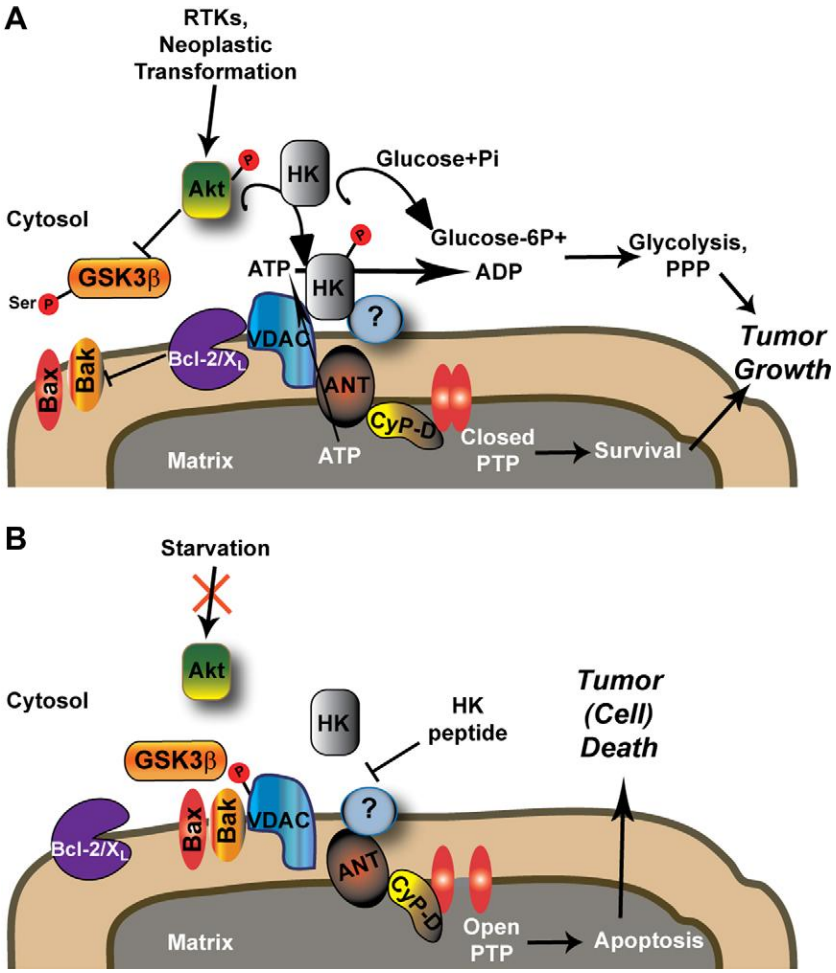

Figure 2. Mitochondrial hexokinase (HK) regulates PTP opening. (A) HK is bound to mitochondrial outer membrane through Akt activation by receptor tyrosine kinases (RTKs) or by neoplastic transformation. Akt can phosphorylate HK directly, or it can prevent VDAC1 phosphorylation by inhibiting GSK3 β, and thus favoring HK and Bcl-2/X_L association to VADC. HK utilizes the ATP synthesized by mitochondria to start glucose metabolism, and stabilizes the PTP in a closed state However, VDAC is dispensable for HK interaction with mitochondria, suggesting that

unidentified partner(s) are involved in this process. (B) Akt inactivation, or treatment with a HK peptide, induces HK detachment from the OMM leading to PTP opening and cell death. Notably, PTP opening induced by HK detachment from mitochondria does not require VDAC (adopted from [74]).

on the specific interactions with VDAC1 isoform, making unclear the role of VDACs in hexokinase-dependent modulation of cell death [64, 65]. However, most of these reports are based on the observation that HK interacts with purified VDAC channels reconstituted into the lipid bi-layers, and/or on the observations of the ability of HK to alter channel conductance and apoptosis induction in the presence of and mutated forms of VDAC [65, 66]. Several studies indicate that HK II must have additional binding partners on the mitochondrial surface. For instance, Chiara *et al.* [67] showed that HK II displacement from the OMM with a cell permeable synthetic peptide corresponding to the hydrophobic N-terminal portion of the enzyme occurred independently of VDAC presence. Notably, the same authors proposed that mitochondrial HK II enhanced resistance to apoptosis, as its detachment triggered cell death through PTP engagement. Also, a more recent study [68] used high resolution two color stimulated emission depletion (STED) microscopy, which enabled to determine the detailed sub-mitochondrial distribution of the three hVDAC isoforms and of HK I with a lateral resolution of ~40 nm. Surprisingly, HK I was seen to co-localize with hVDAC3 isoform, but not significantly with the two other VDAC isoforms. Moreover, rat brain HK binds to yeast mitochondria devoid of VDAC channels at lower affinity, but on many more sites per mitochondrion in confront to yeast mitochondria where human VDAC was expressed [69]. Also, the brain HK I isoenzyme was found to have two distinct binding sites on mitochondria, identified by the ability of the end product G-6-P to promote dissociation of HK I from the organelle. The G-6-P-insensitive pool of mitochondria-bound HK I varies according to species, and it is estimated to represent 10, 40, 60, and 80% for rat, rabbit, bovine and human brain mitochondria, respectively [70, 71].

On the other hand, HK II binding to mitochondria and its consequent anti-apoptotic effect was also interpreted as an antioxidant mechanism consisting in ADP/ATP recycling [72], and as a UCP-3-dependent modulation of mitochondrial ROS [73]. These aspects will be covered in further detail in the next chapter.

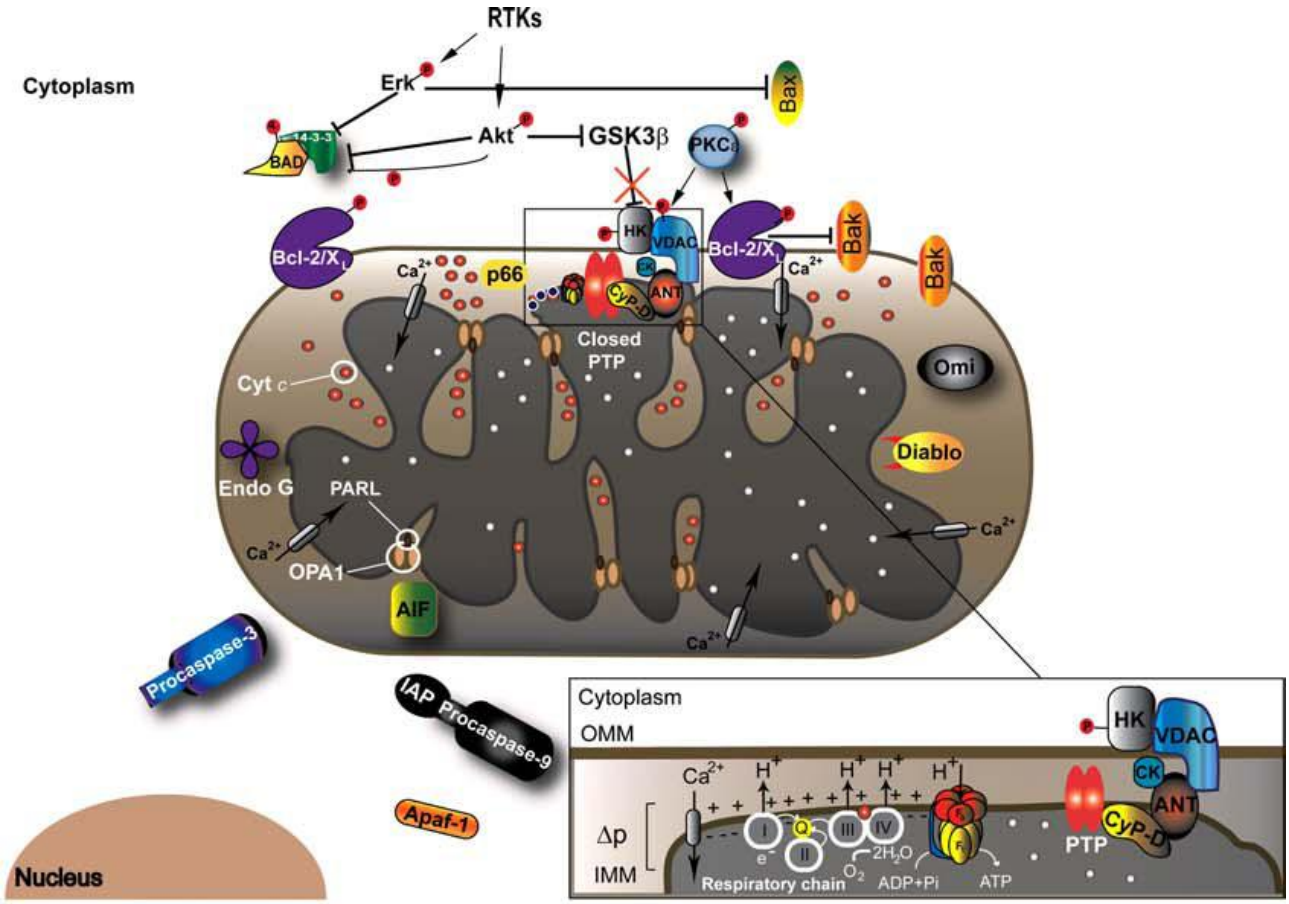

Figure 3. Overview of signaling axes and localization of proteins involved in determining cell faith. Signaling from receptor tyrosine kinases (RTKs) keeps pro-apoptotic Bcl-2 proteins in their inactive state through Erk and Akt (PKB) in healthy mitochondria. Physiological respiratory chain activity and low matrix calcium levels keep the PTP in its closed conformation, preventing OMM permeabilization and release of inter-membrane space pro-apoptotic proteins (adopted from [41]).

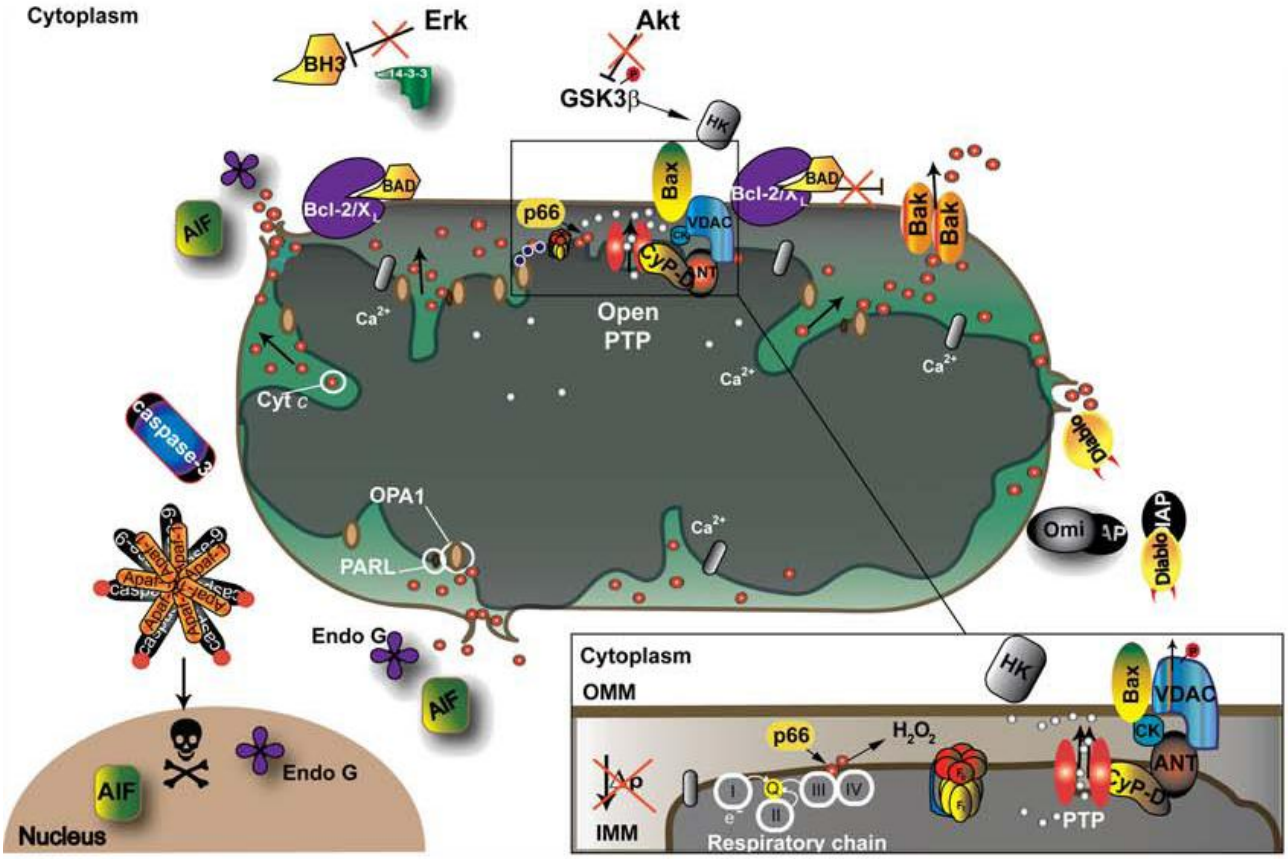

Figure 4. Release of apoptogenic proteins from IMS and subsequent induction of apoptosis. Bcl-2/X_L inactivation, Bax/Bak oligomerization, HK II detachment from OMM are some of the events that can lead to OMM permeability. Notably, activation of Bad constitutes a link between extrinsic, ligand-mediated, and intrinsic apoptotic pathway. Ca^{2+} overload, or increased ROS due to dysfunctional or dysregulated RC and/or due to other mitochondrial ROS producers, induces PTP opening, mitochondrial swelling and rupture of OMM with concomitant release of cyt *c* and other pro-apoptotic proteins to cytoplasm (adopted from [41]).

Mitochondria and ROS

If the only function of mitochondria were ATP production, then the undesirable by-product of the activity for its generation would be reactive oxygen and nitrogen species (ROS/RNS). However, this over-simplified clause becomes true only when levels of ROS/RNS exceed those present at the physiological levels, and when oxidative damage is infringed on DNA, lipids and proteins overwhelming cellular antioxidant defenses. From the idea that ROS generation is an inevitable consequence of oxidative ATP production, resulting in accumulation of unrepaired oxidative damage to macromolecules, the mitochondrial free radical theory of ageing was proposed

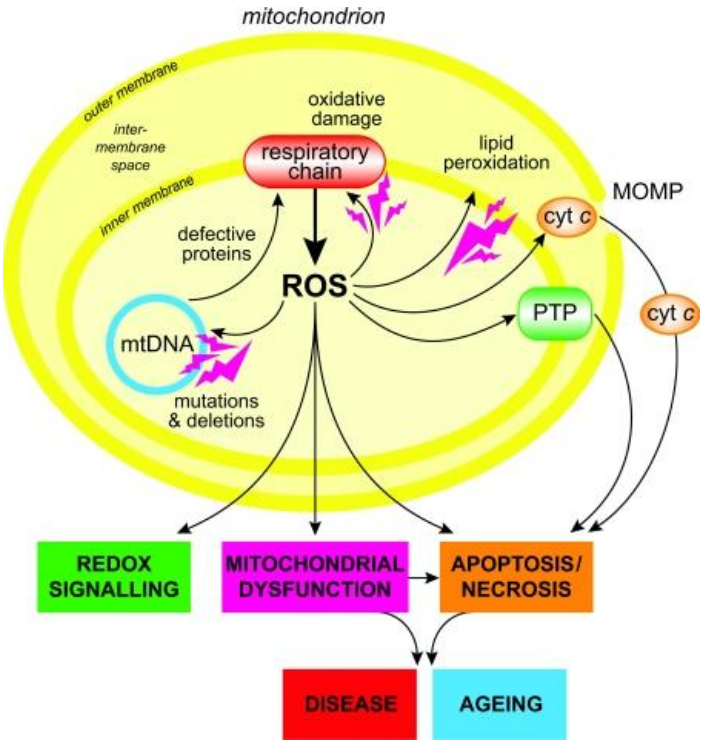

Figure 5. Mitochondria-produced ROS can lead to oxidative damage of mitochondrial proteins, membranes and DNA, thus resulting in the impairment of ATP synthesis and block of other metabolic functions i.e. tricarboxylic acid cycle, fatty acid oxidation, the urea cycle, amino acid metabolism, haem synthesis and FeS centre assembly. Oxidative stress can further induce cytochrome c release and trigger apoptotic cell death, either through induction of the mitochondrial permeability transition pore opening or through permeabilization of outer mitochondrial membrane. In addition, mitochondrial ROS may act as a modulatable redox signal, reversibly affecting the activity of a range of functions in the mitochondria, cytosol and nucleus (adopted from [44]).

by D. Harman in 1972 [75]. The progressive and cumulative feature of unrepaired cell damage

would therefore make a basis for aging and aging-related diseases such as neurodegeneration, cancer, atherosclerosis, inflammation and others. However, mitochondria-generated oxidative stress is not the only cause of ageing in mammals, but it is an important stressor in ageing-related diseases and some pathological conditions i.e. ischemia-reperfusion injury [76].

Inside the cell, ROS homeostasis is maintained by the counteracting role of detoxifying mechanisms and antioxidant systems, comprised of enzymes and reducing molecules. A persistent and overwhelming increase in ROS levels, or a dysfunction in detoxifying and antioxidant systems, lead to the condition of oxidative stress and uncontrolled oxidation, where the rates of ROS production exceed rates of their metabolism [44, 76]. Superoxide anion, which can be formed by the leakage of electrons from the respiratory chain or by NAPDH oxidases, is promptly converted into hydrogen peroxide by a rapid enzymatic reaction performed by Cu/Zn superoxide dismutase (SOD) in the cytoplasm or by MnSOD in the mitochondrial matrix [76]. Mice lacking mitochondrial superoxide scavenging enzyme MnSOD have the life-span of only 10–20 days even in the presence of antioxidants [77, 78], while cytoslic Cu/ZnSOD knock-out is not lethal [79], showing that extra-mitochondrial superoxide is less toxic.

H_2O_2 acts in concert with thiol redox systems such as glutathione and thioredoxin, where glutathione pool constitutes the largest antioxidant defense of the cell and its concentrations are as high as 5mM in the liver [80]. The active cysteine residue of this tripeptide acts as a proton donor and enables direct scavenging of a wide variety of reactive species such as superoxide anion ($O_2^{\bullet -}$), hydroxyl radical ($OH^{\bullet -}$), singlet oxygen ($^1O^2$), protein and DNA radicals, and peroxides such as hydroperoxides (H_2O_2), peroxynitrite ($OONO^-$), and lipid peroxides ($LOO^{\bullet}$). Generally, around 90% or more of total GSH is present in its reduced form, which after being synthesized in cytoplasm is transported into other cell organelles like mitochondria, peroxisomes, nuclear matrix, and the endoplasmic reticulum (ER) [80].

Cellular ROS sources are primarily mitochondria, followed by non-mitochondrial ROS producers cytochrome P-450 enzymes found in ER, peroxisomes and NADPH oxidases [76]. The

contribution of mitochondria to total ROS levels of the cell depends on their quantity and metabolic activity, being dependent on the cell or tissue type. Seven separate sites of superoxide production have been currently identified in mammalian mitochondria: site IQ and site IF on respiratory chain (RC) complex I, site $IIIQ_o$ on RC complex III, pyruvate dehydrogenase, glycerol 3-phosphate dehydrogenase, electron transferring flavoproteinQ oxidoreductase (ETFQOR) and 2-oxoglutarate dehydrogenase [76]. The sites with the greatest capacities to produce ROS are at complex I (site IQ) and complex III (site IIIQo), but which of the specific sites of mitochondrial ROS production is most active in cells in the absence of inhibitors of the electron transport chain is unclear. Other sites like glycerol 3-phosphate dehydrogenase can have significant maximum rates in specific conditions [81].

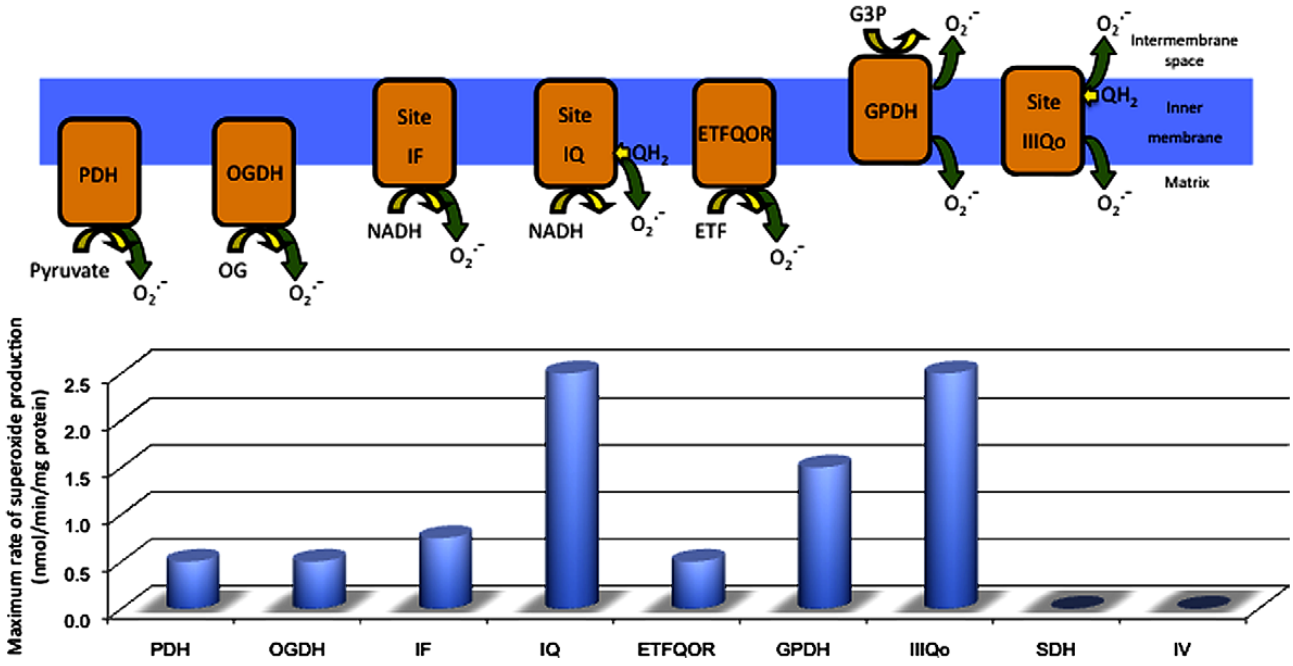

Figure 6. Seven identified sites of superoxide production in mitochondria and topology of the anion source. The sites and the topology of their superoxide production are shown in the upper diagram, while in the lower panel representative values of the maximum superoxide production rate from each site, and from SDH (succinate dehydrogenase; complex II) and complex IV are shown. PDH, pyruvate dehydrogenase; OGDH, 2-oxoglutarate dehydrogenase; site IF, the FMN-containing NADH binding site of complex I; site IQ, ubiquinone reduction site of complex I; ETFQOR, electron transferring flavoprotein ubiquinone

oxidoreductase; GPDH, glycerol 3-phosphate dehydrogenase; site IIIQo, the outer quinone-binding site of the Q-cycle in complex III. Shown values are for rat skeletal muscle mitochondria (adopted from [76]).

Complex I can produce superoxide at high rates during reverse electron transport from succinate to NAD+, although the physiological relevance is unclear [82]. During physiological forward electron transport from NAD-linked substrates, most mitochondria produce superoxide at very low rates (less than 0.1%) which become high after addition of inhibitors such as rotenone (for complex I) or antimycin A (for complex III) [44].

Maintenance of efficient aerobic metabolism by high NAD^+/NADH ratio and the provision of ADP and Pi are important controllers of mitochondrial ROS production. Mild uncoupling of oxidative phosphorylation by uncoupling proteins (UCPs) has also been suggested to limit mitochondrial ROS production by decreasing $\Delta\psi_m$. Chemical uncouplers such as FCCP and dinitrophenol, and the over-expression of UCPs, have been shown in *in vitro* systems to decrease mitochondrial ROS emission [83].

Maillou*xet. al.* [73] recently showed that UCP3 is required to maintain high rates of aerobic metabolism in cells grown in high-glucose and in muscle of fed mice. Knocking-out or inhibiting UCP3 resulted in a slight but significant metabolic shift toward glycolytic metabolism, increased glucose uptake and increased sensitivity to oxidative challenge. In $UCP3^{-/-}$ cells or following UCP3 inhibition a diminished HK II association with OMM was observed.

Da-Silva *et al.* [72] showed that mitochondrial biding of HK I in isolated rat brain mitochondria diminishes rates of H_2O_2 formation upon adding ADP and glucose, whereas H_2O_2 production was not altered by ADP and glucose in HK-depleted mitochondria. However, physiological relevance of ROS produced by isolated mitochondria fuelled on succinate, which favors reverse electron transport and high rates of superoxide at complex I, is not clear. Despite this

fact, it is undeniable that mitochondrial association of HK modulates ROS levels, although the exact molecular mechanisms are unknown.

Low levels of intracellular ROS are emerging as an important intracellular signaling system, which could also transmit information from mitochondria to the nucleus and vice versa [44]. Above a certain threshold, however, ROS are involved in a variety of pathological conditions. The mitochondrial free radical theory of ageing, proposed by D. Harman in 1972 [75], accumulation of unrepaired oxidative damage to macromolecules, postulates that a progressive and cumulative unrepaired oxidative cell damage would make a basis for aging and aging-related diseases such as neurodegeneration, atherosclerosis, inflammation and ischemia-reperfusion injury [76].

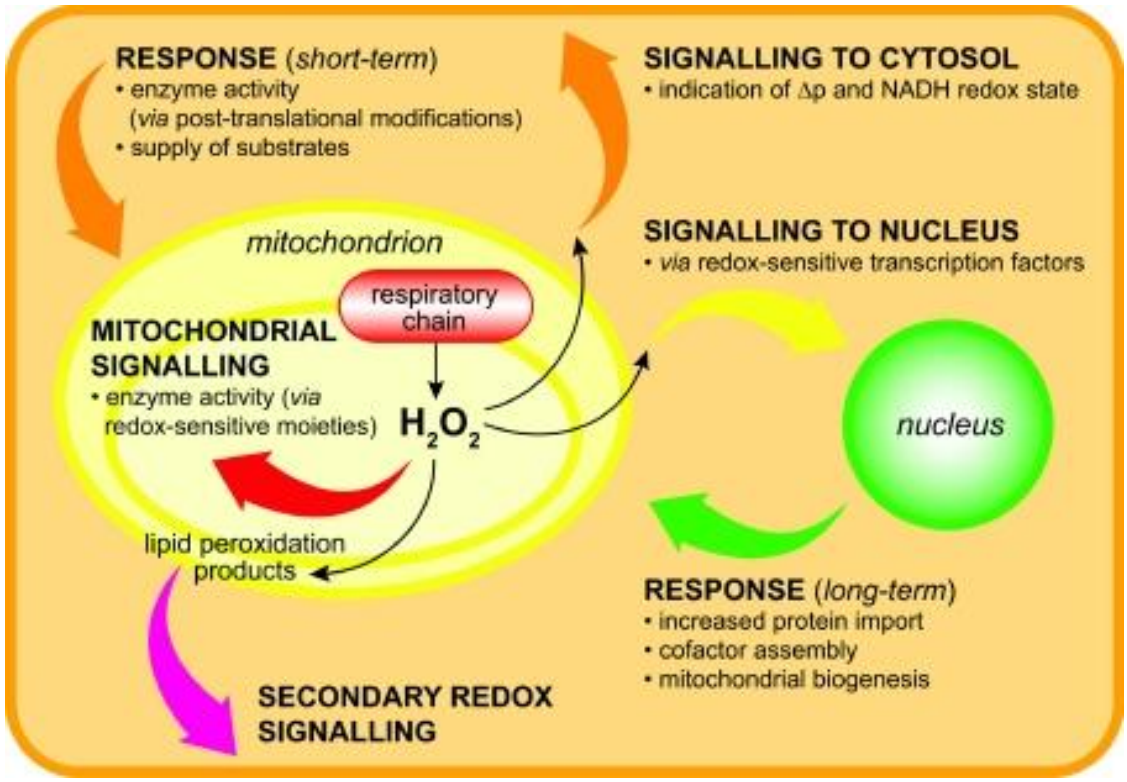

Figure 7. Mitochondrial ROS as signaling mechanism. Mitochondria-generated ROS, and especially the defusable end-product of superoxide dismutation H_2O_2, can reversibly alter the activity of proteins by originating intra- or inter-protein disulfides and glutathionylated proteins by reacting with GSH and critical protein thiols. This can occur with mitochondrial, cytosolic or nuclear enzymes, carriers or transcription factors, transiently altering their activities, which can be restored by reducing the modified protein thiol by

endogenous thiol reductants such as GSH or thioredoxin. Since the rates of H_2O_2 production in mitochondria depend on Δp or the redox state of the NADH pool, ROS can act as a retrograde signal to the rest of the cell, reporting on mitochondrial status. Short-term consequences may consist in modification of substrates supply to the mitochondria, or, in a long run, may consist in modifying redox-sensitive transcription factors that adjust the production of mitochondrial components. External signals may modify $O_2^{\bullet-}$ production from the respiratory chain by post-translational modification. Lipid peroxidation products may act as secondary redox signals (adopted from [44]).

Mitochondria and signaling

Kinase signalling is crucial in the transmission of signals from the environment to the cell interior, and among different cellular compartments. In recent years, it is becoming increasingly clear that reversible phosphorylation events have an important role in shaping mitochondrial functions, such as fusion, fission, apoptosis and metabolism and in connecting it with the rest of the cell [84].

Growing evidence from literature shows that both protein kinases and phosphatases are present both in mitochondrial intermembrane space and in matrix. However, it remains unknown how these enzymes can cross the mitochondrial membranes as very often they lack an obvious mitochondrial targeting sequence. In this sense, a recent breakthrough has been made by identifying cytosolic endopeptidases which process typically non-mitochondrial proteins and unmask a cryptic mitochondrial targeting sequence [85]; similar mechanisms of mitochondrial targeting could work for kinases and phosphatases.

Intracellular scaffolds for signalling molecules such as PKA anchoring proteins (AKAPs; REF), and RICKs and RACKs, receptors for inactive/active PKC, respectively [86] are found on the

external face of the outer mitochondrial membrane (OMM). PKA associated to mitochondria through AKAP binding mediates the pro-survival effect of IL-3 by phosphorylating and inhibiting the pro-apoptotic protein BAD, but also acutely accelerates the transport of cholesterol into mitochondria, a rate limiting step in steroidogenesis [87, 88]. Dynamin-related protein 1 (Drp1), a high molecular weight GTPase that participates in mitochondrial fission and cell death [89, 90], is also a substrate for mitochondria-tethered PKA.

Other kinases like Raf kinases, ERKs and several isoforms of PKC have been shown to undergo translocation to mitochondria. C-Raf is recruited to mitochondria by its interaction with Bcl-2 and Bag-1 (Bcl-2-binding protein), where it sustains a pro-survival function by eliciting phosphorylation of BAD [91].

Different isoforms of PKC, like PKCα, PKCδ and PKCε have been observed on the OMM. However, reports on effects of PKCδ and PKCε on the regulation of mitochondria-dependent cell death show that these two kinases affect mitochondria in substantially different fashion and this probably depends on the particular cell type or stimulus used. Activated PKCδ was seen to translocate onto mitochondria in several cell models and in different pro-apoptotic settings, where it triggered IMM depolarization, release of cyt*c* and the subsequent apoptosis induction [92]. PKCε received considerable interest as a participant in ischemia/reperfusion injury and ischemic preconditioning, where its mitochondrial translocation confers protection against I/R damage, while the preconditioning benefits are abolished by interfering with PKCε docking on mitochondria [93].

Proteomic studies supply growing evidence about the existence of mitochondrial phospho-proteins. Zhao *et al.* [94] revealed the presence of 155 distinct phosphorylation sites, present in 77 different proteins in mitochondria isolated from resting human muscle biopsies. Most of these phosphorylations were on serine residues (116), but they also identified phosphothreonine (23) and phosphotyrosine (16) residues; phosphorylated proteins were involved in oxidative phosphorylation, Kreb's cycle, lipid metabolism, amino acid degradation, calcium homeostasis, apoptosis and in membrane transport. Deng *et al.* [95] analyzed the phosphoproteome of

mitochondria from murine cardiomyocytes, finding a total of 236 phosphorylation sites mapped to 181 phospho-proteins. These proteomic studies underline the importance of phosphorylative regulation of electron transport chain (ETC) machinery, whose fine tuning, or alternatively dysfunction, determine mitochondrial and cellular fitness through ROS production, and supply of ATP, metabolites and reducing equivalents.

Phosphorylation axes that impinge on PTP regulation have also been described by our laboratory [96]. In this work, fractions of ERK2 and GSK3β were both observed inside mitochondria, and an ERK2/GSK3β pathway regulated an unprecedented Ser/Thr phosphorylation of CyP-D in different cancer cell lines. GSK3β-dependent phosphorylation of CyP-D resulted in increased probability of PTP opening.

In cells, tyrosine phosphorylation is promoted by receptor and non-receptor tyrosine kinases (TK). 58 out of 90 unique tyrosine kinase genes identified in the human genome encode receptor tyrosine kinase proteins, while other form a soluble cytosolic pool of non-receptor TKs [84]. TKs bind extracellular growth factors, cytokines, and hormones and control critical processes, such as proliferation and differentiation, cell survival and metabolism, cell migration and cell-cycle progression [84]. TKs were shown not only to be key regulators of normal cellular processes, but also to have a critical role in the development and progression of many types of cancer. The bulk of phosphorylation characterized in the mitochondrial IMS appears to be on tyrosine residues. In fact, tyrosine kinase activity was observed over 20 years ago in mitochondrial compartments [97]. Specifically, in the presence of exogenous ATP and tyrosine phosphatase inhibitor sodium peroxyvanadate, brain mitochondria undergo extensive tyrosine phosphorylation. Different labs have observed the tyrosine phosphatases Shp-2 and PTP1B, in either the inter-membrane space or in both matrix and IMM [86]. IMM is a target for tyrosine phosphorylation of proteins involved in bioenergetics, such as subunit I of RC complex IV and creatine kinase, and apoptosis (cyt*c* and adenine nucleotide translocase 1, ANT1). Salvi *et al.* has found members of the Src family tyrosine kinases, c-Src and Fyn, to be bound on both membranes in the IMS [98] and the observation of c-

Src association to brain mitochondria was subsequently confirmed by others, in brain [99] and in heart [95] mitochondria. The presence of c-Src within or associated with mitochondria provides a link between kinase and redox signaling since different studies have reported on ROS-dependent activation of c-Src through oxidation of Cys^{245} in its SH2 domain and of Cys^{487} in its catalytic domain [100, 101]. Hypoxia-induced increase in mitochondrial ROS resulted in redox activation of c-Src through cysteines 245 and 487 followed by the activation of the NF-κB pro-survival pathway, whose activation was insufficient for cell survival if ROS were further increased [100]. Giannoni *et al.* [101] showed that the oxidative activation of c-Src through these same cysteine residues occurs during cell adhesion and anchorage-dependent cell growth. Moreover, oxidant-insensitive mutants of Src C245A and C487A showed a greatly decreased invasiveness, serum-independent and anchorage-independent growth, and tumor onset, underlying the importance of Src redox regulation in tumorigenesis [101].

Type	Enzyme	Submitochondrial localization
Nonreceptor Tyr kinase	Abl	NR
	Src	Intermembrane space and membrane facing it
		Outer membrane
Receptor Tyr kinase	EGFR	Inner membrane
Dual-specificity phosphatase	TIM50	Inner membrane
	MAPK phosphatase I (MKP-1)	NR
Tyr phosphatase	Shp-2	Intermembrane space
	PTP-D1	Cytosolic surface of outer membrane

Table 2. Some of the tyrosine kinases and phosphatases involved in mitochondrial tyrosine phosphorylation, with their observed sub-mitochondrial localization. With respect to other subcellular compartments these kinases and phosphatases are present in mitochondria at low amounts and they generally lack canonical mitochondrial targeting sequences (adopted from [102]).

Materials and Methods

Cells

Human osteosarcoma (SAOS-2) cells were purchased from ATCC, and human rhabdomyosarcoma cells (RD) were a kind gift of Dr. L. Vergani (Department of Neurosciences, University of Padua, Italy). Cells were grown in Dulbecco's modified Eagle's medium (DMEM) supplemented with 10% fetal bovine serum (Invitrogen), 100 units/ml penicillin and 100 μg/ml streptomycin, in a humidified atmosphere of 5% of CO_2 at 37°C. DMPK was stably expressed in SAOS-2 cells by sub-cloning DMPK cDNA (NM_004409.3, Origene) into the pcDNA3.1(+) vector (Invitrogen) and selecting the cells with 150μg/ml of zeocin (Invivogen) for two weeks. Endogenous DMPK was silenced in RD cells by the use of short hairpin RNA sequences present in pLKO.1-PURO vector (Sigma) and selected with 1 μg/ml of puromycin for two weeks. Serum and glucose depletion was performed for the indicated times after washing the cells twice in PBS and by adding DMEM without serum and glucose (Sigma, 5030) supplemented with 4 mM L-glutamine, 1 mM sodium pyruvate, 44 mM sodium bicarbonate and 10 mM HEPES.

Cell transfection with calcium phosphate

In order to perform transfections, cells were grown in standard medium in 25 cm^2 flasks (BD Falcon). While still non-confluent, cells were treated with DNA-calcium-phosphate (Ca-Pi) co-precipitates as described in [103] for 4 h at 5% of CO_2 and 37°C. 10% glycerol solution in phosphate buffered saline was then added for 1 minute to enhance the expression of transfected DNA. After 48 h

antibiotics for selection were added to medium and maintained to obtain a mixed culture of stably transfected cells.

Cell lysates

Prior to lysis cells were washed in PBS solution (140 mM NaCl, 2.7 mM KCl, 10.1 mM Na_2PO_4, 1.8 mM KH_2PO_4) and detached from flasks with the use of trypsin 0.05% (Invitrogen) at 37°C. After centrifugation at 900 *rcf* for 5 minutes cells were resuspended at 4°C in lysis buffer (140 mM NaCl, 20 mM Tris-HCl pH 7.4, 5 mM EDTA, 10% glycerol, 1% Triton X-100 in the presence of phosphatase and protease inhibitors, Sigma). After 30 minutes on ice, lysates were cleared through a centrifugation at 13000 *rcf* for 25' minutes at 4°C. Supernatants were collected and stored at -80°C. If the lysates were required for the analysis of protein phosphorylation states the cells were washed in PBS at 4°C and detached on ice with the cell scraper (BD Falcon) in the presence of lysis buffer.

Isolation of mitochondria

Mitochondria were isolated from cells through differential centrifugations. To obtain mitochondria, cells were homogenized with an electrical potter (Sigma) in a buffer composed by 250 mM sucrose, 10 mM Tris-HCl, 0.1 mM EGTA-Tris, phosphatase and protease inhibitors (Sigma), pH 7.4. Large cell residues such as nuclei and plasma membrane fractions were separated by two mild centrifugations (700 *rcf,* 10 min), and mitochondria were then spun down at a higher speed (7000 *rcf,* 10 min) and washed twice (7000 rcf, 10 min). When mitochondria were isolated for the analysis of protein phosphorylation states the cells were washed in PBS at 4°C and detached on ice with the use of a cell scraper (BD Falcon) in the presence of ice-cold PBS. All procedures were carried out at 0–4°C.

The protease digestion of isolated mitochondria was performed on 50 μg of mitochondria, with trypsin ranging from 0,5 to 20 μg per sample, at 4°C for 1h. Where indicated, 0.1% SDS was added before trypsin. After trypsin inactivation, mitochondria were spun (18000*rcf*, 10 min, 4°C) and lysed.

Protein quantification

Total protein content was quantified using the BCA Protein Assay Kit (Thermo Scientific-Pierce). The BCA Protein Assay is based on two main reactions: first, the reduction of Cu^{2+} to Cu^{+} by cysteine, cystine, tryptophan, tyrosine residues and peptide bonds in an alkaline medium. Second, the reduced cuprous cation (Cu^{+}) is chelated by two molecules of bicinchoninic acid (BCA). The water-soluble BCA/copper complex exhibits a strong linear absorbance at 562 nm in the protein concentration range starting from 0,5 μg/mL to 1,5 mg/mL. BSA (Sigma) was used as a standard. Absorbance was read on a BioPhotometer plus spectrophotometer (Eppendorf).

SDS-PAGE and Western immunoblotting

Cell extracts were prepared at 4°C in lysis buffer supplemented with protease and phosphatase inhibitors. Samples were then denatured in loading buffer (SDS 10%, TRIS 250 mM pH 6.8, glycerol 50%, β-mercaptoethanol 12,5%, brome phenol blue 0.02%), separated in reducing conditions on SDS-polyacrylamide gels (8-12 % acrylamide for running gels, 4% for stacking gels) and transferred onto nitrocellulose Hybond-C Extra membranes (Amersham) or PVDF 0,22 μm membranes (Millipore). Molecular standards used for electrophoreses were SeeBlue® Plus2 Pre-Stained Standard (Invitrogen) and Precision plus prestained protein standard (Biorad).

Primary antibodies were incubated overnight at 4°C with gentle shaking in 5% milk solubilized in TBS TWEEN 0.1%, or in TBS TWEEN 0.1% alone. Horseradish peroxidase-conjugated secondary

antibodies (1:10000, GE Healthcare) were incubated for 1 hour at room temperature in 5% milk with TBS TWEEN 0,1%. Proteins were visualized by enhanced chemiluminescence reaction (Millipore and Euroclone) using Amersham Hyperfilm ECL autradiography film (GE Healthcare) and developed by Amersham Biosciences Hyperprocessor (Amersham).

Co-immunoprecipitation assays

Co-immunoprecipitations were performed using 1-2 mg of total cellular lysate. Extracts were pre-cleared with sepharose A or G (Sigma) for 1 h at 4°C in agitation. After this phase, lysates were centrifuged at 7000 *rcf* for 1 minute and separated from sepharose. Cleared lysates were supplemented with fresh sepharose conjugated with the antibody against the protein of interest (conjugation was done on ice using 30 μl of packed Sepharose and 2 μg of antibody per mg of total protein) and incubated overnight at 4°C with gentle shaking. Lysates were centrifuged at 7000 *rcf* for 1 minute and supernatants were collected and stored at -80°C. The precipitated sepharose was gently washed three times in lysis buffer and denatured at 100°C for 5 minutes in loading buffer 2x and loaded on SDS PAGE gel.

Fluorescence microscopy

Mitochondrial membrane potential was measured by following the accumulation of tetramethyl rhodamine methyl ester (TMRM) in non-quenching mode. Cells were seeded onto 24-mm-diameter round glass coverslips and grown for 24 hours in 10% FBS DMEM. The loading of the cell-permeable potentiometric probes in cell, and therefore in mitochondria, is affected by the activity of the plasma membrane multidrug resistance pump (MDR), which is inhibited by cyclosporin A (CsA). Inhibition of

the MDR causes an increase in fluorescence signal due to higher cytosolic concentration of the probe. In order to prevent this artifact, all experiments where CsA was used to inhibit the permeability transition pore (PTP), an analog (cyclosporin H, CsH) that inhibits the multidrug resistance pump but not the cyclophilin-D was used in all other samples to normalize the conditions of probe accumulation. Cells were washed once and then incubated in serum-free DMEM supplemented with 1.6 µM CsA or CsH and 10 nM TMRM for 30 minutes. At the end of each experiment, mitochondria were depolarized by the addition of 4 µM of the protonophore carbonyl cyanide p-trifluoromethoxyphenylhydrazone (FCCP). Images were acquired with an Olympus IX71/IX51 inverted microscope (Center Valley,PA). Fluorescence was detected by using 568 nm band-pass excitation and 585 nm long-pass emission filter setting. Data were acquired and analyzed with CellR software (Olympus). Clusters of several mitochondria (5-10) were identified as regions of interest, and normalized for background fluorescence. Sequential digital images were acquired every minute, and the average fluorescence intensity of all relevant regions was recorded and stored for subsequent analysis.

ATP determination

Total cell ATP levels were measured by using the ATP Determination Kit (Molecular Probes) following the producer's instructions. Briefly, 10^5 cells were seeded in 12 well plates 24 h prior to incubation in different media. Cells were washed twice in PBS, and incubated with the inhibitors oligomycin 6 µM (last 45 minutes), 2-deoxyglucose 25 mM (8 h), in complete or serum and glucose free medium for 8 h. Cells were then washed, lysed and protein content determined as described previously. ATP was measured by recording the luminescence produced by luciferase according to the following reaction:

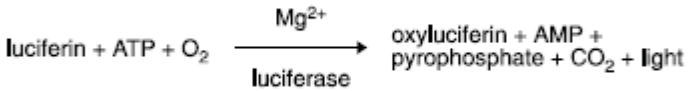

Bioluminescence of 100 μl reactions was recorded with Fluoroskan Ascent FL instrument (Thermo) and normalized to the amount of protein.

Flow cytometry analysis of mitochondrial depolarization, mitochondrial superoxide, cell death and mitochondrial mass

Flow cytometry recordings were performed as described [104]. Measurements of mitochondrial membrane potential and mitochondrial superoxide were performed by pre-incubating the adherent cells with 10 nM TMRM or 1 μM Mitosox, respectively, for 30 minutes prior to the detachment (for long term serum and glucose depletion) or treatment with diamide. Analysis of cell death and mitochondrial mass was done by incubating the cells with the fluorophores after having them detached with trypsin. Briefly, detection of phosphatidyl serine exposure on the cell surface (increased FITC-conjugated Annexin-V staining) and loss of plasma membrane integrity (propidium iodide, PI permeability and staining) was done by incubating the cells with FITC-conjugated Annexin-V (Roche) and 1 μg/ml of PI in 135 mM NaCl, 10 mM HEPES, 5 mM $CaCl_2$ buffer for 15 minutes in gentle shaking at 37°C. Mitochondrial mass was assessed by incubating an equal number of cells in the basic buffer supplemented with 20 μM N-acridine orange, which binds mitochondrial cardiolipin, for 15 minutes in gentle shaking at 37°C. At the end of the incubation, cells were diluted in additional 200 μl of basic buffer and analyzed on a FACS Canto II flow cytometer (Becton Dickinson). Data acquisition and analysis were performed using FACS Diva software.

Analysis of the oxygen consumption rate (OCR) of cell monolayers

These experiments were performed with an Extracellular Flux Analyzer XF-24 (Seahorse Bioscience). $3x10^4$ cells per well were plated the day before the experiment in a 24 well plate in complete DMEM. Prior to experiment, medium was changed to Running DMEM (4 mM glutamine, 1 mM sodium pyruvate, no serum, sodium bicarbonate or HEPES), with or without 25 mM glucose. Cells were pre-incubated in running DMEM for 1 h at 37°C without CO_2. The instrument measures the oxygen consumption rate (OCR) and the extracellular acidification rate (ECAR) using fluorophores contained in a sensor cartridge that is hydrated for 24 h at 37°C without CO_2. Compounds can be added to each well in four sequential injections. We measured the basal OCR, the fraction of the respiration used to produce ATP (oligomycin sensitive), the maximal respiration (FCCP), and the mitochondria-independent OCR (rotenone and antimycin insensitive).

Assay of thioredoxin reductase and glutathione reductase activities

$3x10^5$ cells were plated in 6-wells plate and grown in complete or serum and glucose free medium for 8 h. After incubation, cells were harvested and washed with PBS. Each sample was lysed with a modified RIPA buffer: 150 mM NaCl, 50 mM Tris-HCl, 1 mM EDTA, 0.1% SDS, 0.5% DOC, 1% Triton X100, 1 mM NaF, and an antiprotease cocktail (Roche) containing 0.1 mM PMSF. After 40 minutes of incubation at 0°C, lysates were centrifuged at 14,000 *rcf* for 5 minutes. The obtained supernatants were tested for enzyme activities. Aliquots (200 µg) of lysates were subjected to thioredoxin reductase determination in a final volume of 500 µl of 0.2 M Na^+K^+ phosphate buffer (pH 7.4) with 5 mM EDTA, containing 1 mM DTNB. After 2 minutes the reaction was started with 0.25

mM NADPH. Glutathione reductase activity was estimated at 25°C on 200 µg protein/ml in 0.1 M Tris/HCl buffer (pH 8.1) containing 0.2 mM NADPH. Reactions were started by the addition of 1 mM GSSG and followed spectrophotometrically at 340 nm.

Determination of glutathione concentration and redox state

$3x10^5$ cells were plated in 6-wells plate and grown in complete or serum and glucose free medium for 8h. After incubation, medium was rapidly removed and cells were washed with PBS and then deproteinized in each well with 2.5 ml of 6% meta-phosphoric acid and scraped. After 10 minutes at 4°, the deproteinized samples were centrifuged and the supernatant was neutralized with 15% of Na_3PO_4. Aliquots of neutralized samples were tested for total glutathione [105] and 300 µL were derivatized with 6 µl of 2-vinylpyridine to remove the reduced glutathione in order to determine the oxidized glutathione [106]. In addition, pellets obtained after deproteinization were washed with 1 ml of ice-cold acetone, centrifuged at 11,000 *rcf*, dried and then dissolved in 62.5 mM Tris-HCl buffer (pH 8.1) containing 1 % SDS and utilized for protein determination.

Results

1. Identification of cell models for the study of DMPK

In order to study the biological function(s) of DMPK, we chose to both re-express the mitochondria-anchored isoform A [24] in a cell model which does not present detectable levels of endogenous protein, and to knock-down DMPK expression in cells which normally express it at physiological levels. In this manner we obtained both a gain- and a loss-of-function model.

From the initial screening of DMPK expression levels in different cell lines, we chose SAOS-2 cells as a model for DMPK re-expression and rhabdomyosarcoma cells for silencing endogenous DMPK (Fig.1.1). Additional criteria were also ease of transfection, proliferation rates and tissue of origin, since DMPK protein reduction affects skeletal muscle and cardiac tissues [4-6].

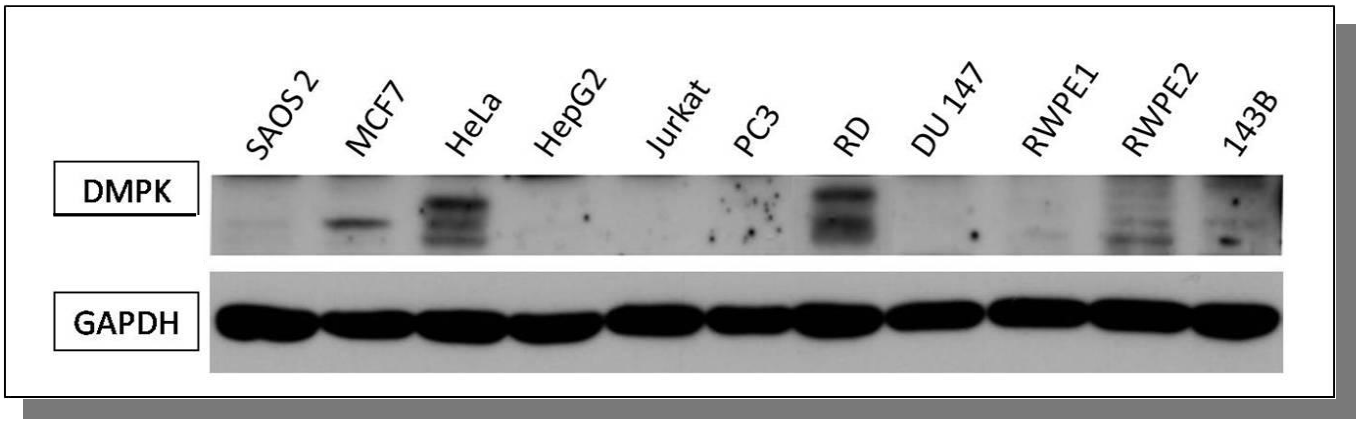

Figure 1.1. DMPK protein levels in different human cell lines. Osteosarcoma cells (SAOS-2) were chosen for re-expression of human DMPK isoform A and rhabdomyosarcoma cells of muscle origin for silencing of the endogenous protein.

Re-expression of DMPK-A in SAOS-2 cells was performed by calcium phosphate transfection method as described in Materials and Methods. The selected cells (SAOS-2 DMPK) were amplified as a bulk culture and kept in a medium supplemented with 50 µg/ml of zeocin (Figure 1.2).

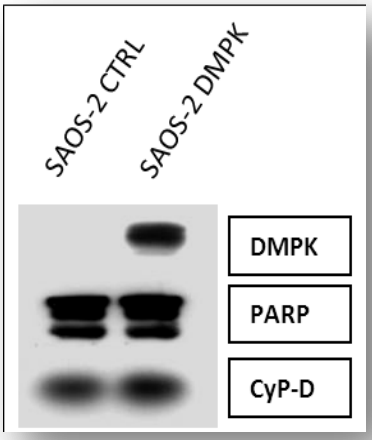

Figure 1.2. DMPK protein levels in stably expressing SAOS-2 cells. 50 µg of total cell lysate were loaded on SDS gel. Nuclear enzyme PARP and mitochondrial protein cyclophilin D were used as loading controls.

It was reported [23, 24] that human DMPK isoform A can anchor on the outer mitochondrial membrane (OMM) by its C-terminal hydrophobic tail. Therefore, as a first step I evaluated which amount of the re-expressed protein was located in the mitochondrial fraction. As shown in Figure 1.3, after separating the mitochondrial and cytosolic fractions of SAOS-2 cells I found that DMPK is almost exclusively found in the mitochondria-enriched fraction. Densitometric analysis showed that in equal amount of mitochondria and cytosol the DMPK is distributed for 98,5% in the first and for 1,5% in the second fraction respectively. After correcting for the total amount of mitochondrial and cytosolic protein obtained from the sub-fractionation, we obtain that at least 85% of total re-expressed DMPK protein is associated to the mitochondrial fraction. This percentage is most likely even higher since cytosolic proteins diffuse more easily from disrupted cells, while only a fraction of mitochondria are actually extracted.

I then investigated in which submitochondrial fraction the re-expressed DMPK is found. To this purpose, I performed a partial protease digestion of isolated mitochondria in order to follow the progressive disappearance of the external (peripheral) mitochondrial proteins and then of the proteins of internal mitochondrial compartments by increasing trypsin concentration.

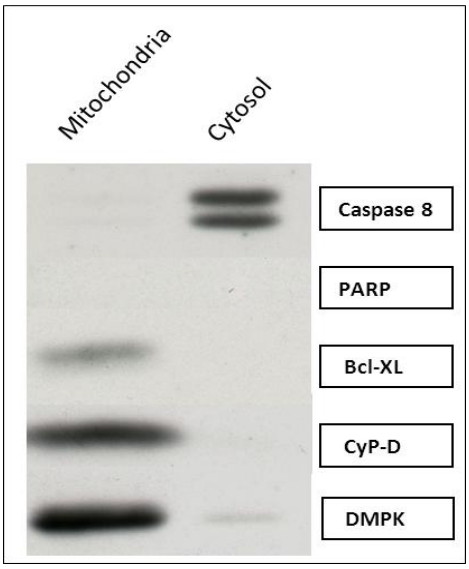

Figure 1.3. Sub-cellular fractionation of SAOS-2 cells shows the expected mitochondrial localization of re-expressed DMPK isoform A. Inactive caspase 8 (55/50 kDa) was used as a cytosolic marker, PARP as a marker of nuclear integrity, and Bcl-X_L and CyP-D as mitochondrial markers.

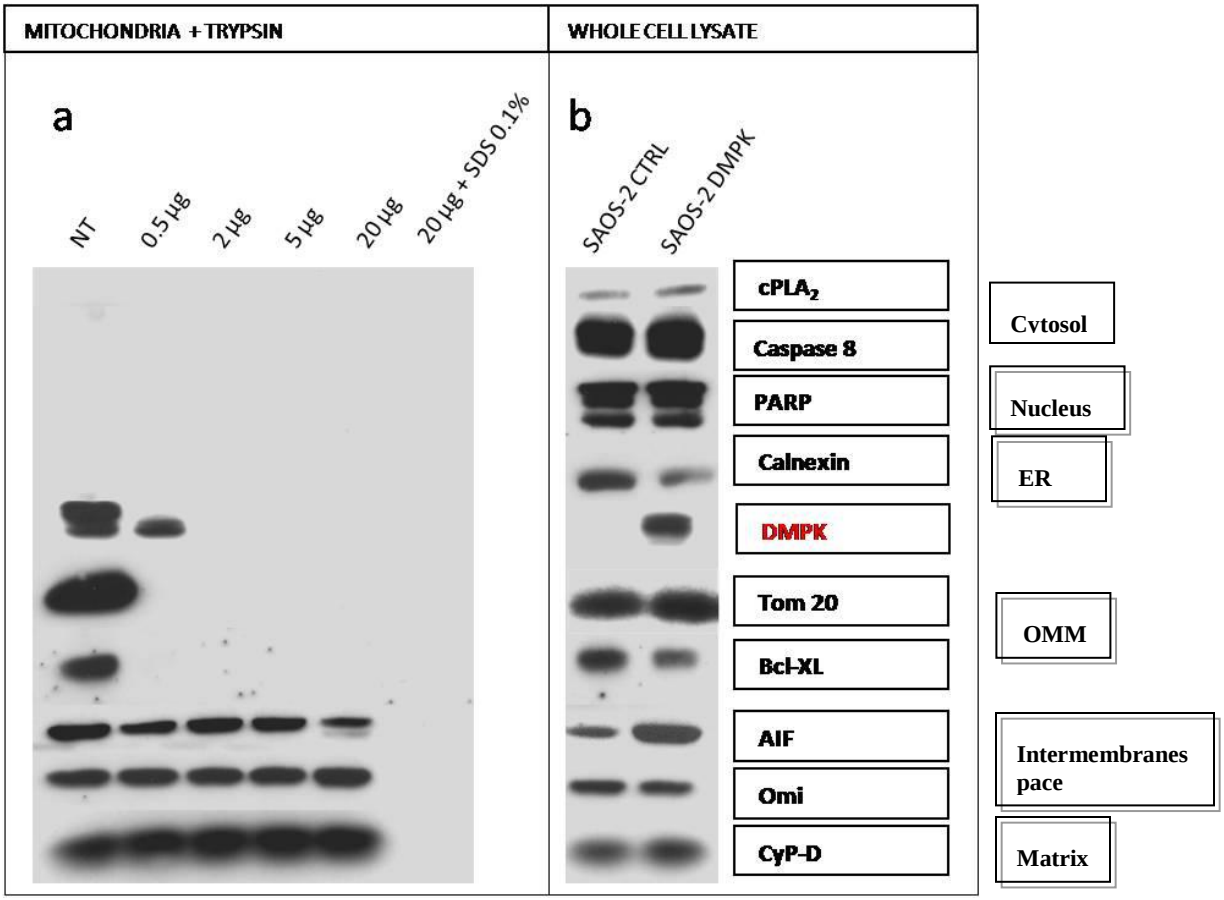

Figure 1.4. Partial protease digestion of mitochondria isolated from SAOS-2 cells. 50 µg of mitochondria were incubated with indicated amounts of trypsin for 1 h on ice, blocked with protease inhibitor and then lysed (NT - not treated). Where indicated, SDS was added in order to completely solubilize mitochondrial membranes.

As shown in Figure 1.4 a substantial part of DMPK is digested at the lowest trypsin concentration of 0,5 µg, such as the outer mitochondrial membrane proteins Tom20 and Bcl-X_L; and DMPK becomes completely degraded at 2 µg of trypsin. Notably, the intermembrane space proteins AIF and Omi are not affected by much higher trypsin amounts, confirming that re-expressed DMPK isoform A is anchored on the OMM facing cytoplasm.

Silencing of endogenous DMPK protein in rhabdomyosarcoma cells was achieved by stably transfecting the cells with shRNA containing constructs (Sigma). The obtained bulk culture showed a reduction in total DMPK protein of more than 50% as illustrated in Figure 1.5.

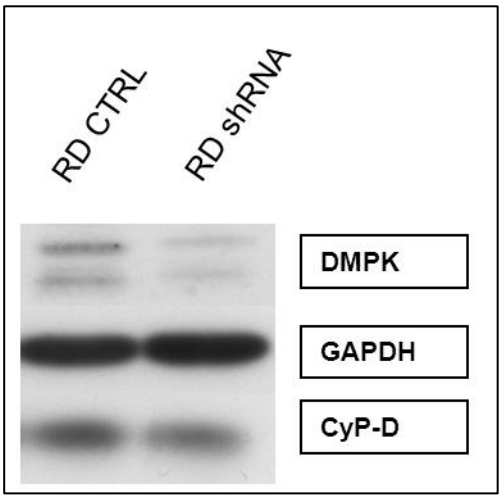

Figure 1.5. Levels of endogenous DMPK protein in human rhabdomyosarcoma control cells and in cells transfected with short hairpin RNA against DMPK coding sequence. Cytosolic protein GAPDH and mitochondrial cyclophilin D were used as loading controls.

More importantly, the fraction of DMPK associated with mitochondria in rhabdomyosarcoma cells is completely silenced (Figure 5.2), which makes this cell model an inverse mirror of the gain-of-function SAOS-2 DMPK cells.

The obtained cell lines were used to assess the role of DMPK in modulating mitochondria-related biological processes such as cell death, metabolism and redox state of the cell.

2. DMPK expression does not affect mitochondrial membrane potential or mitochondrial mass

It has been recently reported that transient over-expression of DMPK isoform A causes spontaneous fragmentation and perinuclear clustering of mitochondria, with mitochondrial depolarization, release of cytochrome *c* and apoptotic cell death [25]. These effects were not due to the DMPK kinase activity, but rather to the insertion of the C-terminal tail into the OMM, and were observed only in a fraction of DMPK-expressing cells, indicating that these observations may be due to non-physiological levels of the expressed protein. In order to verify if DMPK re-expression in SAOS-2 cells could have similar effects on mitochondrial distribution and membrane potential, I compared the mitochondrial membrane potential between DMPK-expressing and control cells. By a fluorescence microscopy inspection of cells loaded with the potentiometric dye TMRM, no DMPK-dependent alteration in the overall distribution of mitochondria was found (Fig. 2.1).

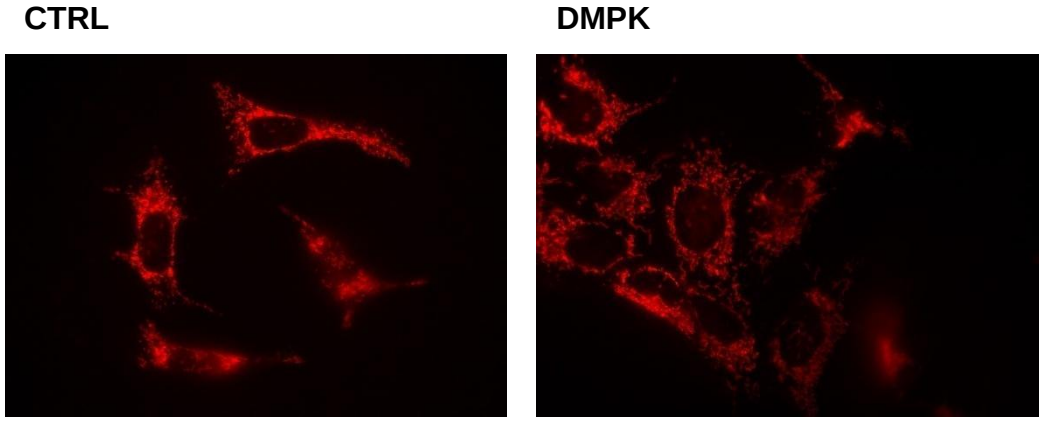

Figure 2.1. Representative images of control and DMPK-expressing SAOS-2 cells loaded with the potentiometric probe TMRM.

Moreover, the analysis of mitochondria-containing regions of interest (ROI) showed that there are no significant differences in mitochondrial membrane potential ($\Delta\psi_m$) between control and DMPK expressing cells (Figure 2.2).

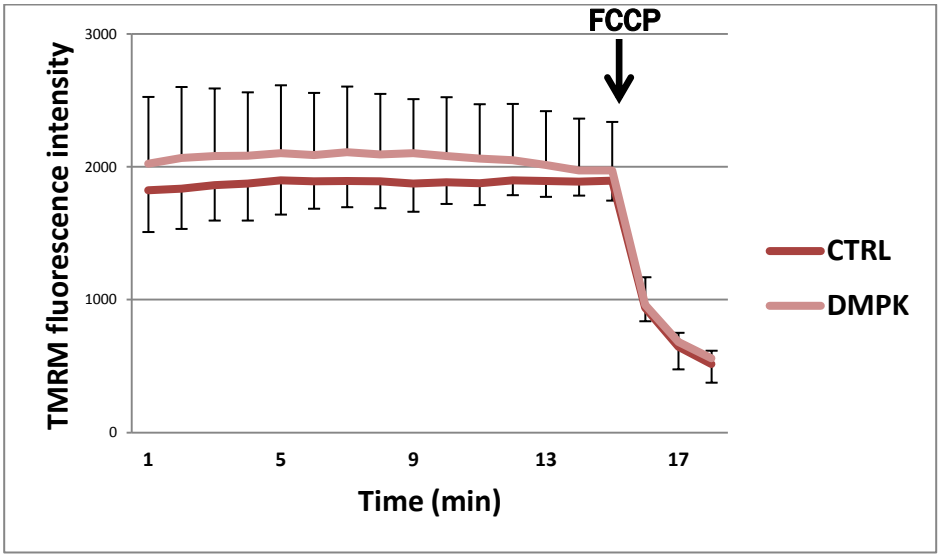

Figure 2.2. Quantitative analysis of mitochondria loaded with TMRM. The mean TMRM fluorescence intensity is not altered by DMPK expression in SAOS-2 cells.

In order to evaluate the same parameter on a much wider scale, a flow cytometry analysis was performed on populations of 10^4 cells loaded with the same fluorescent probe. This assay confirmed that no difference in mitochondrial membrane potential is triggered by DMPK (Fig. 2.3). Since the instrument measures the fluorescence intensity of the whole cell, I confirmed this result by using a buffer based on K^+ as the main cation, in order to depolarize the plasma membrane and to eliminate any eventual probe fluorescence of cytosolic origin. Again, no difference in mitochondrial potential could be appreciated between the two cell types.

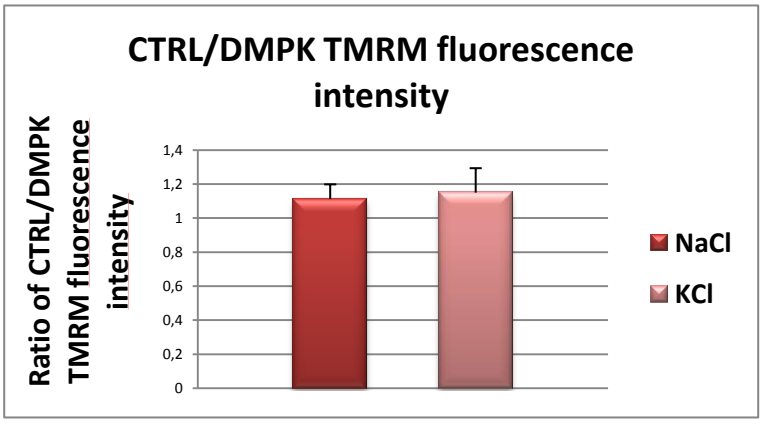

Figure 2.3. Flow cytometry analysis of mitochondrial membrane potential. The result is shown as the ratio of control versus DMPK expressing cells fluorescence intensity.

In order to be confident that there are no major alterations in mitochondrial homeostasis, a control of mitochondrial mass was performed. Cells were incubated with the fluorescent probe N-acridine orange (NAO), which binds mitochondrial fatty acid cardiolipin. Although NAO enters mitochondria following the membrane potential gradient (negative inside), we can use it to evaluate mitochondrial mass indirectly since the DMPK expression did not alter the $\Delta\psi_m$. As shown in Figure 2.4, I found that cells maintain the same NAO fluorescence intensity following DMPK expression, indicating that there are no changes, at least in un stimulated conditions, in the homeostasis of mitochondrial mass.

Taken together, these results indicate that no gross change in mitochondrial function, biosynthesis or degradation are elicited by DMPK expression in the SAOS-2 cell model.

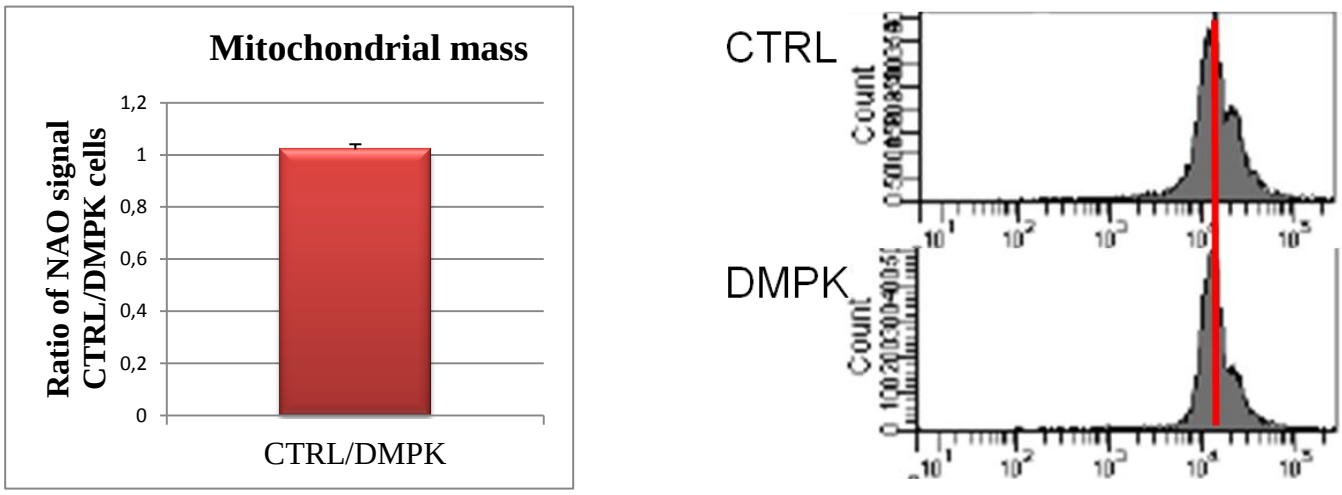

Figure 2.4. Flow cytometry analysis of N-acridine orange signal indicative of mitochondrial mass. The result is shown as the ratio of fluorescence intensity between control and DMPK-expressing cells. On the right, two representative histograms of fluorescence distribution are shown.

3. DMPK and stress

DMPK expression in SAOS-2 cells did not have any dramatic effect in basal conditions, but the possibility existed that it could affect the mitochondrial response to stressing conditions. Therefore I exposed cells to a pro-oxidant challenge, a typical stress affecting mitochondria. Surprisingly, the presence of DMPK markedly diminished the extent of mitochondrial depolarization caused by the pro-oxidant compound diamide (Figure 3.1).

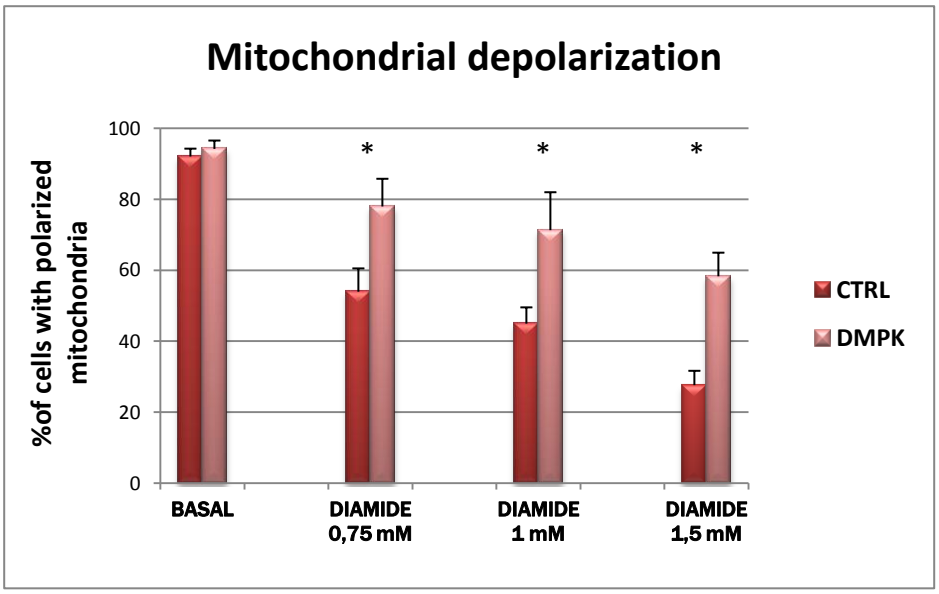

Figure 3.1. DMPK expression protects from diamide-induced mitochondrial depolarization. Bars represent the percentages of cells with polarized mitochondria (*p<0,05).

Notably, DMPK expression alters the mitochondrial redox status both in basal conditions and after the diamide treatment, diminishing the superoxide levels in all conditions (Fig. 3.2).

This piece of data was considered a proof of concept of an anti-oxidant function of DMPK. As a further step, I decided to investigate the molecular mechanisms through which DMPK regulates the levels of mitochondrial reactive oxygen species (ROS). A more physiological stimulus which would affect the mitochondrial sources of ROS was required, in order to assess whether its effect on mitochondria could be influenced by the DMPK. A serious of different metabolically stressful

conditions (e.g. prolonged serum, glucose or serum and glucose starvation conditions) were tested by analyzing both cell death and mitochondrial superoxide levels.

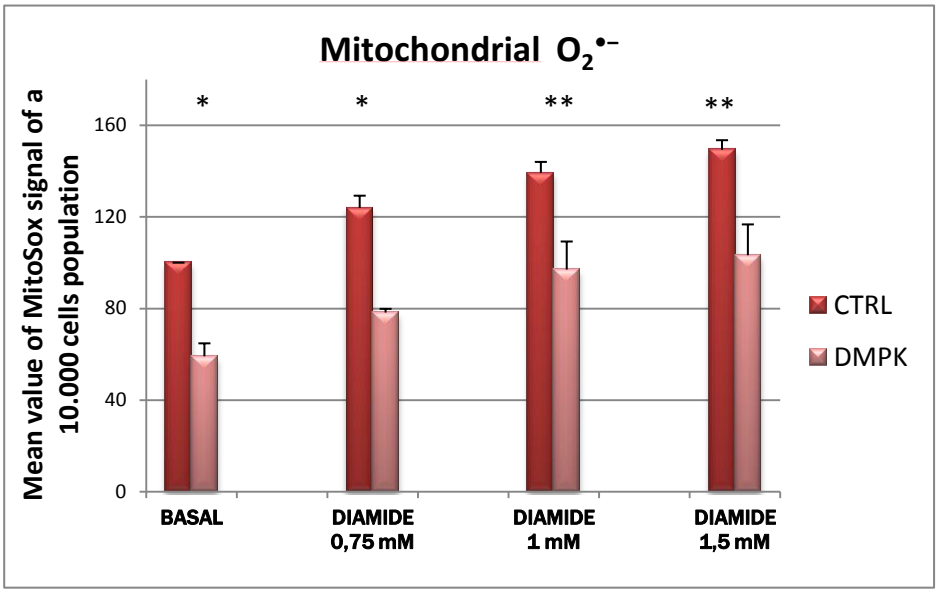

Figure 3.2. Flow cytometry analysis of mitochondrial superoxide levels in SAOS-2 cells after diamide treatment. Values were arbitrarily normalized to the basal condition of control cells, which was made equal to 100 (*p<0,01: ** p<0,05).

I found that a prolonged (24 h) serum and glucose depletion caused a marked reduction in the percentage of viable SAOS-2 control cells. This percentage was doubled by the expression of DMPK, whereas the antioxidant N-acetyl cystein (NAC) almost completely prevented the noxious effect of starvation, indicating that a ROS increase is the most probable cause of cell death (Figure 3.3).

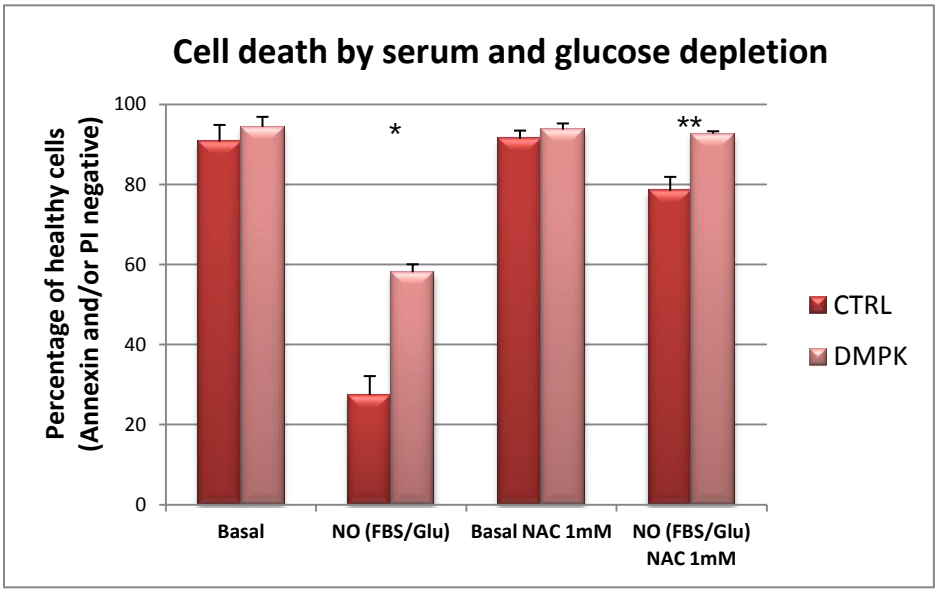

Figure 3.3. Cytofluorimetric analysis of cell death (24 h serum and glucose starvation) in SAOS-2 cells. Bars represent the percentage of viable (Annexin and PI negative) cells (*p<0,01; ** p<0,05).

Serum and glucose depletion caused a huge increase of mitochondrial $O_2^{\bullet-}$, which was attenuated by the expression of DMPK (Figure 3.4). Both the $O_2^{\bullet-}$ levels and the percentage of dead cells were recovered by the antioxidant NAC, thus indicating that serum and glucose depletion induced cell death through an unrestrained increase of ROS of mitochondrial origin.

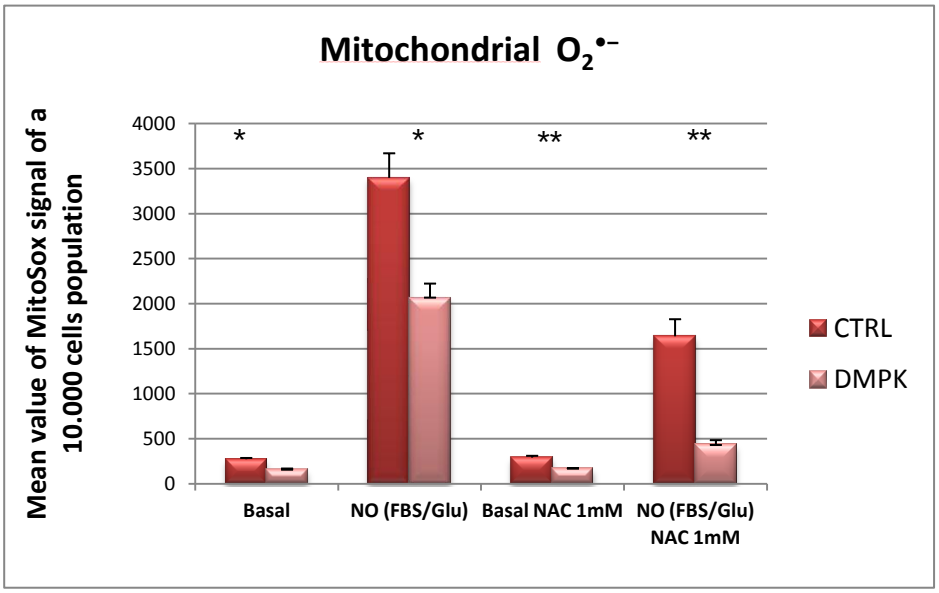

Figure 3.4. Cytofluorimetric analysis of mitochondrial $O_2^{\bullet-}$ production in SAOS-2 cells (24 h serum and glucose starvation). Bars represent mean MitoSox value of a 10 000 cells population (*p<0,05; ** p<0,005).

Taken together, these data unveil an anti-oxidant function of the re-expressed DMPK isoform A. Thus, it was of fundamental importance to check whether this function is a simple artifact observed after DMPK expression in a non-endogenous context, or if DMPK displays a general survival activity under conditions of oxidative stress. I therefore moved to rhabdomyosarcoma cells which constitutively express DMPK . As shown in Figure 3.5 the rhabdomyosarcoma cells are less sensitive to serum and glucose depletion than SAOS-2 cells, since the percentage of living cells is notably higher. Still, DMPK silencing sensitized the cells to serum and glucose depletion.

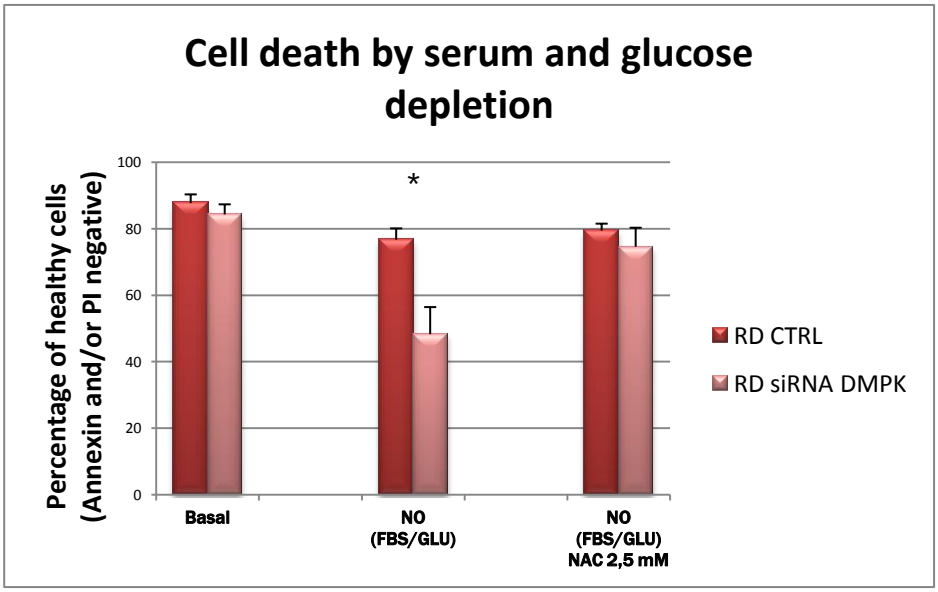

Figure 3.5. Cytofluorimetric analysis of cell death (24 h serum and glucose starvation). Bars represent the percentage of viable (Annexin and PI negative) rhabdomyosarcoma cells (* p<0,05).

Remarkably, the down-regulation of endogenous DMPK protein levels of RD cells correlated with the increase of the levels of mitochondrial superoxide, confirming thus the role of DMPK in modulating mitochondrial ROS levels (Figure 3.6). Thus, DMPK-dependent regulation of mitochondrial ROS levels is an intrinsic and physiological function of the endogenous protein, and not an acquired role due to the expression in a non-physiological context, such as SAOS-2 cells.

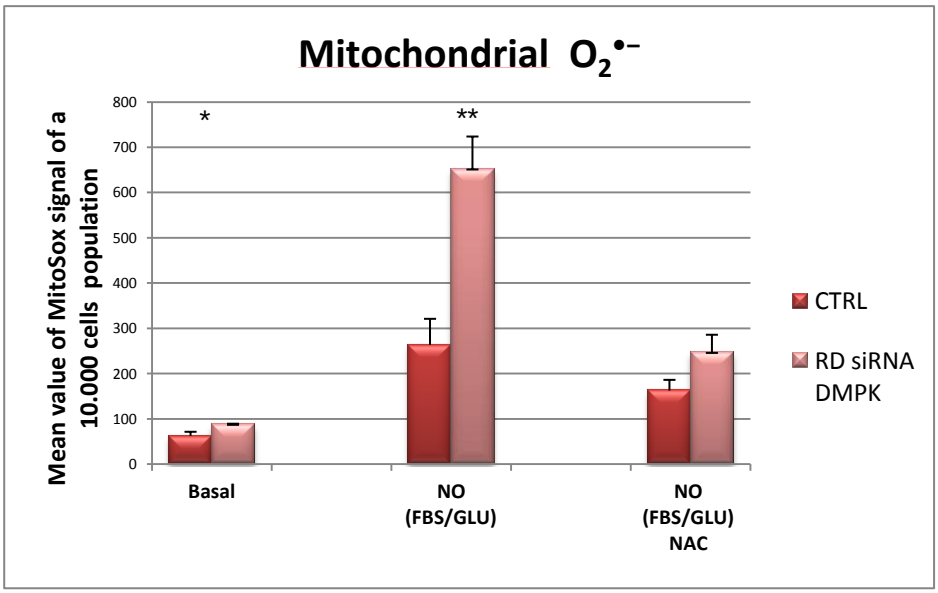

Figure 3.6. Cytofluorimetric analysis of mitochondrial $O_2^{\bullet-}$ levels in RD cells (24 h serum and glucose starvation). Mean values of MitoSox probe of 10 000 cells populations (*p<0,01; ** p<0,005).

4. Mitochondrial metabolism and antioxidant defenses

In order to gain further insight into the mechanisms by which DMPK modulates mitochondrial ROS levels, several parameters were analyzed. Total ATP levels were measured in order to see if DMPK expression alters the activity of the two main pathways of energy production, oxidative phosphorylation (OXPHOS) and glycolysis. ATP was measured in both complete and serum and glucose free medium. As shown in figure 4.1, the global ATP levels were comparable with or without DMPK, and DMPK expression did not alter the ratio of ATP derived from OXPHOS *vs*. the one obtained by glycolisis. In fact, after OXPHOS inhibition with oligomycin or glycolysis inhibition with 2-deoxyglucose (2-DG), no major difference could be observed between SAOS-2 control and DMPK expressing cells. Notably, both cell lines derived most of their ATP from glycolysis (and possibly by other metabolic pathways like glutaminolysis and lipid metabolism) in the presence of glucose in the medium, while the oxidative phosphorylation became the only ATP source when glucose was absent. The effect of 2-DG on ATP levels is explained by the fact that 2-DG is phosphorylated by hexokinase to 2-DG-6 phosphate, which at the same time depletes the ATP and blocks the downstream glycolysis. Therefore, the reduction of ATP levels in the presence of 2-DG is not only due to the block of glycolysis, but also to the ATP consumed when 2-DG itself is phosphorylated. In parallel, I measured ATP levels after 8 hours of serum and glucose depletion. In these conditions, a complete switch to oxidative phosphorylation was observed, as pyruvate and glutamine were present in the medium. As the difference in mitochondrial superoxide levels with or without DMPK is maximized (remind a figure otherwise it is not clear), this difference probably stems from the activity of the respiratory chain. This experiment also highlighted that the difference in cell death elicited by these starvation conditions are most likely not due to different ATP reserves between control and DMPK-expressing cells.

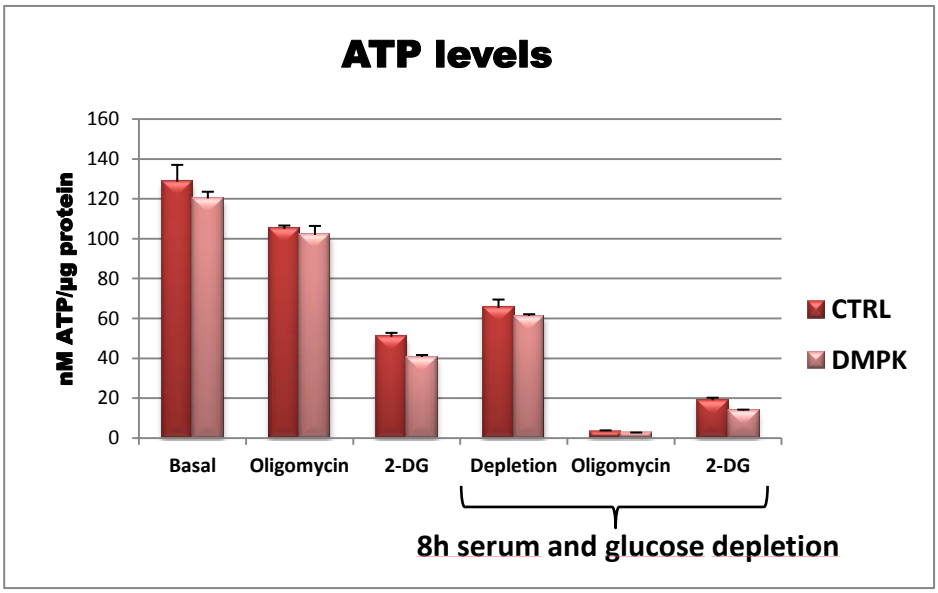

Figure 4.1. Total ATP levels expressed as nM ATP/µg protein in basal conditions (full medium) and in serum and glucose free medium. 6 µM of oligomycin were added 45 min prior to lysis, and 25 mM 2-deoxyglucose were added for 8 h.

DMPK could exert a role on the activity of key enzymes for the maintenance of cell antioxidant defenses, thus counteracting non-physiological levels of ROS. To verify this possibility, I assayed the reduced glutathione pool and the reduced thioredoxin pool, along with the levels of oxidized and total glutathione. Indeed, an inhibition of one of these two antioxidant systems could lead to a decreased capacity in buffering an increased oxidative damage. As illustrated in Figures 4.2 and 4.3 the glutathione reductase and thioredoxin reductase activities were not altered by re-expressing or silencing the DMPK in SAOS-2 and RD cells, respectively. Levels of total glutathione were not altered either, but differences were observed in the percentage of oxidized glutathione. These differences seem rather a consequence than a cause of increased ROS in the absence of DMPK, since both the levels of total glutathione, and the recycling activity of glutathione reductase are not altered.

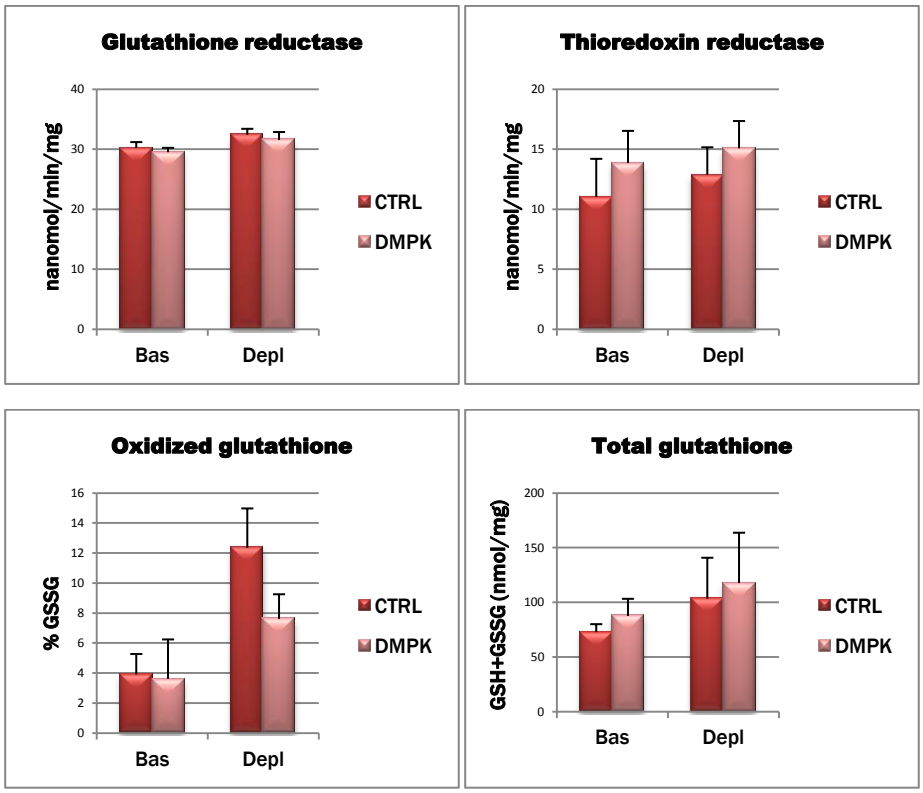

Figure 4.2. Upper graphs: activities of glutathione reductase and thioredoxin reductase of SAOS-2 cells in basal conditions (full medium) and in serum and glucose free medium (8 h depletion), expressed as nmol/min/mg of protein. Lower graphs: levels of oxidized glutathione expressed as percentage of total glutathione, and levels of total glutathione expressed as nmol/mg of protein.

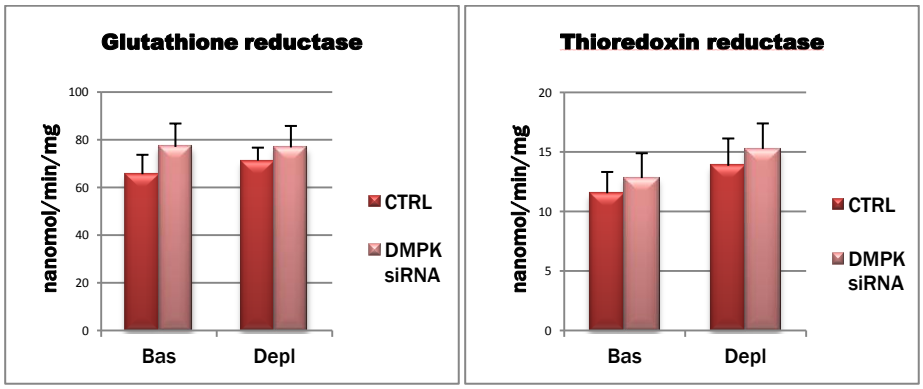

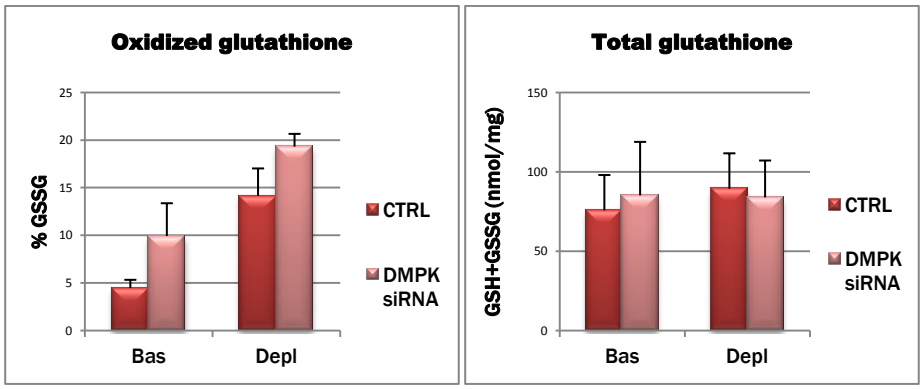

Figure 4.3. Upper graphs: activities of glutathione reductase and thioredoxin reductase of rhabdomyosarcoma cells in basal conditions (full medium) and in serum and glucose free medium (8 h depletion), expressed as nmol/min/mg of protein. Lower graphs: levels of oxidized glutathione expressed as percentage of total, and levels of total glutathione expressed as nmol/mg of protein.

The activity of the respiratory chain is one of the most important sources of mitochondrial superoxide, which is most frequently formed at the level of complexes I and III when electrons leak to O_2. The rates of $O_2^{\bullet-}$ formation are dictated by the concentration of potential electron donors, by the local concentration of oxygen and by the second-order kinetic constants for the reactions between them [44]. Therefore, data of oxygen consumption rate in serum and glucose depleted conditions can allow to understand whether the $O_2^{\bullet-}$ flux is dependent on changes in RC activity. I exploited a last-generation extracellular flux analyzer (XF24 Seahorse) to assess the oxygen consumption rate (OCR) of adherent cells in the closest-to-physiological conditions, on monolayers of intact cells. The addition of respiratory chain inhibitors permits to discriminate between basal, maximal and mitochondria-independent OCR. As illustrated in the upper panel of Figure 4.4, the respiratory activity of SAOS-2 cells is not altered by DMPK expression, while after 4 h of serum and glucose depletion, the DMPK expressing cells show higher rates of oxygen consumption in both basal and uncoupled (FCCP) respiration. However, the small differences observed require further analysis after cell exposure to longer depletion times. Should this difference be confirmed, modulation of RC activity by DMPK under starvation conditions could at least partially account for DMPK-dependent modulation of the mitochondrial superoxide levels.

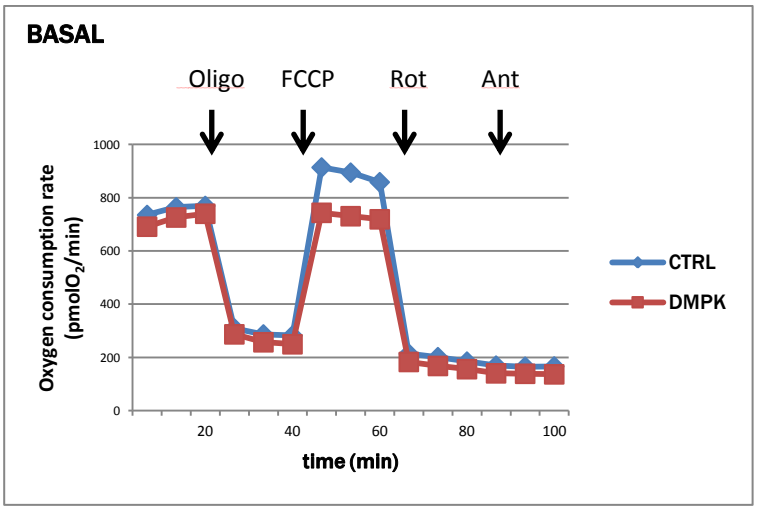

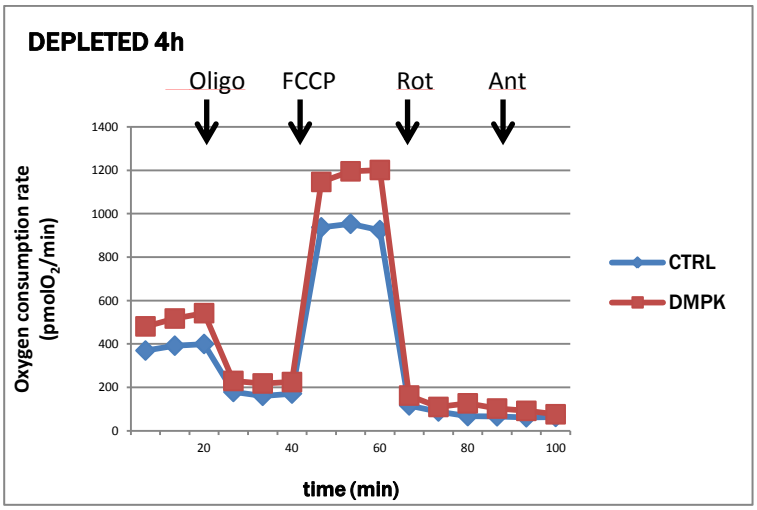

Figure 4.4. Oxygen consumption rate (OCR) of adherent SAOS-2 cells measured by Seahorse instrument in basal (up) and serum and glucose depleted medium (4 h, bellow). Data is shown as the velocity of oxygen consumption in picomols of O_2 per minute per 45 µg of total protein.

5. Molecular mechanisms of DMPK-driven regulation of mitochondrial superoxide

Mitochondrial superoxide anion can be produced in two distinct compartments, the intermembrane space and the matrix, meaning that there is at least one lipid bi-layer separating the

source of the anion and the localization of DMPK kinase. Therefore, DMPK most likely modulates mitochondrial ROS in an indirect manner, through interaction with other mitochondrial proteins that transduce regulatory signals from the cytosol-mitochondrion interface to the inner organelle compartments. To elucidate how DMPK affects mitochondria-related signaling cascades and other pro-survival proteins, the mitochondrial localization and activity (phosphoryaltion status) of candidate pathways was first evaluated. Secondly, I searched for DMPK-interacting partners onto mitochondria, and I investigated whether stress conditions could modulate DMPK activity by affecting the phosphorylation status of the kinase itself or of any of its interactors.

Three different conditions were taken into account: basal (complete medium), serum and glucose depleted (8 h), and serum and glucose depleted (8 h) and then stimulated with the addition of 10% serum for 15 minutes to obtain the maximal signaling activation. I found that DMPK expression increased the proportion of isoform II of hexokinase (HK II) associated to the OMM. Moreover, I could detect a fraction of Ser/Thr kinase GSK3 (glycogen synthase kinase 3) in mitochondria (Figure 5.1). Mitochondrial GSK3 was more inhibited by phosphorylation of the Ser9/21 residues after serum and glucose depletion in the presence of DMPK (Figure 5.1). Importantly, both kinases modulate

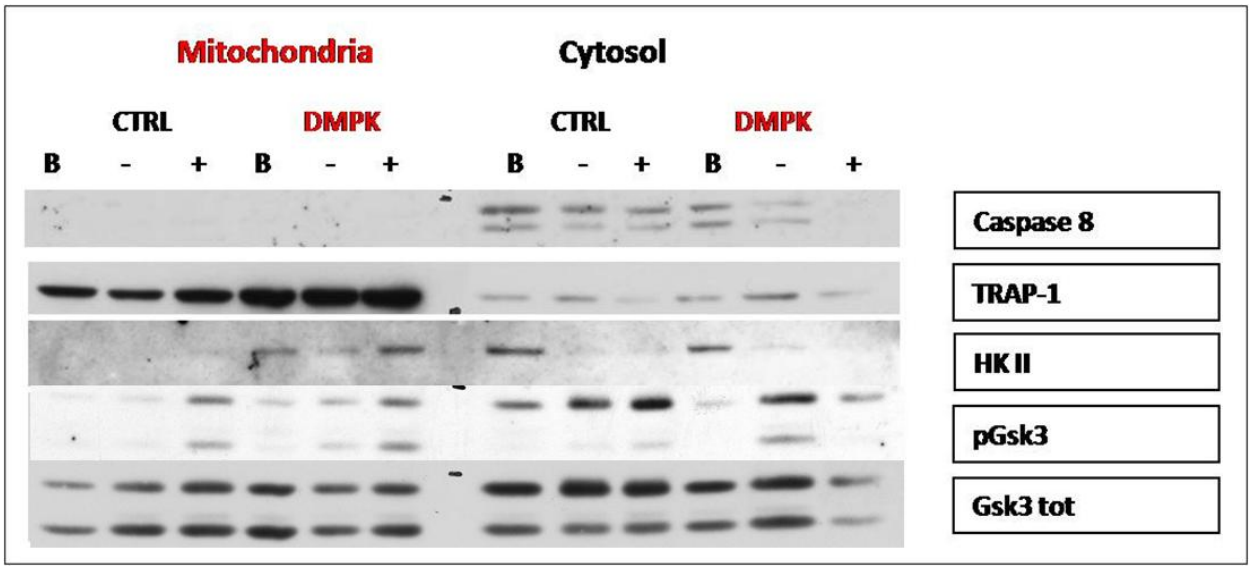

Figure 5.1. Western blot of mitochondrial and cytosolic fractions isolated from SAOS-2 cells in: (**B)** basal (complete medium), (**-)** serum and glucose depleted (8 h), and (**+)** serum and glucose depleted (8 h) and then stimulated with addition of 10% serum for 15 minutes to obtain the maximal signaling activation.

permeability transition pore (PTP) opening; mitochondrial association of HK II inhibits pore opening [40, 58, 61, 62], and CyP-D phosphorylation by mitochondrial GSK3 facilitates PTP opening [37].

The same analysis was performed in rhabdomyosarcoma cells with consistent results, as the silencing of the endogenous DMPK protein resulted in a decrease of the mitochondrial fraction of HK II, and in a decrease of the inhibitory phosphorylation of glycogen synthase kinase 3 (GSK3), as shown in figures 5.2 and 5.3.

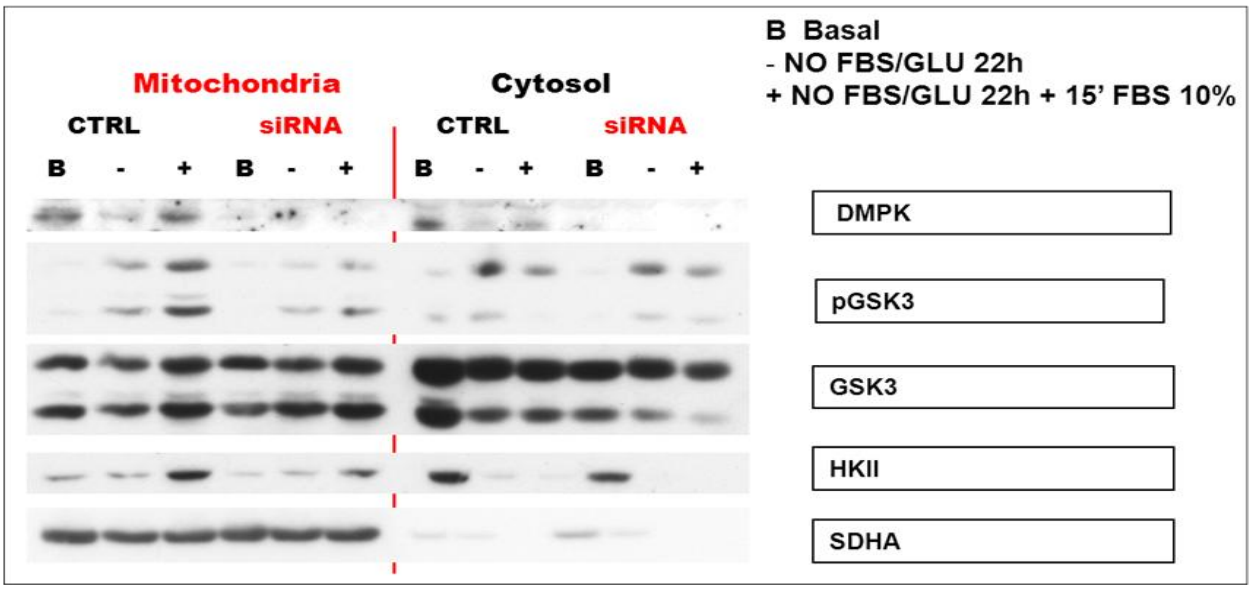

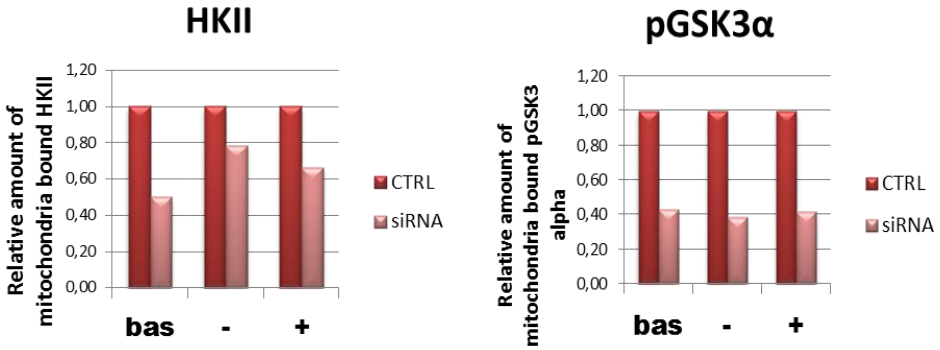

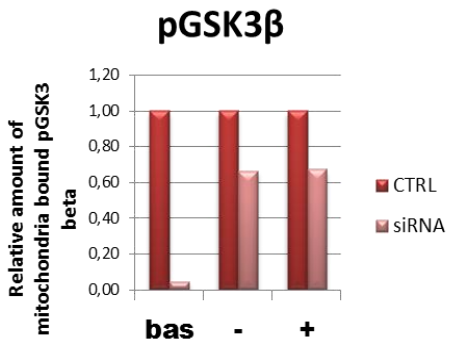

Figure 5.2. Western blot of mitochondrial and cytosolic fractions isolated from rhabdomyosarcoma cells in: (**B)** basal (complete medium), (**-)** serum and glucose depleted (22 h), and (+**)** serum and glucose depleted (22 h) and then stimulated with the addition of 10% serum for 15 minutes to obtain the maximal signaling activation. Below, quantification of western blots for HK II and pGSK α/β (Ser9/21).

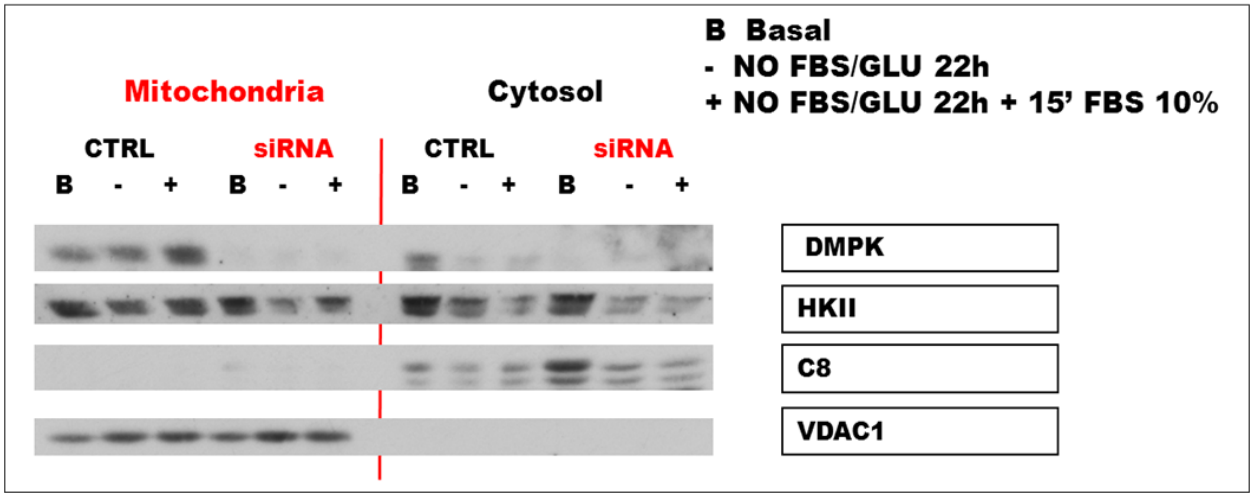

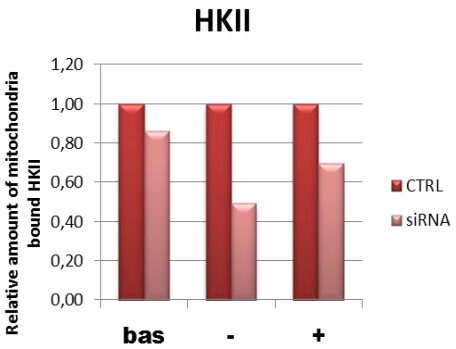

Figure 5.3. Western blot of mitochondrial and cytosolic fractions isolated from rhabdomyosarcoma cells (up) as in Figure 5.2. with the quantification of the mitochondria-associated HK II (left).

I used a pharmacological approach in order to elucidate the relevance of these two DMPK-dependent mitochondrial changes in the regulation of survival pathways. I used the PTP inhibitor cyclosporine A (CsA), the antioxidants NAC and Trolox (an analog of vitamin E), and the HK II inhibitor 5-thioglucose (5-TG) in order to asses if targeting the PTP or HK II could differentially modulate depletion-induced cell death in cells with or without DMPK. Cell death was analyzed by Annexin-V and propidium iodide staining after 16 h of serum and glucose depletion. This shorter time frame was chosen in order to evaluate the efficacy of the inhibitors at the time point "when not all is yet lost", i.e. before the level of cell death reached a maximal plateau. CsA inhibits plasma membrane multi drug resistance (MDR) pump and cell cyclophilins, among which cytosolic CyP-A complexed with CsA creates a binding site for Ser/Thr phosphatase calcineurin (CN). This binding leads to the inhibition of CN, lack of nuclear factor of activated T cell (NFAT) activation and suppression of NFAT

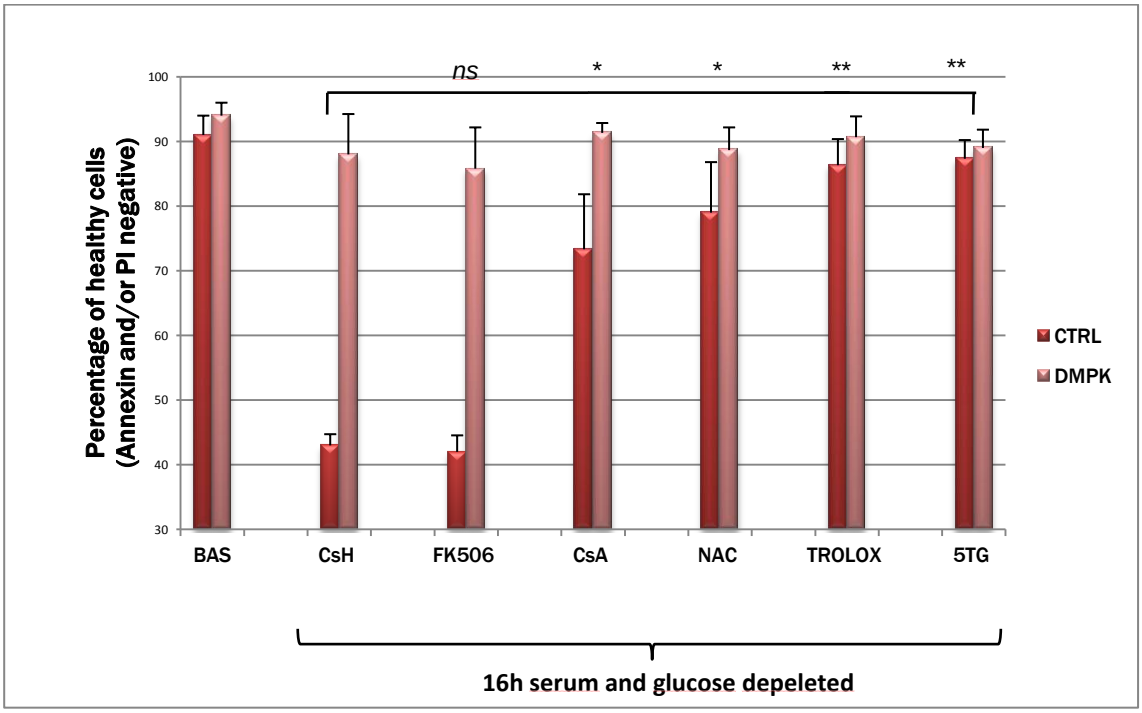

Figure 5.4. Cytofluorimetric analysis of cell death. Bars represent the percentage of viable (Annexin and PI negative) cells (*p<0.05, ** p<0.005). All compounds were added at the beginning of the serum and glucose depletion (Csh, FK506, CsA 0,8 µM, NAC 2,5 mM, Trolox 100 µM, and 5-TG 10 mM).

driven transcription [107]. Cyclosporine H (CsH) and FK506 were used as negative controls for CsA, to exclude a possible contribution of MDR or calcineurin inhibition, respectively. As shown in Figure 5.4, depletion-induced cell death was markedly enhanced in control SAOS-2 cells with respect to SAOS-2 DMPK cells; CsA almost completely prevented cell death in control SAOS-2 cells, and this was not due to CsA side-effects on MDR or calcineurin. Both N-acetyl cysteine and Trolox prevented cell death, and most surprisingly the HK II inhibitor 5-TG completely prevented death in control cells.

5-TG is the closest glucose analog which competes for the glucose binding site on HK II, and when bound, inhibits the enzymatic activity. Since the cell death analysis was performed after 16 h of glucose depletion it was unlikely to assume that the protective effect of 5-TG could have something to do with modulating HK II enzymatic activity in the absence of its physiological substrate. An alternative possibility was that 5-TG could modulate HK II binding to OMM and in this way regulate the susceptibility of mitochondria to undergo the permeability transition. If correct, this hypothesis implies that the anti-apoptotic function of HK II is independent of its enzymatic activity. To elucidate

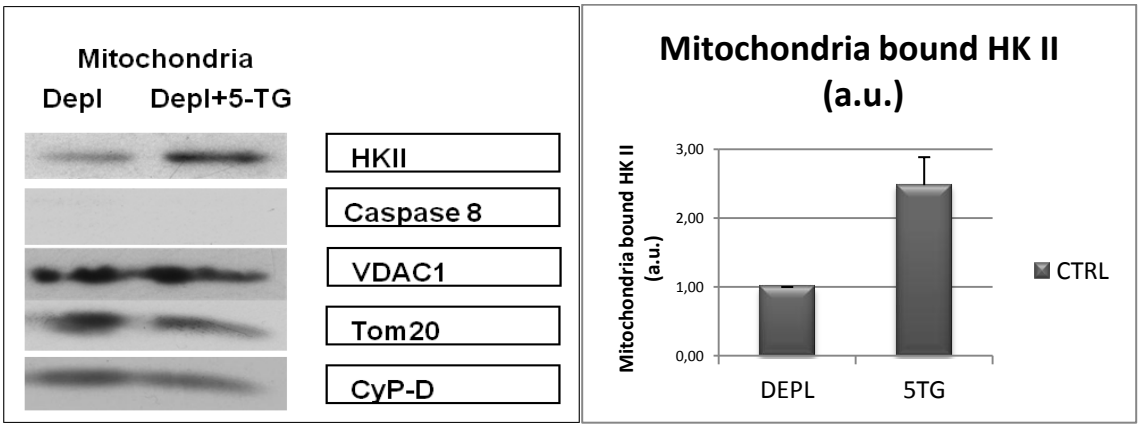

Figure 5.5. Western blot of mitochondria isolated from 8 h serum and glucose depleted SAOS-2 control cells. Where indicated, 10 mM 5-TG was added at the beginning of treatment. On the right, quantification of mitochondrial HK II normalized *vs*.Tom20, VDAC1 and CyP-D.

if 5-TG can modulate HK II association with the OMM in the presence of 5-TG, I isolated mitochondria from SAOS-2 control cells depleted of serum and glucose for 8 h, with or without 5-TG

in the medium. As illustrated in Figure 5.5, 5-TG increased the amount of mitochondrial HK II more than two-fold.

Furthermore, 5-TG decreased the levels of mitochondrial superoxide to one third in SAOS-2 control cells exposed to starvation conditions (Figure 5.6). Taken together, these data indicate that following serum and glucose deprivation the mere HK II localization on the OMM is sufficient to both down-modulate mitochondrial ROS levels and to inhibit cell death, without requirement of HK II enzymatic activity.

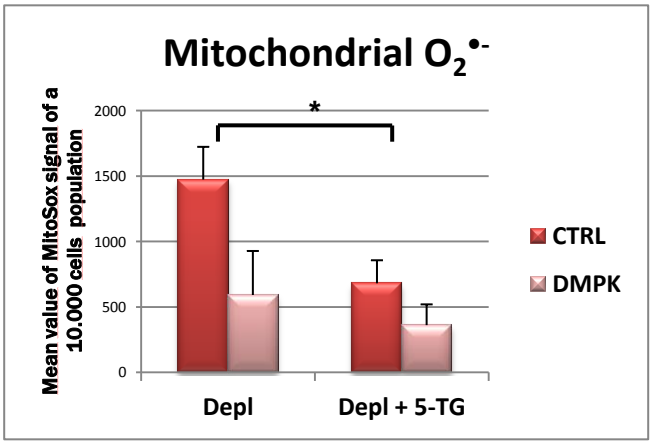

Figure 5.6. Cytofluorimetric analysis of mitochondrial $O_2^{\bullet-}$ levels (16 h serum and glucose starvation) in the absence or presence of 10 mM 5-TG. Mean values of MitoSox probe of 10 000 cells populations (*p<0,001). Increase of mitochondria-associated HK II results in decrease of mitochondrial superoxide.

In order to approach the role of HK II in modulating mitochondrial superoxide levels from a different angle, a cell-permeable synthetic peptide was used to selectively detach HK II from the OMM. This peptide, dubbed TAT-HK II, is formed by the hydrophobic N-terminus of HK II, which is the portion of the enzyme that takes contact with the mitochondrial surface, linked to a fragment of the HIV1-Tat to render it membrane-permeable [40]. Rotenone and antimycin A, which inhibit RC complex I and III, respectively, were also used, and mitochondrial superoxide levels were assessed by using the Mitosox probe on cells in basal conditions and after a 8 h serum and glucose depletion. Figure 5.7 reports the ratio of the Mitosox fluorescence intensity of control *vs.* DMPK-expressing SAOS-2 cells. Each bar shows CTRL vs. DMPK ratio either in complete medium (basal) or after 8 h in serum and glucose depleted medium in the presence of the indicated compounds.

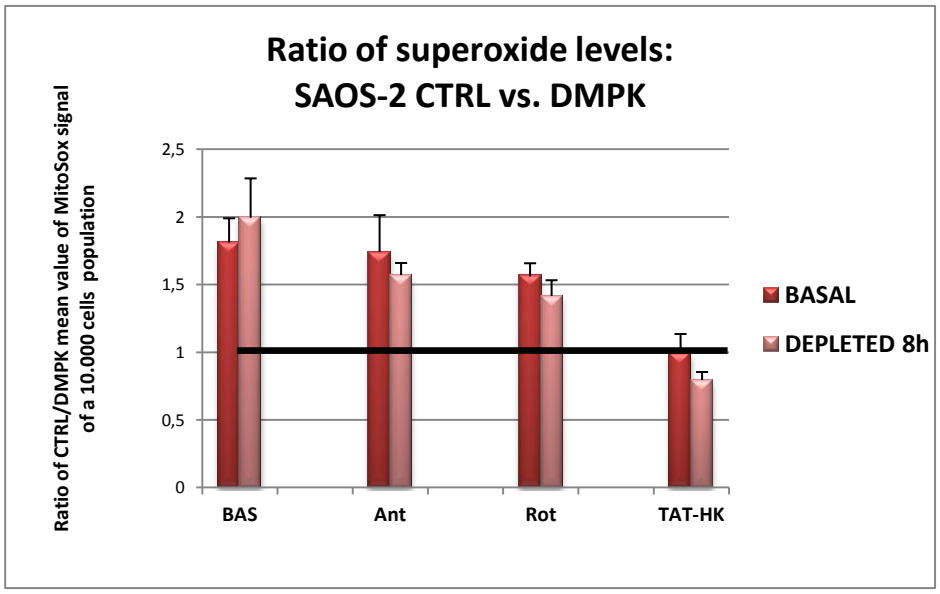

Figure 5.7. Cytofluorimetric analysis of mitochondrial $O_2^{\bullet -}$ levels (8 h serum and glucose depletion). Antimycin A (1 µM), rotenone (4 µM) and TAT-HK II (20 µM) were added for 45 minutes before cells were processed for analysis. Bars represent the ratio of the Mitosox fluorescence intensity between control and DMPK-expressing SAOS-2 cells for the indicated condition.

As depicted in the figure, HK II detachment from the OMM with the TAT-HK II peptide completely abrogates differences in mitochondrial superoxide levels. Taken together with the data on the effect of 5-TG, these observations put the HK II in central place for the DMPK-dependent modulation of the mitochondrial redox state. The fact that antimycin A and rotenone do not abolish DMPK-dependent differences in mitosox fluorescence does not exclude the possibility that respiratory chain activity is responsible for the maintenance of those same differences. Thus, HK II could be an upstream modulator.

6. How does DMPK increase HK II association with mitochondria?

Both DMPK and HK II are anchored on the cytosolic side of the OMM, making it possible that they physically interact with each other. This possibility was tested by immunoprecipitating HK II,

since the DMPK immunoprecipitation yielded extremely low amounts of immunoprecipitated protein. Remarkably, DMPK was found to co-immunoprecipitate with HK II, both in basal conditions and after a 8 h serum and glucose depletion (Figure 6.1).

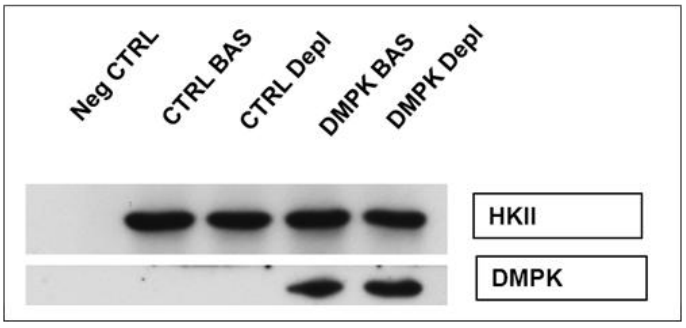

Figure 6.1. HK II immunoprecipitation. DMPK co-immunoprecipitates with HK II in SAOS-2 cells, both in basal and 8 h serum and glucose depleted conditions. Lysate of DMPK-expressing SAOS-2 cells with sepharose was used as negative control.

Next, I looked if there was any detectable post-translational modification (phosphorylation) in DMPK and/or HK II, as modulation of phosphorylation events could be a regulatory mechanism of the complex stability and/or function. To this aim, I immunoprecipitated either Ser/Thr or Tyr phosphorylated proteins. An unexpected result was obtained from phospho-Tyr immunoprecipitation: DMPK turned out to be strongly tyrosine-phosphorylated, and its tyrosine phosphorylation was increased after serum and glucose depletion (Figure 6.2).

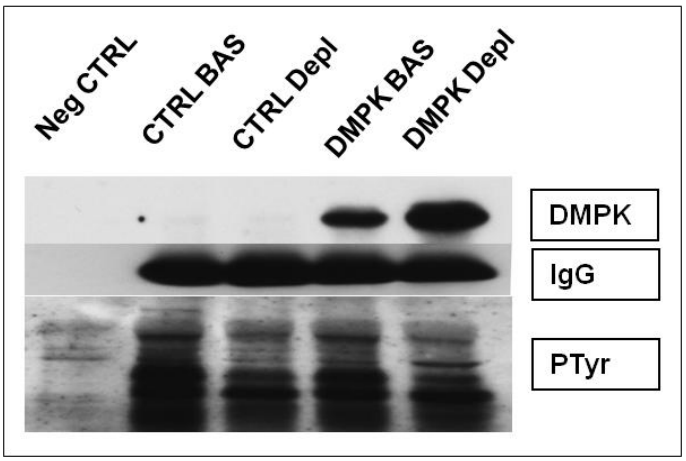

Figure 6.2. Phospho-Tyr immunoprecipitation of proteins with phosphorylated tyrosine residue(s). DMPK is tyrosine phosphorylated and this phosphorylation increases after serum and glucose depletion.

Among non-receptor tyrosine kinases that could account for this DMPK phosphorylation, the most probable candidates are members of the Src family of Tyr kinases. Most of these enzymes are found in specific cellular subsets, while Src itself is ubiquitously expressed. c-Src was found to co-immunoprecipitate with HK II; remarkably, the HK II-c-Src association was strongly increased in the presence of DMPK (Figure 6.3). Furthermore, only in SAOS-2 DMPK cells at least a portion of c-Src interacting with HK II was in its active form (i.e. phosphorylated at Tyr416).

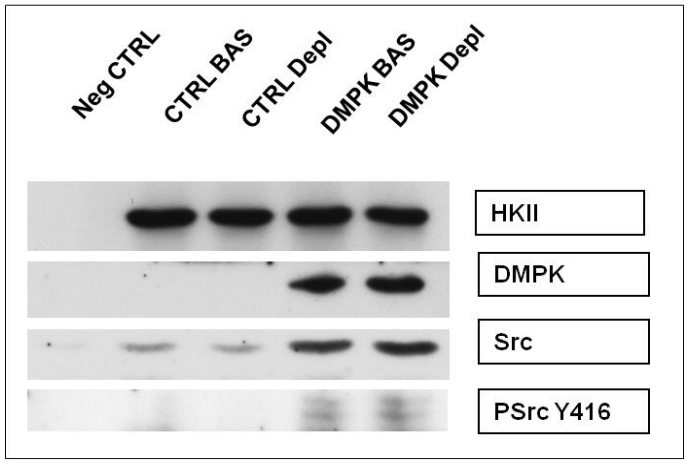

Figure 6.3. HK II immunoprecipitation. Along with DMPK co-immunoprecipitation with HK II, c-Src non-receptor tyrosine kinase also increases its association with HK II in the presence of DMPK, and part of this interacting c-Src fraction is active (phosphorylated in tyrosine 416).

Next, the observed interactions between HK II, Src and DMPK were cross-checked by Src immunoprecipitation. As shown in Figure 6.4 we found both HK II and DMPK to co-immunoprecipitate with c-Src, and DMPK association with Src increased following 8 h serum and glucose depletion.

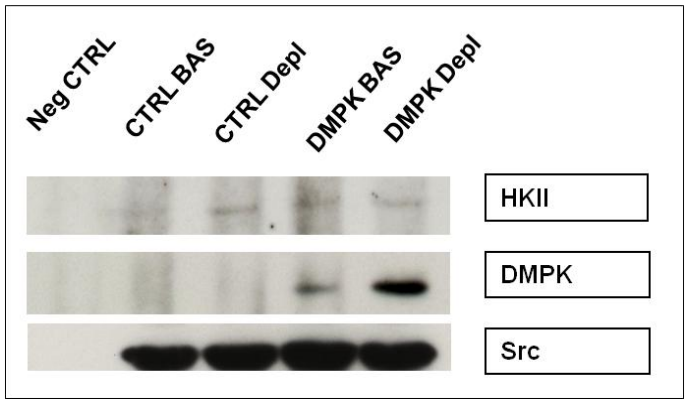

Figure 6.4. c-Src immunoprecipitation. Both HK II and DMPK co-immunoprecipitate with c-Src, and DMPK association with Src increases following 8 h serum and glucose depletion.

Still as a preliminary evidence, it was also found that DMPK expression abolished the c-Src phosphorylation in Ser/Thr residues. Figure 6.5 shows the result of a pSer/pThr immunoprecipitation in which pSer/pThr phosphorylated Src was found in SAOS-2 control but not DMPK expressing cells.

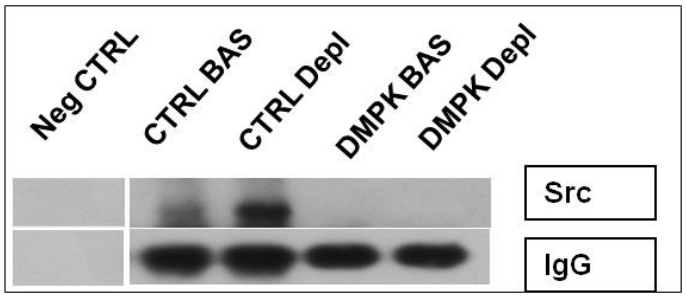

Figure 6.5. pSer/pThr immunoprecipitation. Src is phosphorylated on Ser/Thr residues in SAOS-2 control cells, and this phosphorylation is abolished by DMPK expression.

Finally, the functional relevance of this novel trimeric complex was assayed. Src was first inhibited by a potent and specific dual-site c-Src inhibitor, SrcI-1, and afterwards HK II was detached from mitochondria with the TAT-HK displacing peptide. In this way, two of the three components of

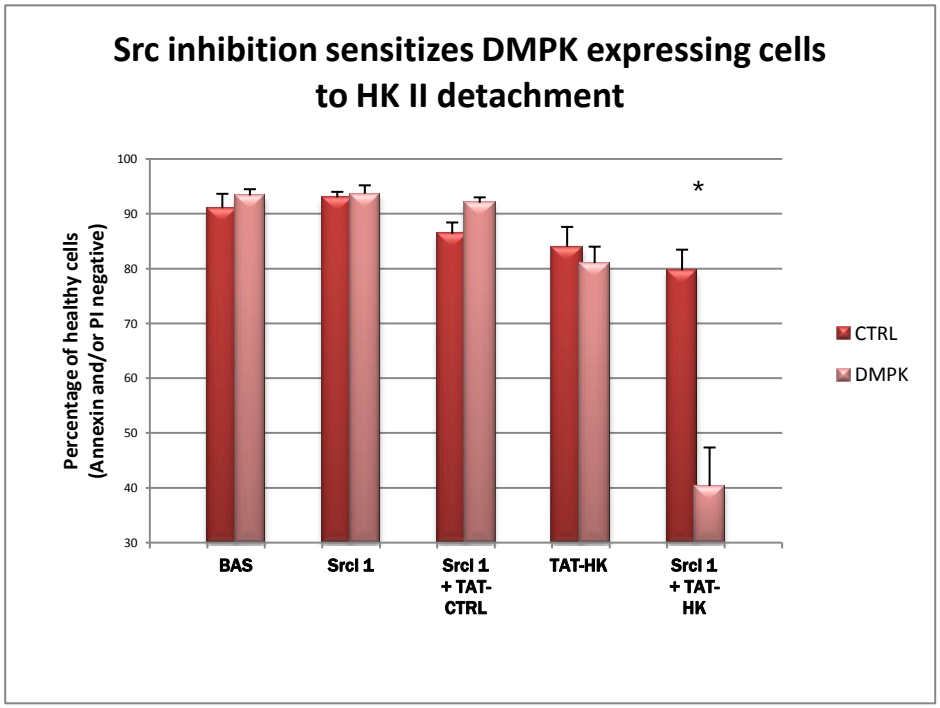

Figure 6.6. Cytofluorimetric analysis of cell death. Bars represent the percentage of viable (Annexin and PI negative) SAOS-2 cells (*$p<0.05$). 10 µM of SrcI-1 were pre-incubated for 30 minutes, following 45 minutes of 20 µM TAT-CTRL or TAT-HK II peptide, in serum-free medium.

the complex are targeted directly, while the relevance of the non-druggable DMPK can be evaluated by confronting control and DMPK expressing cells. As illustrated in Figure 6.6, the Src inhibitor alone has no effect on cell viability, as well as the Src inhibitor plus a TAT-CTRL peptide. The TAT-HK II peptide reduces cell survival very modestly at the concentration used, but when combined with the Src inhibitor it dramatically increases cell death only in DMPK expressing cells, where Src-DMPK-HK II complex is present. Thus, Src activity is crucial for increased DMPK-dependent HK II association with the OMM.

These data lead to a working model in which cell viability is increased in a DMPK-dependent fashion through the modulation of mitochondrial superoxide levels. The interaction of DMPK and Src with HK II favors the HK II association with OMM, which in turn decreases superoxide anion produced by mitochondria, and rescues the cell from death in conditions where $O_2^{\bullet -}$ concentration rises above physiological levels.

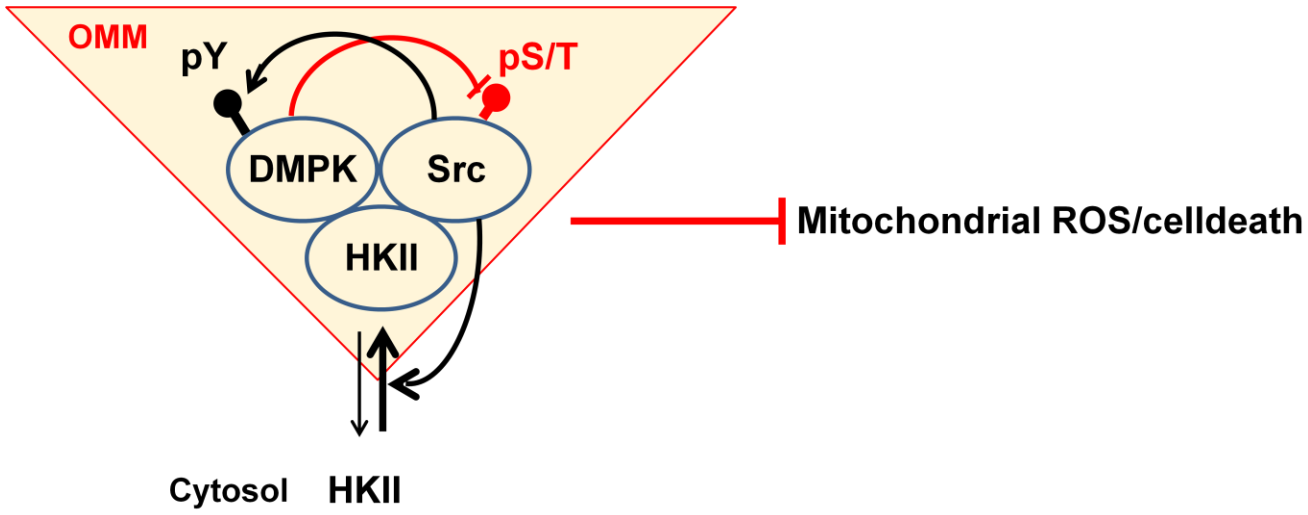

Figure 6.7. Working model of DMPK-dependent increased cell viability due to the modulation of mitochondrial superoxide levels.

Discussion

In this study I have analyzed the role of mitochondria-associated DMPK, relative to the function of the organelle and of the cell. The most frequent adult muscular dystrophy, myotonic dystrophy type 1, shows a reduction of DMPK protein levels, and mice lacking *dmpk* develop late onset myophaty and cardiac defects similar to those of DM1 patients [4-6]. Although mouse knock-out does not reproduce entire spectrum of DM1 clinical features, it clearly develops some of the symptoms in the tissues where the protein is normally expressed [3]. As reported by Oude Ophuis *et al.* [25], DMPK high molecular weight isoforms are mostly found in skeletal muscle and cardiac tissue, where they were seen to co-localize with mitochondria. A more detailed analysis of Wansink *et al*. showed them to be anchored on the outer mitochondrial membrane [23, 24]. Finally, Oude Ophuis *et al.* also reported [36] that a transient expression of human isoform A (hDMPK-A) induced spontaneous mitochondrial clustering in the perinuclear region, followed by depolarization, release of cytochrome c and apoptosis. These results have prompted us to examine in more detailed manner the role of DMPK in shaping the mitochondrial function, with the aim to uncover the underlying molecular mechanisms.

To this purpose, we have used a gain-of function and a loss-of function approach which consisted in expressing hDMPK-A in cell line that did not show detectable levels of endogenous protein, and in silencing the endogenous DMPK in a cell line of muscle origin where the protein is normally expressed. Thus, any mitochondrial parameter regulated by the mitochondria-associated DMPK should vary in the opposite direction in these two cell lines.

In SAOS-2 cells, DMPK was enriched in the mitochondrial fraction, as seen in immunoblot performed on fractions obtained after standard differential centrifugation separation of sub-cellular fractions. Importantly, re-expression of DMPK isoform A in SAOS-2 cells resulted in almost

complete mitochondrial association of the expressed protein, thus the observed effects can be interpreted as direct modeling of mitochondrial function by the associated DMPK, rather than an indirect consequence of its effects on other non-mitochondrial targets. Silencing of endogenous DMPK in rhabdomyosarcoma cells did not target specifically the mitochondria-associated high molecular weight isoforms, which are predominantly expressed in confront to lower MW cytosolic isoforms in muscle derived cells. Yet, when levels of mitochondria-bound DMPK were evaluated on isolated mitochondria (Figure 5.2 and 5.3), no detectable band could be observed indicating that mitochondria-associated DMPK was completely silenced. Protease digestion of mitochondria isolated from SAOS-2 cells (Figure 1.4) showed that hDMPK-A associates to outer mitochondrial membrane, since its digestion profile was similar to those of other two OMM proteins Tom20 and Bcl-X_L. The presence of two distinct DMPK bands is most likely indicative of its phosphorylation status, probably due to its auto-phosphorylative activity as reported by Wansink [23].

Intriguingly, stably transfected SAOS-2 cells did not show alterations of mitochondrial membrane potential due to the expression of hDMPK-A, as it was reported by Oude Ophuis *et al.* [36] when transiently expressing the same isoform by viral vectors. This inconsistency can be explained by the stress given by the transfection method, combined with a high viral load. In fact, a construct containing only DMPK-A C-terminal tail equally induced perinuclear clustering of mitochondria and subsequent apoptosis [36] indicating that those phenomena were independent of protein function as a whole. When SAOS-2 cells were put in a condition of acute oxidative stress elicited by a thiol oxidant diamide, DMPK-A expression decreased the rates of mitochondrial depolarization, thus conferring a protective effect (Figure 3.1). Diamide-induced depolarization is most likely not due to a modest increase of mitochondrial superoxide levels (Figure 3.2), but rather due to its action on reactive thiol sites of permeability transition pore or other proteins involved in maintenance of inside negative membrane potential.

However, expression of hDMPK-A resulted in 40 percent decrease in mitochondrial superoxide levels, so I looked for a more physiological condition in which this difference would be amplified. Combined serum and glucose depletion was seen to induce higher levels of cell death in SAOS-2 control cells (Figure 3.3), while absence of serum or glucose alone affected both cell lines equally (data not shown). On the contrary, silencing of endogenous DMPK in RD cells increased their susceptibility to cell death induced by serum and glucose depletion (Figure 3.5), supporting the idea that observed alterations of cell viability in those conditions are due to variations of DMPK protein levels. Substantial increase of mitochondrial superoxide levels was seen in the same experimental conditions, and this increase was attenuated by the presence of mitochondria-associated DMPK in both cell lines. Thiol-reducing antioxidant N-acetyl cystein kept low $O_2^{\bullet -}$ levels in serum and glucose depletion, and prevented what we conclude to be ROS-induced cell death (Figures 3.4 and 3.6).

Importantly, enzymatic activity of two key antioxidant systems, the glutathione and thioredoxin, as well as levels of total glutathione were not altered by variation of DMPK protein levels in both cell types, indicating that the observed differences in superoxide levels are not due to alterations in antioxidant defenses. Levels of oxidized glutathione were higher when DMPK was absent or silenced, consistently with the increased oxidative stress detected in those conditions (Figures 4.2 and 4.3).

Presence of 1 mM pyruvate and 4 mM L-glutamine in the depletion medium provides cells with energy source through Kreb's cycle and glutaminolysis, respectively. Finally, obtained NADH can be used to fuel the oxidative phosphorylation. In serum and glucose depletion, SAOS-2 cells rely completely on ATP produced by oxidative phosphorylation, since the addition of oligomycin, a specific inhibitor of ATP synthase, exhausts all cellular ATP when added for the last 45 minutes of 8 h depletion (Figure 4.1). Measurement of oxygen consumption rates of adherent SAOS-2 cells by the Extracellular Flux analyzer XF-24 showed that DMPK did not alter the respiration in the

presence of glucose, but after only a short 4 h serum and glucose depletion DMPK expression kept OCR levels higher in confront to control cells, both in basal and FCCP-stimulated (maximal) respiration. The rates of superoxide production depend mostly on the proton gradient, the $NADH/NAD^+$ and $CoQH_2/CoQ$ ratios and the local O_2 concentration, indicating that dynamical fine tuning of Δp and electron donors influences at the same time RC activity and consequent $O_2^{\bullet -}$ production [44]. Thus, respiratory chain activity and its modulation by DMPK presence on the OMM could account as a physiological source of observed superoxide levels in depletion conditions, but further experiments are required to validate this hypothesis.

DMPK expression in SAOS-2 cells and silencing in RD cells caused an alteration in the amount of HK II bound to mitochondria, and also an alteration in the levels of inhibitory Ser9/21 phosphorylation of mitochondrial GSK3 α/β. DMPK presence on the OMM increased mitochondrial binding of HK II, and it also increased GSK3 Ser9/21 inhibitory phosphorylation in both cell types (Figures 5.1-5.3). The relevance of these observations was tested pharmacologically; both HK II binding and GSK3 inhibition prevent PTP opening, and the CyP-D inhibitor cyclosporine A almost completely prevented cell death in SAOS-2 control cells and this was independent of CsA effect on MDR pumps or calcineurin. Both antioxidants NAC and Trolox restored viability of SAOS-2 control cells, indicating this was ROS-induced cell death due to the PTP opening. Most remarkably, the closest glucose analog and a HK II inhibitor 5-TG, completely prevented cell death (Figure 5.4).

Effect of 5-TG was studied in a more detailed manner, and I found that 5-TG increased the amount of HK II bound to mitochondria in SAOS-2 control cells (Figure 5.5), and the increased binding of HK II corresponded to a marked reduction of mitochondrial superoxide (Figure 5.6). This can hardly be explained by the inhibition of HK II enzymatic activity, since the former was reported to have a protective antioxidant effect in isolated mitochondria due to the ATP/ADP recycling mechanism [72]. In this context, it has been recently reported that HK II curtails

mitochondrial ROS in UCP3 (uncoupling protein 3) dependent fashion, but only in the presence of high glucose [73]. However, here I have shown that (*i*) increased HK II binding with mitochondria is seen in DMPK-expressing SAOS-2 cells after prolonged glucose depletion when there is no available substrate for its enzymatic activity, and that (*ii*) use of an inhibitor of HK II enzymatic activity, 5-TG, increases its binding to mitochondria, reduces mitochondrial $O_2^{\bullet -}$ levels and prevents the subsequent cell death in SAOS-2 control cells. These observations imply that HK II modulation of mitochondrial ROS is independent of its enzymatic activity. On the other hand, detachment of HK II from OMM by TAT-HK II peptide abolished differences in superoxide levels due to the DMPK expression in SAOS-2 cells, both in the presence and in the absence of glucose for 8 h (Figure 5.7). This data is another proof of principle of HK II central role in the regulation of mitochondrial ROS upon DMPK expression or silencing.

HK I and II binding to OMM is presumed to occur due to the presence of hydrophobic N-terminal tail of 15 amino acids, but a great body of evidence reports HKs to bind the OMM voltage dependent anion channel (VDAC1) [108] and to mediate their anti-apoptotic functions by this interaction. However, different studies showed that (*i*) HK II detachment from OMM triggers cell death independently of VDAC1/3 [40]; (*ii*) brain HK I does not colocalize significantly with VDAC1 and 2, but it does with VDAC3, in human osteosarcoma cells (U2OS) [68]; and (*iii*) HK I has at least two distinct binding sites on OMM, discriminated by the ability of the end product G-6P to detach the enzyme, whose ratio is 20:80 for G-6P sensitive *vs*. insensitive site in human brain [70].

Although a possible involvement of VDAC1 in the DMPK-dependent modulation of HK II binding to mitochondria still needs to be verified, I first evaluated the possibility of direct interaction between DMPK and HK II. Remarkably, DMPK was co-immunoprecipitated with HK II in SAOS-2 cells (Figure 6.1), and this interaction most likely occurs on the OMM where more than 85% of total DMPK is localized (Figure 1.3). The search of phosphorylative modifications

surprisingly revealed that DMPK was strongly phosphorylated in tyrosine residue(s) (Figure 6.2). *In silico* analysis of DMPK amino acid sequence revealed the presence of a proline rich sequence between residues 347 and 356 RDSVPPFTP resembling the consensus motif (R/K)XXPXXP of class I ligands [109]; this sequence could constitute a Src homology 3 (SH3) binding domain in DMPK protein kinase. Although it differs from the canonical class I consensus sequence, a significant divergency in functional SH3 binding sequences is documented [109-111]. This fact narrowed the circle of potential tyrosine kinases (TKs) to soluble and ubiquitously expressed members of the family, suggesting the Src members as potential candidates, especially those that were already seen to be associated with mitochondria [94, 95, 99]. An additional kinase was found to co-immunoprecipitate with HK II and this was the non-receptor tyrosine kinase Src, whose interaction increased in the presence of DMPK (Figure 6.3). A fraction of detected Src in HK II immunoprecipitates was active, i.e. phosphorylated at Tyr416, only in the presence of DMPK and is most likely responsible for the tyrosine phosphorylation of DMPK. I validated the observed interactions by immunoprecipitating Src: both HK II and DMPK were detected, thus confirming the previously observed interactions.

Despite the novelty of this molecular complex, its functional meaning in the context of DMPK-dependent modulation of mitochondrial ROS is much more relevant. As shown in Figure 6.6, Src has a functional role in keeping HK II associated with mitochondria, since Src inhibition sensitizes only DMPK-expressing cells to HK II detachment from OMM. Concerted DMPK and Src activity may either stabilize the HK II that is already bound to OMM, or alternatively increase the rate of its re-association with the OMM by modifying directly hexokinase or its binding partner(s) on the OMM. Further work is required to elucidate the phosphorylative interplay in this triangle, and possibly to determine the sites of phosphorylations and their functional consequences.

Reported alterations in *dmpk-/-* mice such as late onset progressive myophaty [4] and cardiac abnormalities [5, 6] develop gradually and increase in severity during time. Ultrastructure of

affected *dmpk-/-* muscles was characterized with the loss of ordered organization of sarcomeres and abnormal mitochondria which lost their structural integrity [4]. Cardiac alterations of DM1 patients are remarkably reproduced in homozygous *dmpk-/-*, but also heterozygous mice, and it was shown that *in vitro*-differentiated *dmpk-/-* myotubes exhibit a higher resting $[Ca^{2+}]_i$ than WT myotubes [112]. The same was observed in ventricular cardiomyocytes from *dmpk-/-* mice that displayed enhanced basal contractility of single cardiomyocytes and an associated increase in intracellular $[Ca^{2+}]_i$ [34]. Unfortunately, mitochondrial function or structure in *dmpk-/-* cardiomyocytes was not reported. The late onset of both muscle and cardiac phenotype in *dmpk-/-* mice indicates that progressive accumulation of damage takes place, until the tissue homeostasis and its function become compromised, somehow resembling the Harman's theory of aging [75].

Considering the presented novel findings on the role of DMPK in suppression of mitochondrial ROS, it is tempting to speculate that both cardiac and muscle phenotypes of *dmpk-/-* mice, could be due to the mitochondrial dysfunction. Combined action of increased mitochondrial ROS levels due to the DMPK absence, and a concomitant increase in intracellular Ca^{2+} levels as reported in [4, 34, 112] create ideal conditions for PTP opening [42]. A recent study of differentiating primary muscular satellite cells from DM1 patients have showed that they fuse, differentiate and mature normally, but differentiated myotubes exhibit increased levels of apoptosis and autophagy [113]. Unfortunately, DMPK protein levels were not evaluated, so it will be extremely interesting to asses differentiating capacity and survival of muscle precursor cells in the absence of DMPK, for instance in rhabdomyosarcoma cells.

Involvement of DMPK protein in mitochondrial redox regulation and, as a consequence, in cell death, opens a possibility of its participation in the process of tumorigenesis. A recently reported evidence of association between DM1 and increased rates of observed malignant neoplasms [19, 21] is so far the only correlation of these two pathologies. The proposed hypothetical molecular basis of increased neoplasms in DM1 would consist of up-regulation of

Wnt/β-catenin signaling pathway [19]. However, in Drosophila, the loss of one of the two DMPK homologous genes *lats/warts* leads to excess growth and abnormalities of cell differentiation [20]. Thus, genetic instability due to $CUG_{(n)}$ repeats and their *trans* effect on splicing of other genes from one side, and the novel role of DMPK in modulating mitochondrial ROS, from the other, could consist means of increased cancer risk associated to DM1.

Taken together, these new findings on the DMPK role in modulating the mitochondrial function, open a new window on possible pathogenic mechanisms related to variations of DMPK protein levels. Involvement of c-Src and HK II, proteins involved in oncogenic transformation [101] and cancer metabolism respectively [63], could thus provide a mechanistic link between tissue degeneration and increased cancer risk in DM1.

References

1. Cho, D.H., and Tapscott, S.J. (2007). Myotonic dystrophy: emerging mechanisms for DM1 and DM2. Biochim. Biophys. Acta 1772, 195-204.

2. Ranum, L.P., and Day, J.W. (2004). Myotonic dystrophy: RNA pathogenesis comes into focus. Am. J. Hum. Genet. 74, 793-804.

3. Kaliman, P., and Llagostera, E. (2008). Myotonic dystrophy protein kinase (DMPK) and its role in the pathogenesis of myotonic dystrophy 1. Cell Signal. 20, 1935-1941.

4. Reddy, S., Smith, D.B., Rich, M.M., Leferovich, J.M., Reilly, P., Davis, B.M., Tran, K., Rayburn, H., Bronson, R., Cros, D., Balice-Gordon, R.J., and Housman, D. (1996). Mice lacking the myotonic dystrophy protein kinase develop a late onset progressive myopathy. Nat. Genet. 13, 325-335.

5. Berul, C.I., Maguire, C.T., Gehrmann, J., and Reddy, S. (2000). Progressive atrioventricular conduction block in a mouse myotonic dystrophy model. J. Interv. Card Electrophysiol. 4, 351-358.

6. Berul, C.I., Maguire, C.T., Aronovitz, M.J., Greenwood, J., Miller, C., Gehrmann, J., Housman, D., Mendelsohn, M.E., and Reddy, S. (1999). DMPK dosage alterations result in atrioventricular conduction abnormalities in a mouse myotonic dystrophy model. J. Clin. Invest 103, R1-R7.

7. Sarkar, P.S., Appukuttan, B., Han, J., Ito, Y., Ai, C., Tsai, W., Chai, Y., Stout, J.T., and Reddy, S. (2000). Heterozygous loss of Six5 in mice is sufficient to cause ocular cataracts. Nat. Genet. 25, 110-114.

8. Mahadevan, M.S., Yadava, R.S., Yu, Q., Balijepalli, S., Frenzel-McCardell, C.D., Bourne, T.D., and Phillips, L.H. (2006). Reversible model of RNA toxicity and cardiac conduction defects in myotonic dystrophy. Nat. Genet. 38, 1066-1070.

9. Kanadia, R.N., Johnstone, K.A., Mankodi, A., Lungu, C., Thornton, C.A., Esson, D., Timmers, A.M., Hauswirth, W.W., and Swanson, M.S. (2003). A muscleblind knockout model for myotonic dystrophy. Science 302, 1978-1980.

10. Orengo, J.P., Chambon, P., Metzger, D., Mosier, D.R., Snipes, G.J., and Cooper, T.A. (2008). Expanded CTG repeats within the DMPK 3' UTR causes severe skeletal muscle wasting in an inducible mouse model for myotonic dystrophy. Proc. Natl. Acad. Sci. U. S. A 105, 2646-2651.

11. Storbeck, C.J., Sabourin, L.A., Waring, J.D., and Korneluk, R.G. (1998). Definition of regulatory sequence elements in the promoter region and the first intron of the myotonic dystrophy protein kinase gene. J. Biol. Chem. 273, 9139-9147.

12. Carrasco, M., Canicio, J., Palacin, M., Zorzano, A., and Kaliman, P. (2002). Identification of intracellular signaling pathways that induce myotonic dystrophy protein kinase expression during myogenesis. Endocrinology 143, 3017-3025.

13. Bonaldo, P., Braghetta, P., Zanetti, M., Piccolo, S., Volpin, D., and Bressan, G.M. (1998). Collagen VI deficiency induces early onset myopathy in the mouse: an animal model for Bethlem myopathy. Hum. Mol. Genet. 7, 2135-2140.

14. Palma, E., Tiepolo, T., Angelin, A., Sabatelli, P., Maraldi, N.M., Basso, E., Forte, M.A., Bernardi, P., and Bonaldo, P. (2009). Genetic ablation of cyclophilin D rescues mitochondrial defects and prevents muscle apoptosis in collagen VI myopathic mice. Hum. Mol. Genet. 18, 2024-2031.

15. Pelargonio, G., dello, R.A., Sanna, T., De, M.G., and Bellocci, F. (2002). Myotonic dystrophy and the heart. Heart 88, 665-670.

16. Krentz, A.J., Clark, P.M., Cox, L., Williams, A.C., and Nattrass, M. (1992). Hyperproinsulinaemia in patients with myotonic dystrophy. Diabetologia 35, 1170-1172.

17. Llagostera, E., Catalucci, D., Marti, L., Liesa, M., Camps, M., Ciaraldi, T.P., Kondo, R., Reddy, S., Dillmann, W.H., Palacin, M., Zorzano, A., Ruiz-Lozano, P., Gomis, R., and Kaliman, P. (2007). Role of myotonic dystrophy protein kinase (DMPK) in glucose homeostasis and muscle insulin action. PLoS. One. 2, e1134.

18. O'Cochlain, D.F., Perez-Terzic, C., Reyes, S., Kane, G.C., Behfar, A., Hodgson, D.M., Strommen, J.A., Liu, X.K., van den Broek, W., Wansink, D.G., Wieringa, B., and Terzic, A. (2004). Transgenic overexpression of human DMPK accumulates into hypertrophic cardiomyopathy, myotonic myopathy and hypotension traits of myotonic dystrophy. Hum. Mol. Genet. 13, 2505-2518.

19. Mueller, C.M., Hilbert, J.E., Martens, W., Thornton, C.A., Moxley, R.T., III, and Greene, M.H. (2009). Hypothesis: neoplasms in myotonic dystrophy. Cancer Causes Control 20, 2009-2020.

20. Justice, R.W., Zilian, O., Woods, D.F., Noll, M., and Bryant, P.J. (1995). The Drosophila tumor suppressor gene warts encodes a homolog of human myotonic dystrophy kinase and is required for the control of cell shape and proliferation. Genes Dev. 9, 534-546.

21. Gadalla, S.M., Lund, M., Pfeiffer, R.M., Gortz, S., Mueller, C.M., Moxley, R.T., III, Kristinsson, S.Y., Bjorkholm, M., Shebl, F.M., Hilbert, J.E., Landgren, O.,

Wohlfahrt, J., Melbye, M., and Greene, M.H. (2011). Cancer risk among patients with myotonic muscular dystrophy. JAMA 306, 2480-2486.

22. Pearce, L.R., Komander, D., and Alessi, D.R. (2010). The nuts and bolts of AGC protein kinases. Nat. Rev. Mol. Cell Biol. 11, 9-22.

23. Wansink, D.G., van Herpen, R.E., Coerwinkel-Driessen, M.M., Groenen, P.J., Hemmings, B.A., and Wieringa, B. (2003). Alternative splicing controls myotonic dystrophy protein kinase structure, enzymatic activity, and subcellular localization. Mol. Cell Biol. 23, 5489-5501.

24. van Herpen, R.E., Oude Ophuis, R.J., Wijers, M., Bennink, M.B., van de Loo, F.A., Fransen, J., Wieringa, B., and Wansink, D.G. (2005). Divergent mitochondrial and endoplasmic reticulum association of DMPK splice isoforms depends on unique sequence arrangements in tail anchors. Mol. Cell Biol. 25, 1402-1414.

25. Oude Ophuis, R.J., Mulders, S.A., van Herpen, R.E., van, d., V, Wieringa, B., and Wansink, D.G. (2009). DMPK protein isoforms are differentially expressed in myogenic and neural cell lineages. Muscle Nerve 40, 545-555.

26. Groenen, P.J., Wansink, D.G., Coerwinkel, M., van den Broek, W., Jansen, G., and Wieringa, B. (2000). Constitutive and regulated modes of splicing produce six major myotonic dystrophy protein kinase (DMPK) isoforms with distinct properties. Hum. Mol. Genet. 9, 605-616.

27. Roberts, R., Timchenko, N.A., Miller, J.W., Reddy, S., Caskey, C.T., Swanson, M.S., and Timchenko, L.T. (1997). Altered phosphorylation and intracellular distribution of a (CUG)n triplet repeat RNA-binding protein in patients with myotonic dystrophy and in myotonin protein kinase knockout mice. Proc. Natl. Acad. Sci. U. S. A 94, 13221-13226.

28. Kuyumcu-Martinez, N.M., Wang, G.S., and Cooper, T.A. (2007). Increased steady-state levels of CUGBP1 in myotonic dystrophy 1 are due to PKC-mediated hyperphosphorylation. Mol. Cell 28, 68-78.

29. Adrian, R.H., and Bryant, S.H. (1974). On the repetitive discharge in myotonic muscle fibres. J. Physiol 240, 505-515.

30. Pusch, M. (2002). Myotonia caused by mutations in the muscle chloride channel gene CLCN1. Hum. Mutat. 19, 423-434.

31. Zhang, X.Q., Wang, J., Carl, L.L., Song, J., Ahlers, B.A., and Cheung, J.Y. (2009). Phospholemman regulates cardiac Na+/Ca2+ exchanger by interacting with the exchanger's proximal linker domain. Am. J. Physiol Cell Physiol 296, C911-C921.

32. Mounsey, J.P., John, J.E., III, Helmke, S.M., Bush, E.W., Gilbert, J., Roses, A.D., Perryman, M.B., Jones, L.R., and Moorman, J.R. (2000). Phospholemman is a substrate for myotonic dystrophy protein kinase. J. Biol. Chem. 275, 23362-23367.

33. Muranyi, A., Zhang, R., Liu, F., Hirano, K., Ito, M., Epstein, H.F., and Hartshorne, D.J. (2001). Myotonic dystrophy protein kinase phosphorylates the myosin phosphatase targeting subunit and inhibits myosin phosphatase activity. FEBS Lett. 493, 80-84.

34. Pall, G.S., Johnson, K.J., and Smith, G.L. (2003). Abnormal contractile activity and calcium cycling in cardiac myocytes isolated from DMPK knockout mice. Physiol Genomics 13, 139-146.

35. Kaliman, P., Catalucci, D., Lam, J.T., Kondo, R., Gutierrez, J.C., Reddy, S., Palacin, M., Zorzano, A., Chien, K.R., and Ruiz-Lozano, P. (2005). Myotonic dystrophy protein kinase phosphorylates phospholamban and regulates calcium uptake in cardiomyocyte sarcoplasmic reticulum. J. Biol. Chem. 280, 8016-8021.

36. Oude Ophuis, R.J., Wijers, M., Bennink, M.B., van de Loo, F.A., Fransen, J.A., Wieringa, B., and Wansink, D.G. (2009). A tail-anchored myotonic dystrophy protein kinase isoform induces perinuclear clustering of mitochondria, autophagy, and apoptosis. PLoS. One. 4, e8024.

37. Mulders, S.A., van, H.R., Gerrits, L., Bennink, M.B., Pluk, H., de Boer-van Huizen RT, Croes, H.J., Wijers, M., van de Loo, F.A., Fransen, J., Wieringa, B., and Wansink, D.G. (2011). Abnormal actomyosin assembly in proliferating and differentiating myoblasts upon expression of a cytosolic DMPK isoform. Biochim. Biophys. Acta 1813, 867-877.

38. Harmon, E.B., Harmon, M.L., Larsen, T.D., Yang, J., Glasford, J.W., and Perryman, M.B. (2011). Myotonic dystrophy protein kinase is critical for nuclear envelope integrity. J. Biol. Chem. 286, 40296-40306.

39. Harmon, E.B., Harmon, M.L., Larsen, T.D., Paulson, A.F., and Perryman, M.B. (2008). Myotonic dystrophy protein kinase is expressed in embryonic myocytes and is required for myotube formation. Dev. Dyn. 237, 2353-2366.

40. Elmore, S. (2007). Apoptosis: a review of programmed cell death. Toxicol. Pathol. 35, 495-516.

41. Rasola, A., and Bernardi, P. (2007). The mitochondrial permeability transition pore and its involvement in cell death and in disease pathogenesis. Apoptosis. 12, 815-833.

42. Rasola, A., and Bernardi, P. (2011). Mitochondrial permeability transition in Ca(2+)-dependent apoptosis and necrosis. Cell Calcium 50, 222-233.

43. Benard, G., Bellance, N., Jose, C., Melser, S., Nouette-Gaulain, K., and Rossignol, R. (2010). Multi-site control and regulation of mitochondrial energy production. Biochim. Biophys. Acta 1797, 698-709.

44. Murphy, M.P. (2009). How mitochondria produce reactive oxygen species. Biochem. J. 417, 1-13.

45. Zong, W.X., and Thompson, C.B. (2006). Necrotic death as a cell fate. Genes Dev. 20, 1-15.

46. Kannan, K., and Jain, S.K. (2000). Oxidative stress and apoptosis. Pathophysiology. 7, 153-163.

47. Saito, M., Korsmeyer, S.J., and Schlesinger, P.H. (2000). BAX-dependent transport of cytochrome c reconstituted in pure liposomes. Nat. Cell Biol. 2, 553-555.

48. Shimizu, S., Narita, M., and Tsujimoto, Y. (1999). Bcl-2 family proteins regulate the release of apoptogenic cytochrome c by the mitochondrial channel VDAC. Nature 399, 483-487.

49. Tuppen, H.A., Blakely, E.L., Turnbull, D.M., and Taylor, R.W. (2010). Mitochondrial DNA mutations and human disease. Biochim. Biophys. Acta 1797, 113-128.

50. Rinaldi, T., Dallabona, C., Ferrero, I., Frontali, L., and Bolotin-Fukuhara, M. (2010). Mitochondrial diseases and the role of the yeast models. FEMS Yeast Res. 10, 1006-1022.

51. Bernardi, P. (1999). Mitochondrial transport of cations: channels, exchangers, and permeability transition. Physiol Rev. 79, 1127-1155.

52. Costantini, P., Chernyak, B.V., Petronilli, V., and Bernardi, P. (1996). Modulation of the mitochondrial permeability transition pore by pyridine nucleotides and dithiol oxidation at two separate sites. J. Biol. Chem. 271, 6746-6751.

53. Costantini, P., Colonna, R., and Bernardi, P. (1998). Induction of the mitochondrial permeability transition by N-ethylmaleimide depends on secondary oxidation of critical thiol groups. Potentiation by copper-ortho-phenanthroline without dimerization of the adenine nucleotide translocase. Biochim. Biophys. Acta 1365, 385-392.

54. Bernardi, P., Broekemeier, K.M., and Pfeiffer, D.R. (1994). Recent progress on regulation of the mitochondrial permeability transition pore; a cyclosporin-sensitive pore in the inner mitochondrial membrane. J. Bioenerg. Biomembr. 26, 509-517.

55. Szabo, I., De, P., V, and Zoratti, M. (1993). The mitochondrial permeability transition pore may comprise VDAC molecules. II. The electrophysiological properties of VDAC are compatible with those of the mitochondrial megachannel. FEBS Lett. 330, 206-210.

56. Baines, C.P., Kaiser, R.A., Sheiko, T., Craigen, W.J., and Molkentin, J.D. (2007). Voltage-dependent anion channels are dispensable for mitochondrial-dependent cell death. Nat. Cell Biol. 9, 550-555.

57. Basso, E., Fante, L., Fowlkes, J., Petronilli, V., Forte, M.A., and Bernardi, P. (2005). Properties of the permeability transition pore in mitochondria devoid of Cyclophilin D. J. Biol. Chem. 280, 18558-18561.

58. Baines, C.P., Kaiser, R.A., Purcell, N.H., Blair, N.S., Osinska, H., Hambleton, M.A., Brunskill, E.W., Sayen, M.R., Gottlieb, R.A., Dorn, G.W., Robbins, J., and Molkentin, J.D. (2005). Loss of cyclophilin D reveals a critical role for mitochondrial permeability transition in cell death. Nature 434, 658-662.

59. Nakagawa, T., Shimizu, S., Watanabe, T., Yamaguchi, O., Otsu, K., Yamagata, H., Inohara, H., Kubo, T., and Tsujimoto, Y. (2005). Cyclophilin D-dependent mitochondrial permeability transition regulates some necrotic but not apoptotic cell death. Nature 434, 652-658.

60. Basso, E., Petronilli, V., Forte, M.A., and Bernardi, P. (2008). Phosphate is essential for inhibition of the mitochondrial permeability transition pore by cyclosporin A and by cyclophilin D ablation. J. Biol. Chem. 283, 26307-26311.

61. Sileikyte, J., Petronilli, V., Zulian, A., Dabbeni-Sala, F., Tognon, G., Nikolov, P., Bernardi, P., and Ricchelli, F. (2011). Regulation of the inner membrane mitochondrial permeability transition by the outer membrane translocator protein (peripheral benzodiazepine receptor). J. Biol. Chem. 286, 1046-1053.

62. Wilson, J.E. (2003). Isozymes of mammalian hexokinase: structure, subcellular localization and metabolic function. J. Exp. Biol. 206, 2049-2057.

63. Mathupala, S.P., Ko, Y.H., and Pedersen, P.L. (2009). Hexokinase-2 bound to mitochondria: cancer's stygian link to the "Warburg Effect" and a pivotal target for effective therapy. Semin. Cancer Biol. 19, 17-24.

64. Pastorino, J.G., and Hoek, J.B. (2003). Hexokinase II: the integration of energy metabolism and control of apoptosis. Curr. Med. Chem. 10, 1535-1551.

65. Abu-Hamad, S., Zaid, H., Israelson, A., Nahon, E., and Shoshan-Barmatz, V. (2008). Hexokinase-I protection against apoptotic cell death is mediated via interaction with the voltage-dependent anion channel-1: mapping the site of binding. J. Biol. Chem. 283, 13482-13490.

66. Gottlob, K., Majewski, N., Kennedy, S., Kandel, E., Robey, R.B., and Hay, N. (2001). Inhibition of early apoptotic events by Akt/PKB is dependent on the first committed step of glycolysis and mitochondrial hexokinase. Genes Dev. 15, 1406-1418.

67. Chiara, F., Castellaro, D., Marin, O., Petronilli, V., Brusilow, W.S., Juhaszova, M., Sollott, S.J., Forte, M., Bernardi, P., and Rasola, A. (2008). Hexokinase II detachment from mitochondria triggers apoptosis through the permeability transition pore independent of voltage-dependent anion channels. PLoS. One. 3, e1852.

68. Neumann, D., Buckers, J., Kastrup, L., Hell, S.W., and Jakobs, S. (2010). Two-color STED microscopy reveals different degrees of colocalization between hexokinase-I and the three human VDAC isoforms. PMC Biophys. 3, 4.

69. Aflalo, C., and Azoulay, H. (1998). Binding of rat brain hexokinase to recombinant yeast mitochondria: effect of environmental factors and the source of porin. J. Bioenerg. Biomembr. 30, 245-255.

70. de Cerqueira, C.M., and Wilson, J.E. (2002). Functional characteristics of hexokinase bound to the type a and type B sites of bovine brain mitochondria. Arch. Biochem. Biophys. 397, 106-112.

71. Golestani, A., Ramshini, H., and Nemat-Gorgani, M. (2007). A study on the two binding sites of hexokinase on brain mitochondria. BMC. Biochem. 8, 20.

72. da-Silva, W.S., Gomez-Puyou, A., de Gomez-Puyou, M.T., Moreno-Sanchez, R., De Felice, F.G., de, M.L., Oliveira, M.F., and Galina, A. (2004). Mitochondrial bound hexokinase activity as a preventive antioxidant defense: steady-state ADP formation as a regulatory mechanism of membrane potential and reactive oxygen species generation in mitochondria. J. Biol. Chem. 279, 39846-39855.

73. Mailloux, R.J., Dumouchel, T., Aguer, C., deKemp, R., Beanlands, R., and Harper, M.E. (2011). Hexokinase II acts through UCP3 to suppress mitochondrial reactive oxygen species production and maintain aerobic respiration. Biochem. J. 437, 301-311.

74. Rasola, A., Sciacovelli, M., Pantic, B., and Bernardi, P. (2010). Signal transduction to the permeability transition pore. FEBS Lett. 584, 1989-1996.

75. Harman, D. (1972). The biologic clock: the mitochondria? J. Am. Geriatr. Soc. 20, 145-147.

76. Brand, M.D. (2010). The sites and topology of mitochondrial superoxide production. Exp. Gerontol. 45, 466-472.

77. Lebovitz, R.M., Zhang, H., Vogel, H., Cartwright, J., Jr., Dionne, L., Lu, N., Huang, S., and Matzuk, M.M. (1996). Neurodegeneration, myocardial injury, and perinatal death in mitochondrial superoxide dismutase-deficient mice. Proc. Natl. Acad. Sci. U. S. A 93, 9782-9787.

78. Li, Y., Huang, T.T., Carlson, E.J., Melov, S., Ursell, P.C., Olson, J.L., Noble, L.J., Yoshimura, M.P., Berger, C., Chan, P.H., Wallace, D.C., and Epstein, C.J. (1995). Dilated cardiomyopathy and neonatal lethality in mutant mice lacking manganese superoxide dismutase. Nat. Genet. 11, 376-381.

79. Ho, Y.S., Gargano, M., Cao, J., Bronson, R.T., Heimler, I., and Hutz, R.J. (1998). Reduced fertility in female mice lacking copper-zinc superoxide dismutase. J. Biol. Chem. 273, 7765-7769.

80. Franco, R., and Cidlowski, J.A. (2009). Apoptosis and glutathione: beyond an antioxidant. Cell Death. Differ. 16, 1303-1314.

81. Drahota, Z., Chowdhury, S.K., Floryk, D., Mracek, T., Wilhelm, J., Rauchova, H., Lenaz, G., and Houstek, J. (2002). Glycerophosphate-dependent hydrogen peroxide production by brown adipose tissue mitochondria and its activation by ferricyanide. J. Bioenerg. Biomembr. 34, 105-113.

82. Muller, F.L., Liu, Y., Abdul-Ghani, M.A., Lustgarten, M.S., Bhattacharya, A., Jang, Y.C., and Van, R.H. (2008). High rates of superoxide production in skeletal-muscle mitochondria respiring on both complex I- and complex II-linked substrates. Biochem. J. 409, 491-499.

83. Harper, M.E., Green, K., and Brand, M.D. (2008). The efficiency of cellular energy transduction and its implications for obesity. Annu. Rev. Nutr. 28, 13-33.

84. Lemmon, M.A., and Schlessinger, J. (2010). Cell signaling by receptor tyrosine kinases. Cell 141, 1117-1134.

85. Boopathi, E., Srinivasan, S., Fang, J.K., and Avadhani, N.G. (2008). Bimodal protein targeting through activation of cryptic mitochondrial targeting signals by an inducible cytosolic endoprotease. Mol. Cell 32, 32-42.

86. Foster, D.B., Van Eyk, J.E., Marban, E., and O'Rourke, B. (2009). Redox signaling and protein phosphorylation in mitochondria: progress and prospects. J. Bioenerg. Biomembr. 41, 159-168.

87. Li, H., Degenhardt, B., Tobin, D., Yao, Z.X., Tasken, K., and Papadopoulos, V. (2001). Identification, localization, and function in steroidogenesis of PAP7: a peripheral-type benzodiazepine receptor- and PKA (RIalpha)-associated protein. Mol. Endocrinol. 15, 2211-2228.

88. Liu, J., Cavalli, L.R., Haddad, B.R., and Papadopoulos, V. (2003). Molecular cloning, genomic organization, chromosomal mapping and subcellular localization of mouse PAP7: a PBR and PKA-RIalpha associated protein. Gene 308, 1-10.

89. Chang, C.R., and Blackstone, C. (2007). Cyclic AMP-dependent protein kinase phosphorylation of Drp1 regulates its GTPase activity and mitochondrial morphology. J. Biol. Chem. 282, 21583-21587.

90. Cribbs, J.T., and Strack, S. (2007). Reversible phosphorylation of Drp1 by cyclic AMP-dependent protein kinase and calcineurin regulates mitochondrial fission and cell death. EMBO Rep. 8, 939-944.

91. Jin, S., Zhuo, Y., Guo, W., and Field, J. (2005). p21-activated Kinase 1 (Pak1)-dependent phosphorylation of Raf-1 regulates its mitochondrial localization, phosphorylation of BAD, and Bcl-2 association. J. Biol. Chem. 280, 24698-24705.

92. Sumitomo, M., Ohba, M., Asakuma, J., Asano, T., Kuroki, T., Asano, T., and Hayakawa, M. (2002). Protein kinase Cdelta amplifies ceramide formation via mitochondrial signaling in prostate cancer cells. J. Clin. Invest 109, 827-836.

93. Chen, L., Hahn, H., Wu, G., Chen, C.H., Liron, T., Schechtman, D., Cavallaro, G., Banci, L., Guo, Y., Bolli, R., Dorn, G.W., and Mochly-Rosen, D. (2001). Opposing cardioprotective actions and parallel hypertrophic effects of delta PKC and epsilon PKC. Proc. Natl. Acad. Sci. U. S. A 98, 11114-11119.

94. Zhao, X., Leon, I.R., Bak, S., Mogensen, M., Wrzesinski, K., Hojlund, K., and Jensen, O.N. (2011). Phosphoproteome analysis of functional mitochondria isolated from resting human muscle reveals extensive phosphorylation of inner membrane protein complexes and enzymes. Mol. Cell Proteomics. 10, M110.

95. Deng, N., Zhang, J., Zong, C., Wang, Y., Lu, H., Yang, P., Wang, W., Young, G.W., Wang, Y., Korge, P., Lotz, C., Doran, P., Liem, D.A., Apweiler, R., Weiss, J.N., Duan, H., and Ping, P. (2011). Phosphoproteome analysis reveals regulatory sites in major pathways of cardiac mitochondria. Mol. Cell Proteomics. 10, M110.

96. Rasola, A., Sciacovelli, M., Chiara, F., Pantic, B., Brusilow, W.S., and Bernardi, P. (2010). Activation of mitochondrial ERK protects cancer cells from death through inhibition of the permeability transition. Proc. Natl. Acad. Sci. U. S. A 107, 726-731.

97. Piedimonte, G., Silvotti, L., Chamaret, S., Borghetti, A.F., and Montagnier, L. (1986). Association of tyrosine protein kinase activity with mitochondria in human fibroblasts. J. Cell Biochem. 32, 113-123.

98. Salvi, M., Brunati, A.M., Bordin, L., La, R.N., Clari, G., and Toninello, A. (2002). Characterization and location of Src-dependent tyrosine phosphorylation in rat brain mitochondria. Biochim. Biophys. Acta 1589, 181-195.

99. Arachiche, A., Augereau, O., Decossas, M., Pertuiset, C., Gontier, E., Letellier, T., and Dachary-Prigent, J. (2008). Localization of PTP-1B, SHP-2, and Src exclusively in rat brain mitochondria and functional consequences. J. Biol. Chem. 283, 24406-24411.

100. Lluis, J.M., Buricchi, F., Chiarugi, P., Morales, A., and Fernandez-Checa, J.C. (2007). Dual role of mitochondrial reactive oxygen species in hypoxia signaling: activation of nuclear factor-{kappa}B via c-SRC and oxidant-dependent cell death. Cancer Res. 67, 7368-7377.

101. Giannoni, E., Buricchi, F., Raugei, G., Ramponi, G., and Chiarugi, P. (2005). Intracellular reactive oxygen species activate Src tyrosine kinase during cell adhesion and anchorage-dependent cell growth. Mol. Cell Biol. 25, 6391-6403.

102. Salvi, M., Brunati, A.M., and Toninello, A. (2005). Tyrosine phosphorylation in mitochondria: a new frontier in mitochondrial signaling. Free Radic. Biol. Med. 38, 1267-1277.

103. Batard, P., Jordan, M., and Wurm, F. (2001). Transfer of high copy number plasmid into mammalian cells by calcium phosphate transfection. Gene 270, 61-68.

104. Rasola, A., and Geuna, M. (2001). A flow cytometry assay simultaneously detects independent apoptotic parameters. Cytometry 45, 151-157.

105. Tietze, F. (1969). Enzymic method for quantitative determination of nanogram amounts of total and oxidized glutathione: applications to mammalian blood and other tissues. Anal. Biochem. 27, 502-522.

106. Anderson, M.E. (1985). Determination of glutathione and glutathione disulfide in biological samples. Methods Enzymol. 113, 548-555.

107. Hansson, M.J., Mattiasson, G., Mansson, R., Karlsson, J., Keep, M.F., Waldmeier, P., Ruegg, U.T., Dumont, J.M., Besseghir, K., and Elmer, E. (2004). The nonimmunosuppressive cyclosporin analogs NIM811 and UNIL025 display nanomolar potencies on permeability transition in brain-derived mitochondria. J. Bioenerg. Biomembr. 36, 407-413.

108. Pastorino, J.G., and Hoek, J.B. (2008). Regulation of hexokinase binding to VDAC. J. Bioenerg. Biomembr. 40, 171-182.

109. Jia, C.Y., Nie, J., Wu, C., Li, C., and Li, S.S. (2005). Novel Src homology 3 domain-binding motifs identified from proteomic screen of a Pro-rich region. Mol. Cell Proteomics. 4, 1155-1166.

110. Tian, L., Chen, L., McClafferty, H., Sailer, C.A., Ruth, P., Knaus, H.G., and Shipston, M.J. (2006). A noncanonical SH3 domain binding motif links BK channels to the actin cytoskeleton via the SH3 adapter cortactin. FASEB J. 20, 2588-2590.

111. Mayer, B.J. (2001). SH3 domains: complexity in moderation. J. Cell Sci. 114, 1253-1263.

112. Benders, A.A., Groenen, P.J., Oerlemans, F.T., Veerkamp, J.H., and Wieringa, B. (1997). Myotonic dystrophy protein kinase is involved in the modulation of the Ca2+ homeostasis in skeletal muscle cells. J. Clin. Invest 100, 1440-1447.

113. Loro, E., Rinaldi, F., Malena, A., Masiero, E., Novelli, G., Angelini, C., Romeo, V., Sandri, M., Botta, A., and Vergani, L. (2010). Normal myogenesis and increased apoptosis in myotonic dystrophy type-1 muscle cells. Cell Death. Differ. 17, 1315-1324.